



MODELLING THE POPULATION DYNAMICS OF ANTARCTIC KRILL

The Timing of Reproduction and
the Impact of Climate Change

Von der Fakultät für Mathematik und Naturwissenschaften der Carl
von Ossietzky Universität Oldenburg zur Erlangung des Grades und
Titels eines **Doktors der Naturwissenschaften (Dr. rer. nat.)**
angenommene Dissertation

von **Siri Rackebrandt**

geboren am 02.09.1988 in Göttingen.

Erstgutachter: Prof. Dr. Bernd Blasius
Zweitgutachter: Prof. Dr. Volker Grimm

Tag der Disputation: 02.12.2016

SUMMARY

Antarctic krill (*Euphausia superba*) is a shrimp-like crustacean from the order Euphausiacea and one of the most abundant pelagic species in the Southern Ocean. It is an important predator on lower trophic levels such as phytoplankton as well as a prey for higher trophic levels such as whales and thus it occupies a central position in the Southern Ocean food web. In addition, it is an increasingly important fishery resource. The life cycle of Antarctic krill is highly complex and finely tuned to the strong seasonal changes in its environment. One crucial aspect of this life cycle is the right timing of the reproduction. Adult krill need high phytoplankton concentrations to fuel the energy-demanding reproduction. At the same time, their offspring also depend on the highly productive summer months to be able to survive the following winter. Due to the short period of the year with high food availability, the spawning has to be timed precisely. It has therefore been suggested that krill has developed a biological clock – i.e. it uses environmental cues which predict the upcoming conditions to initiate and terminate the reproduction. Possible environmental cues for the start or termination of the reproductive season could be the daylength or food availability, but their exact role in the timing of the reproduction is not yet clear.

One aim of this thesis was to elucidate the importance of these two environmental factors for the krill population using a mathematical model. For this purpose, a new population model was developed. In contrast to earlier studies, the two most important food sources (pelagic and sea ice phytoplankton) and their dependence on environmental factors such as light, sea ice conditions and iron availability are considered as well. This basic reference model without a clock reproduces the annual dynamics of juvenile and adult krill observed in nature. Analyses of the model results have shown that the most important process in the life cycle of krill is the maturation from juveniles to adults. Changes in this process can lead to multi-annual cycles of the krill population or chaotic behaviour. This process should be analyzed further considering the interannual variations in krill density observed in nature. In a second step, the model was extended by a biological clock and the implications of four different combinations of daylength and food availability as a trigger to start and terminate the reproductive season were analyzed. None of the four clock setups lead to a qualitative change in the krill dynamics. Thus, none of the clock setups can be rejected as biologically unfeasible. All four clock setups lead to a decrease in krill density compared to the reference model without a clock. The exact magnitude of this decrease depends on the parameters of the clock setup, for example at which critical daylength krill starts the reproduction. Some of the values of the parameters lead to a particularly strong decrease, but considering the

current latitudinal extent of the distribution area of krill, these parameter values can be ruled out as biologically unfeasible .

The second aim of this thesis was to analyze the impact of climate change on krill. The environment in the Southern Ocean is changing in many ways. Either krill has to adapt to these changes – for example a short sea ice season – or it might be forced to move to higher latitudes to escape the unfavourable environmental conditions in his current distribution area. Considering the possible dependence of a biological clock on the daylength, it has been suggested that moving south could lead to a mismatch between the reproductive period and the food availability and thus a decline of the krill population. The two scenarios – krill moving south and krill experiencing a shorter sea ice season – were both analyzed using the reference model without a clock and the extended model with the four clock setups. For both climate change scenarios, the model results suggest that krill densities increase due to increased phytoplankton growth. The increased growth is a result of longer days for growth at high latitudes or due to less sea ice that reduces the amount of light reaching the sea surface. The magnitude of the increase in krill density has probably been overestimated, because other – possibly negative – effects of climate change such as ocean acidification have been neglected in the model. Nevertheless, the results of the model have shown that, considering that phytoplankton experiences the same changes in the environment as krill, a desynchronization of the life cycle and the food availability is unlikely.

ZUSAMMENFASSUNG

Antarktischer Krill (*Euphausia superba*) ist eine garnelenartige Krebsart der Ordnung Euphausiacea und eine der häufigsten Arten im Südpolarmeer. Er ist sowohl ein wichtiger Räuber für die unteren trophischen Ebenen wie Phytoplankton als auch eine wichtige Beute für höhere trophische Ebenen wie Wale. Dadurch nimmt der Krill eine zentrale Position im Nahrungsnetz des Südpolarmeeres ein. Des Weiteren gibt es eine zunehmende kommerzielle Nutzung durch Fischerei. Der Lebenszyklus des Antarktischen Krills ist sehr komplex und genau auf die saisonalen Änderungen in seiner Umwelt angepasst. Beispielsweise ist für den Erfolg der Reproduktion der genaue Zeitpunkt sehr entscheidend. Auf der einen Seite sind die geschlechtsreifen Weibchen auf sehr hohe Phytoplankton Konzentrationen für die energieaufwendige Reproduktion angewiesen. Andererseits sind aber auch ihre Nachkommen davon abhängig diese hohen Phytoplankton Konzentrationen im Sommer für ihre Entwicklung nutzen zu können um den folgenden Winter zu überleben. Um die kurzen Zeiten im Jahr mit hoher Primärproduktion optimal zu nutzen, müssen die Weibchen ihre Eier also genau zur richtigen Zeit ablegen. Deswegen wird vermutet, dass der Krill im Laufe der Evolution eine biologische Uhr entwickelt hat, d.h. der Krill nutzt bestimmte Signale in der Umwelt um gute Bedingungen für die Reproduktion vorherzusagen. Mögliche Signale für den Beginn oder das Ende des jährlichen Reproduktionszykluses könnten die Tageslänge oder die Nahrungsverfügbarkeit sein. Es ist bisher jedoch unklar welchen Einfluss diese Signale bei der Wahl des richtigen Reproduktionszeitpunkts genau haben.

Ein Ziel dieser Arbeit war es diesen Einfluss auf die Krill Population mit Hilfe eines mathematischen Modells zu untersuchen. Für diesen Zweck wurde im Rahmen dieser Arbeit ein neues Populationsmodell entwickelt. Im Gegensatz zu früheren Modellen wurde in diesem Modell die Nahrung des Krills (d.h. pelagisches und Meereis-Phytoplankton) und dessen Abhängigkeit von Umweltfaktoren wie Licht, Eisbedeckung und Nährstoffverfügbarkeit explizit mit modelliert. Dieses Referenzmodell, das ohne biologische Uhr auskommt, beschreibt den in der Natur beobachteten Jahreszyklus von juvenilem und adultem Krill korrekt. Die Analysen der Modellergebnisse haben gezeigt, dass der wichtigste Prozess im Lebenszyklus des Krills die Entwicklung vom juvenilen zum geschlechtsreifen, adulten Stadium ist. Veränderungen in der Parametrisierung dieses Prozesses können zu Mehrjahreszyklen oder chaotischem Verhalten der Population führen. Da diese Änderungen der Population von Jahr zu Jahr auch in der Natur beobachtet werden können, liegt es nahe diesen Prozess in Zukunft genauer zu untersuchen. In einem zweiten Schritt wurde das Modell um eine biologische Uhr erweitert und die Einflüsse der vier möglichen Kombinationen von Tageslänge und Nahrungsverfüg-

barkeit als Signale für den Start oder das Ende der Reproduktion untersucht. Keiner der vier möglichen Varianten der Uhr ändert das qualitative Verhalten des Jahresverlaufs des Krills, d.h. keine der vier Varianten kann als biologisch unmöglich erachtet werden. Im Vergleich zum Referenzmodell ohne Uhr führen alle vier Uhren zu einem Rückgang des Krills. Die Stärke des Rückgangs hängt dabei von der genauen Parametrisierung der Uhr ab, z.B. von der Tageslänge bei der der Krill sich zu reproduzieren beginnt. Einige dieser Parameterwerte führen zu einem sehr starken Rückgang. Diese können aber auf Grund der räumlichen Ausdehnung des derzeitigen Verbreitungsgebietes des Krills ausgeschlossen werden.

Ein weiteres Ziel dieser Arbeit war es mit Hilfe des Modells den Einfluss des Klimawandels auf den Krill zu analysieren. Das Südpolarmeer ist bereits dabei sich zu verändern. Entweder passt sich der Krill diesen Veränderungen, z.B. einer zeitlich kürzeren Eisbedeckung, an oder er ist womöglich gezwungen sein Verbreitungsgebiet nach Süden zu verlagern. Dies könnte, besonders auf Grund der möglichen Abhängigkeit der biologischen Uhr von der Tageslänge, zu einer zeitlichen Diskrepanz zwischen dem Reproduktionszyklus und der Nahrungsverfügbarkeit führen. Eine solche Diskrepanz hätte vermutlich einen Rückgang der Krillabundanz zur Folge. Beide Szenarien – der Krill wandert nach Süden bzw. der Krill muss sich an eine verkürzte Eissaison anpassen – wurden mit Hilfe des Referenzmodells sowie des um die Uhr erweiterten Modells untersucht. Die Modellergebnisse zeigen, dass die Krillabundanz in beiden Szenarien durch ein erhöhtes Phytoplankton Wachstum zunimmt. Dieses erhöhte Wachstum ergibt sich aus den längeren Tagen bei südlicheren Breitengraden bzw. erhöhter Lichtintensität in der Wassersäule durch Abschmelzen des Eises. Vermutlich wird die Zunahme der Krillabundanz durch das Modell überschätzt, da weitere, möglicherweise negative, Effekte des Klimawandels wie Ozeanversauerung nicht beachtet wurden. Die Modellergebnisse haben jedoch gezeigt, dass dadurch dass das Phytoplankton die gleichen Umweltveränderungen wie der Krill ausgesetzt ist, eine Desynchronisierung zwischen dem Lebenszyklus des Krills und der Nahrungsverfügbarkeit unwahrscheinlich ist.

TABLE OF CONTENTS

Summary	v
Zusammenfassung	vii
Preface	1
1. A Mathematical Model of the Life Cycle of Antarctic Krill	5
1.1. Introduction	5
1.1.1. The Seasonal Environment of the Southern Ocean	6
1.1.2. The Life Cycle of Antarctic Krill	7
1.1.3. Modelling of Antarctic Krill	8
1.2. Model Description	10
1.2.1. Forcing	11
1.2.2. Nutrient	15
1.2.3. Pelagic Phytoplankton	16
1.2.4. Sea Ice Phytoplankton	18
1.2.5. Juvenile Krill	19
1.2.6. Adult Krill	22
1.2.7. Implementation	23
1.2.8. Parametrization	23
1.2.9. Sensitivity Analysis	29
1.3. Results	33
1.3.1. Annual Dynamics	33
1.3.2. Sensitivity Analysis	38
1.3.3. Multi-Annual Dynamics	45
1.4. Short Summary	51
2. The Influence of a Biological Clock on Krill Reproduction	53
2.1. Introduction	53
2.1.1. Types of Annual Rhythms	53
2.1.2. Timing of Krill Reproduction	54
2.2. Model Changes	56

2.3.	Results	58
2.3.1.	Dependence of the Krill Density on the Critical Values	59
2.3.2.	Comparison of the Different Clocks	62
2.4.	Short Summary	64
3.	The Impact of Climate Change on Krill	65
3.1.	Introduction	65
3.2.	Model Changes	68
3.2.1.	Scenario 1: Krill Moves South	68
3.2.2.	Scenario 2: Krill Experiences a Shorter Sea Ice Season	69
3.3.	Results	70
3.3.1.	Scenario 1: Krill Moves South	70
3.3.2.	Scenario 2: Krill Experiences a Shorter Sea Ice Season	74
3.4.	Short Summary	77
4.	Discussion and Conclusions	79
	References	89
A.	Appendix	103
A.1.	Calculation of the Sea Ice Forcing	103
A.2.	Calculation of the Astronomical Irradiance and Daylength	103
A.3.	Calculation of the Light-Dependent Growth Factor	105
A.4.	Calculation of the Conceptual Ice	107
A.5.	The Effect of Climate Change on the Absolute Krill Densities	109
	List of Figures	113
	List of Tables	115

PREFACE

*“Antarctic krill (*Euphausia superba*) is one of the best-studied species of pelagic animal, yet there are still considerable uncertainties about key elements of its biology and of the forces that determine its distribution and abundance.”*

— Nicol (2006)

Antarctic krill (*Euphausia superba*) – hereafter called krill – is a shrimp-like crustacean from the order Euphausiacea. Krill research dates back as far as the 1930’s (Fraser, 1936) and although much progress has since been made, the quote above still holds true. The numerous studies in recent years have shed some more light on the complex life cycle of krill, but many of the accepted concepts stem from earlier studies – especially from the detailed report by Marr (1962).

Krill are circumpolarly distributed all around the Southern Ocean as far north as 50°S. It is the most abundant pelagic species in the Southern Ocean and with an estimated biomass of 60 to 420 Mt probably one of the most abundant animals on Earth (Nicol et al., 2000; Siegel, 2005; Atkinson et al., 2009). Krill plays an important role in the Southern Ocean food web, both as a predator on primary producers and other lower trophic levels and as prey for higher trophic levels such as whales, seals and birds. Due to this role, Quetin and Ross (2009) have described krill as a foundation species – a species “*that controls community dynamics and modulates ecosystem processes [...] and whose loss would lead to system-wide changes in the structure and function of the ecosystem.*” In addition to the important role in the food web, krill is an increasingly important fishery resource. Technological improvements have already led to an increase in the annual catches which will probably continue in the upcoming years (Nicol and Foster, 2003; Nicol et al., 2012).

To cope with the strong seasonal changes in the environment which are characteristic for the Southern Ocean, krill has adapted its life cycle to these conditions. One of these remarkable adaptations to the extreme environment is the reduction in metabolic activity in winter. To survive this period of low food availability, krill even regresses their external sexual organs to save energy (Thomas and Ikeda, 1987). After winter, krill needs to re-develop their sexual organs and spawn at the right time to maximize the probability of survival for its offspring. So far, it is unclear how the timing of the regression and re-development is controlled. The reproductive cycle could be endogenous, but krill could also possess a biological clock mediated by light and/or food availability. Although several experimental studies have attempted to clarify how this cycle works, the details are

still not understood (Thomas and Ikeda, 1987; Kawaguchi et al., 2007; Teschke et al., 2008; Yoshida, 2009; Brown et al., 2011).

As many other regions on Earth, the Southern Ocean is subject to climate change such as increase in temperature, sea ice decline and ocean acidification. There are signs that krill densities are already declining (Atkinson et al., 2004), but it is so far poorly known whether krill will be able to cope with future changes. Understanding how krill will react to changes in its environment, however, is crucial considering its role as a foundation species in the food web as well as the growing commercial interests. The importance of this topic has been underlined by “The 1st Antarctic & Southern Ocean Science Horizon Scan” (Kennicutt II et al., 2015) – a compilation of the 80 key scientific questions in Antarctic research. Two of these questions are related to this thesis:

Q.58 “How will climate change affect existing and future Southern Ocean fisheries, especially krill stocks?”

Q.60 “What are the impacts of changing seasonality and transitional events on Antarctic and Southern Ocean marine ecology, biogeochemistry and energy flow? ”

Q.58 is a rather general question of how krill will react to climate change and what economic effect that might have, but Q.60 has an important point that is often overlooked in climate change discussions. Not only the absolute increase or decrease of an environmental factor (i.e. rising temperatures) is important to consider, but also the changing seasonality of this factor. For krill, for example, a change in the seasonal cycle of primary production might lead to a mismatch between the reproductive cycle and the food availability, which could have drastic consequences for the whole food web.

ABOUT THIS THESIS

The aim of this thesis is to develop a model that is suitable to examine the role of the biological clock and the effect of climate change on krill dynamics.

The description of the new model and the necessary background information about krill biology form the first chapter of this thesis. This part is quite detailed in order to give the reader the possibility to comprehend how the model works and assess the advantages and the disadvantages of the chosen model approach. The new model is essentially an NPZ-model (nutrient-phytoplankton-zooplankton model) with one nutrient, two phytoplankton groups and two different developmental stages of krill.

In the second chapter, the model is extended by a biological clock acting on the reproductive cycle. Since it is still under much debate what controls the timing of the reproductive cycle, the model is set up with four different clocks and their effects on the krill dynamics are analyzed.

In the third chapter of this thesis, the effect of climate change on the population dynamics of Antarctic krill is analyzed. Because it is unclear how exactly the environment will change, two different scenarios are considered and combined with the four clocks from the previous

chapter.

All of these three chapters have the same structure: the necessary background information is followed by the description of the model or changes to the model, the model results and finally a short paragraph summarizing the most important results from this chapter. A synthesis combining the results of all three chapters concludes this thesis.

Acknowledgements

Thank you Bernd for funding and supervising this PhD project and providing me with many opportunities to discuss my work with specialists in the field of krill research.

Thank you Volker for taking time to evaluate this thesis.

A PhD Thesis is not possible without the help of numerous people. Thank you to everyone who contributed to this thesis in one way or another – either by providing data, helping with the development of the model, solving computer problems, answering numerous questions about krill ecology, discussing my work, sharing the office, proofreading this thesis ... or simply by meeting for a coffee.

Above all: Thank you Jo! Without your support, this thesis would have remained an unfinished project.

1

A MATHEMATICAL MODEL OF THE LIFE CYCLE OF ANTARCTIC KRILL

1.1. INTRODUCTION

Antarctic krill (*Euphausia superba*) is the most abundant of the approximately 85 different krill species from the order Euphausiacea (Everson, 2000). The species of this order can be found in all oceans, but – as the name already suggests – Antarctic krill can only be found around the Antarctic continent. Antarctic krill (or short: krill) is found all over the Southern Ocean as far north as the Polar Front (approx. 50 °S in the Atlantic), but it's largest densities can be found around South Georgia and West of the Antarctic Peninsula (Nicol et al., 2000; Atkinson et al., 2004). Krill plays a pivotal role in the Southern Ocean food web, coupling lower trophic levels such as pelagic or sea ice phytoplankton to higher trophic levels such as fish, birds, whales and seals. Krill is a fairly large crustacean species growing up to 65 mm long (Knox, 2006). It has been suggested that it can live up to 10 years but a lifespan of 5 to 8 years is generally more accepted (Quetin and Ross, 2003). Krill has developed a unique life cycle to cope with the harsh environment in the Southern Ocean. It is because of this complex life cycle, the central role of krill in the food web and also increasing commercial interests of the krill fishery, that krill has gained more and more attention.

1.1.1. THE SEASONAL ENVIRONMENT OF THE SOUTHERN OCEAN

The environmental conditions that krill faces in the Southern Ocean are highly seasonal and can strongly differ between regions. This section does not aim to give a complete description of the Southern Ocean environment, but it rather aims at providing an overview of those environmental factors which are most important with regard to krill.

The most important abiotic factor is light. Light intensity in the Southern Ocean can vary strongly depending on the latitude, day of the year, sea ice thickness and atmospheric conditions. In addition to the varying light intensity, the length of the the daily photoperiod is very different between the northern and the southern part of the Southern Ocean. At the northernmost latitude of krill's distribution area, there are about 16 hours of daylight in summer and at least 8 hours in winter. South of the polar cycle (65.5°S), the 24 hours of daylight in summer are contrasted by a few months without any daylight in winter. That has a profound effect on primary production. At high latitudes, phytoplankton growth can be very high in summer, but it will also be confined to a shorter period of time within the year due to the very short days in winter.

The second most important environmental factor is the sea ice cover. It is a very dynamic environment with its maximum extent in September reaching approximately $20 \times 10^6 \text{ km}^2$ and a minimum in February of only 20 % of that area (Knox, 2006). Sea ice has two main purposes for krill: (1) as a feeding ground and (2) as a shelter against larger predators and transport by currents to unfavourable places (Daly and Macaulay, 1991; Meyer et al., 2009; Flores et al., 2012b). Especially the first point is of uttermost importance. Primary production in ice covered water columns is very low due to the low light availability. Sea ice phytoplankton, in contrast, is more shade-adapted and can reach densities that are up to three orders of magnitude higher in winter than those in the water column at that time of the year (Quetin and Ross, 2009). Even though these high densities are only restricted to a short part of the year, sea ice primary production can make up 9 to 25 % of the total primary production in ice covered waters (Arrigo et al., 1997).

An important factor for phytoplankton growth are the iron concentrations. Large areas of the Southern Ocean are so-called HNLC (high nutrient - low chlorophyll) areas. Primary production in these areas is low although macronutrients such as nitrate and phosphate are available in such high concentrations in the Southern Ocean that they cannot be limiting phytoplankton growth (Gran, 1931; Hart, 1934). It has been hypothesized that one reason for the low primary production are the low concentrations of the micronutrient iron, which is an essential element for photosynthesis (Martin, 1990, 1991; Morel et al., 1991). Whether this iron hypothesis is true for all regions of the Southern Ocean is still under much debate.

The mixed layer depth – the depth down to which the water column is completely mixed – is important in regulating iron and phytoplankton concentrations in the upper water column. Iron supply from below the mixed layer depth via mixed layer deepening in winter is an important process to replenish the iron concentration in the surface layer (Tagliabue et al., 2014). On the one hand, these increased iron concentration favour pelagic phytoplankton. But

on the other hand, the deepening of the mixed layer is a disadvantage, because it transports pelagic phytoplankton further down in the water column where light intensities might not be sufficient for phytoplankton growth.

Two environmental factors have not been mentioned so far: temperature and the ocean currents. Both of them are important for the Southern Ocean ecosystem but are considered negligible for the aim of this thesis. Seasonal changes in the temperature amplitude are considerably smaller than 4 to 5 °C in most areas of the Southern Ocean (Clarke, 1988; Knox, 2006) and temperature thus only determines the possible maximum growth rates but not their seasonal cycle. The current system of course plays an important role in determining the distribution patterns of phytoplankton and krill, but since those spatial aspects are not part of this thesis, currents will be neglected.

1.1.2. THE LIFE CYCLE OF ANTARCTIC KRILL

The reason for the great success of Antarctic krill is its adaptation to the extremely seasonal environment. Krill have to undergo a multitude of developmental stages that are closely tied to the environment until they reach adulthood (Fraser, 1936; Jia et al., 2014). The life cycle begins in summer (December - March) when the gravid female krill lay their thousands of eggs. While sinking down in the water column, the eggs undergo development until the embryos hatch at around 700 to 1000 m (Nicol, 2006). The hatched nauplius larvae go through several stages (Nauplius I & II, Metanauplius) while swimming upwards until they reach the surface approximately 30 days after the females have spawned (Fraser, 1936; Marr, 1962). Throughout the rest of the year, the larvae undergo several more developmental stages (Calyptopis I-III, Furcilia I - VI) until they develop to juveniles in late winter/early spring. After a year as juveniles/subadults, they finally develop into mature adults in the following spring – males usually a couple of months earlier than females (Ross et al., 2000).

The whole life cycle strongly depends on the availability of food, but there are two phases where it is particularly important that krill finds enough food: (1) After reaching the surface and developing into the first feeding stage (Calyptopis I), the larvae need to find food within 10 to 14 days (Ross and Quetin, 1989). Since the duration of the life cycle up to this point is fairly constant, it is crucial that the females spawn at the right time in relation to the phytoplankton concentrations. To maximize the chance that the larvae encounter good feeding conditions, one female krill spawns up to ten times within one season (Ross and Quetin, 1983). (2) During the first winter, larvae need to feed to continue their development despite the low phytoplankton concentrations in the water column. Instead of feeding on pelagic phytoplankton, juvenile krill have been reported to feed on the sea ice phytoplankton attached to the bottom of the ice (Daly, 1990; Meyer et al., 2009). The survival of the larvae is also related to the timing of spawning: the longer the larvae can feed in good conditions, the larger the chance of surviving their first winter (Quetin and Ross, 1991).

Adults are not as closely attached to the sea ice, because they have developed other mechanisms to survive the food shortage in winter. Four different overwintering mechanisms are generally accepted (Quetin and Ross, 1991; Meyer, 2012): Shrinkage in size (Ikeda and

Dixon, 1982; Quetin and Ross, 1991), utilization of stored lipids (Quetin and Ross, 1991; Hagen et al., 2001), reduction in metabolic rates (Kawaguchi et al., 1986; Quetin and Ross, 1991; Meyer et al., 2010) and switching to alternative food sources such as zooplankton, benthic phytoplankton and detritus (Kawaguchi et al., 1986; Price et al., 1988). Feeding on sea ice phytoplankton has also been suggested (Marschall, 1988), but in more recent years several studies have found that adult krill are seldom associated with the sea ice in winter (Quetin and Ross, 1991; Quetin et al., 1996; Meyer, 2012; Schaafsma et al., 2016). Only in spring, adult krill might revert to feeding on sea ice algae to be able to meet the high metabolic demand in preparation for reproduction (Meyer, 2012). Teschke et al. (2007) have shown that the reduction in metabolic rates is not dependent on the food availability, but is probably an inherent mechanism triggered by light. This adds another level of complexity to the life cycle which needs to be understood to predict how krill will cope with future changes in its environment.

1.1.3. MODELLING OF ANTARCTIC KRILL

A multitude of krill models exist, which differ greatly in the chosen model approach. Some of them are strongly based on data and fit relatively simple functions to predict krill growth for time periods for which no data is available. Others are based on the knowledge about fundamental processes in the life cycle of krill and its environment and not on specific data. The models can be divided roughly into four categories depending on their research aim: (1) models predicting the somatic growth in length (e.g. Astheimer et al., 1985; Astheimer, 1986; Murphy and Reid, 2001; Atkinson et al., 2006; Candy and Kawaguchi, 2006; Kawaguchi et al., 2006; Wiedenmann et al., 2008; Constable and Kawaguchi, 2012), (2) models aiming to understand the spatial distribution pattern of krill (e.g. Capella et al., 1992; Murphy et al., 1998; Hofmann and Hüsrevoglu, 2003; Fach and Klinck, 2006; Fach et al., 2006; Thorpe et al., 2007; Piñones et al., 2013, 2016), (3) physiology-based models interested in specific processes of the life-cycle (e.g. Hofmann et al., 1992; Hofmann and Lascara, 2000; Fach et al., 2002, 2008; Lowe et al., 2012; Groeneveld et al., 2015; Jager and Ravagnan, 2015), and (4) models aiming to understand the interaction with higher trophic levels or even the whole food web (e.g. Pinkerton et al., 2010). The distinction between these four categories is not strict, and thus models can fall into more than one category. Fach et al. (2002), for example, combine a physiology-based growth model with trajectories from a Lagrangian model to assess whether food concentrations are sufficient to support growth during transport from the Antarctic Peninsula to South Georgia.

All these models have some advantages and disadvantages and a model should be chosen carefully depending on the research question. For example, somatic growth models usually have only a simple dependence on environmental parameters and are thus less useful for predictions of krill densities under climate change scenarios. The advantage of these models is that length-frequency data is sufficient to parametrize the model. These models are an important tool for the calculation of catch limits, because they can be used to predict growth in-between different sampling campaigns (Constable and Kawaguchi,

2012). Physiology-based models, in contrast, provide more biological realism but need detailed knowledge about different physiological processes such as respiration or reproduction. Spatial distribution models and food web models add even more complexity, because they require knowledge about transport processes and the physiology of other organisms respectively.

1.2. MODEL DESCRIPTION

The model developed in this thesis describes the temporal dynamics of Antarctic krill, its food and the environment.

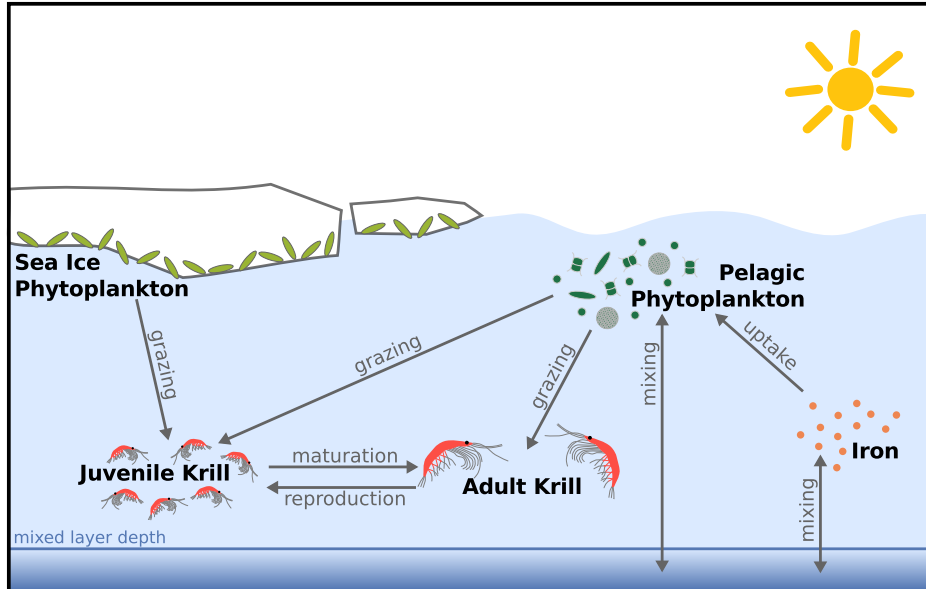


FIGURE 1.1.: Graphical summary of the model. Shown are the five state variables (juvenile krill, adult krill, pelagic phytoplankton, sea ice phytoplankton and iron), the environmental forcing (sea ice cover, light and mixed layer depth) and the processes coupling the state variables which are considered in the model. The mortality fluxes of phytoplankton and krill are not shown for better readability.

Krill undergoes many different developmental stages. For simplicity, this model combines these stages into two classes: juveniles and adults. The difference between the two classes is the ability to mature (juveniles) or reproduce (adults). It has to be mentioned here that in this model, the term “juveniles” combines all developmental stages that cannot reproduce including those stages which are called larvae in the literature – i.e. all the stages from Nauplius I to juveniles/subadults (Fraser, 1936; Jia et al., 2014).

The success of a krill population strongly depends on the food availability. Especially for juvenile krill, food conditions in winter are crucial for their survival (Daly, 1990; Meyer et al., 2002). Krill can feed on phytoplankton as well as small zooplankton such as copepods, but results from stomach analyses show that phytoplankton (diatoms and autotrophic flagellates) is the main food source (Schmidt et al., 2014). In the model, two different phytoplankton groups are considered as a food source for krill: pelagic phytoplankton and sea ice phytoplankton. These two groups don't necessarily have to differ in their species composition, but rather represent two distinct feeding habitats of krill.

The abundance of phytoplankton is strongly related to the seasonality of the environment

and it is therefore important to properly account for environmental effects on phytoplankton in the model. Particularly iron concentrations, light and sea ice conditions and water column stability are important drivers for the development of sufficiently large phytoplankton concentrations to support krill survival (Boyd, 2002; Taylor et al., 2013). Iron is reduced by the uptake of pelagic phytoplankton and thus needs to be explicitly modelled. In contrast to that are the light and sea ice conditions, which are not influenced by phytoplankton and krill. They only depend on the time and, in case of the light, on the latitude and thus can be included as a forcing function.

The model is a 0-dimensional model. All state variables are averaged over the upper mixed layer of the ocean which reaches from the surface to the mixed layer depth. As the name implies, the upper mixed layer is well mixed and it can thus be assumed that krill, phytoplankton and iron are homogeneously distributed. Light decreases exponentially with depth, which is important to consider when calculating the average phytoplankton concentration in the water column. Although krill is a well-studied organism, many details of krill somatic growth and metabolism are not sufficiently well known. Because of this uncertainty, this model is not length-, weight- or age-based as most other models but describes all processes in terms of krill density (krill m^{-3}) – which is also the unit commonly used in krill sampling (i.e. Siegel, 2000). Pelagic phytoplankton and iron concentrations are given in mg C m^{-3} and $\mu\text{mol m}^{-3}$ respectively. In contrast, sea ice phytoplankton densities are given in mg C m^{-2} , because the sea ice phytoplankton is only attached to the bottom of the sea ice and not distributed in the water column.

The five different state variables – iron, pelagic phytoplankton, sea ice phytoplankton, juvenile krill and adult krill – and the environmental forcing – light, sea ice and mixed layer depth – mentioned above are depicted in the conceptual diagram of the model in Figure 1.1. The arrows show how the state variables are coupled by the different processes grazing, mixing, uptake, maturation, reproduction and mortality (not shown), which will be explained in detail on the following pages.

1.2.1. FORCING

1.2.1.1. Sea Ice

Sea ice plays an important role in the life cycle of krill as a major feeding habitat and shelter for juvenile krill (Daly and Macaulay, 1991; Meyer et al., 2009; Flores et al., 2012b). To keep the model conceptual, only the first one of these two aspects is considered – the importance as a feeding habitat – and thus only the sea ice concentration and not its structure is considered in this model.

Sea ice concentrations have been obtained from Nimbus-7 SMMR and DMSP SSM/I-SSMIS Passive Microwave Data of the Atlantic Sector of the Southern Ocean (65 °W to 5 °E, 53 to 65 °S) using the NASA Team algorithm developed by the Oceans and Ice Branch, Laboratory for Hydrospheric Processes at NASA Goddard Space Flight Center (GSFC) for the years 2005 to 2012 (M. Sumner, personal communication, Oct. 2014). To calculate the percentage

of the area covered by sea ice from this data, the number of pixels with an ice cover greater than or equal to 15% was divided by the total number of pixels. A forcing function f_{ice} for the ice cover of each day of the year was obtained by averaging this time series for each day of the year and approximating it by a Fourier series (Figure 1.2 and Appendix A.1).

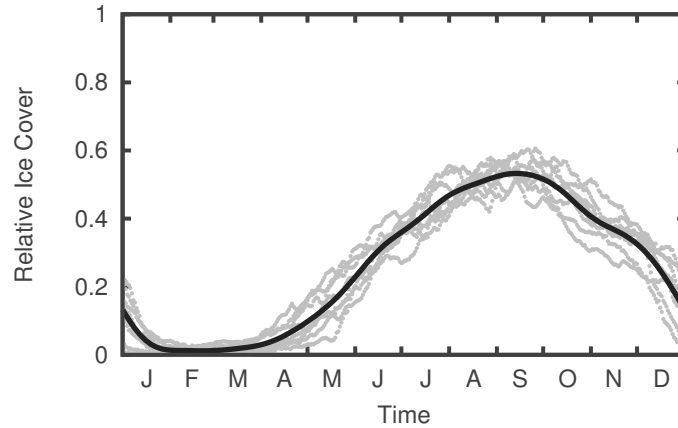


FIGURE 1.2.: Temporal dynamics of the relative ice cover over the course of one year. The data for the years 2005 to 2012 within the area 65 °W to 5 °E, 53 to 65 °S (M. Summer, pers. comm., Oct. 2014) are plotted as light grey points. The dark grey line shows the function $f_{ice}(t)$ used as forcing for the model.

1.2.1.2. Light

Phytoplankton are phototrophic organisms and thus depend on the availability of light for growth. Light intensity naturally varies over the course of a year, but especially at lower latitudes the length of the day (i.e. the number of hours of daylight) plays an important role as well. In summer, phytoplankton experiences very long days with up to 24 h of daylight, while in winter – depending on the latitude – there might be only a few hours of daylight or even none at all. In contrast to the sea ice concentration and mixed layer depth, the light forcing is not obtained from data but by first calculating the astronomical irradiance and from that estimating the light intensity that reaches the sea surface. The detailed calculations of the astronomical irradiance can be found in Appendix A.2. The irradiance received from this calculation is the average daily irradiance I_{ast} at the top of the atmosphere, which only depends on the latitude and the day of the year.

Irradiance at the sea surface: On its way to the sea surface, the irradiance is influenced by several processes. In the Antarctic, three processes are especially important (Knox, 2006): (1) The low angle of the sun over the horizon over large parts of the year increases the surface reflection; (2) Increased storm activity reduces the surface reflection and increases the transmission of light in the water column; (3) Sea ice and especially snow cover considerably

reduce the amount of light reaching the sea surface. How much of the astronomical irradiance reaches the sea surface varies over the year, but due to a lack of data the first two processes and additional processes (e.g. cloud cover) are combined in a constant, dimensionless factor q_{loss} . Although most processes included in this constant are most pronounced in winter and the irradiance reaching the surface will most likely be overestimated during that time of the year, the effect on the outcome of the model will be negligible compared to the uncertainties in other process rates.

From the irradiance reaching the sea surface, only a certain fraction q_{PAR} can actually be used by the phytoplankton for photosynthesis – the photosynthetically active radiation (PAR). Because light-dependent growth parameters of phytoplankton are often given in $\mu\text{mol m}^{-2} \text{s}^{-1}$, a conversion factor q_{W2P} is applied to convert the irradiance from W m^{-2} to $\mu\text{mol m}^{-2} \text{s}^{-1}$. Multiplying the absolute astronomical irradiance with these three factors (q_{loss} , q_{PAR} and q_{W2P}) will give the irradiance at the sea surface when it is not covered by ice. Some part of the study area, however, is always covered by sea ice which considerably reduces the irradiance reaching the sea surface. Thus, the model also needs to account for the fact that sea ice attenuates a large fraction of the irradiance. Since the model only contains the sea ice coverage and not the thickness and the snow cover, it is assumed that a fixed percentage κ of the irradiance is lost on its way through the sea ice. This leads to the following equation for the irradiance at the sea surface I_{net} (Figure 1.3, left):

$$I_{\text{net}} = q_{\text{PAR}} \cdot q_{\text{loss}} \cdot q_{\text{W2P}} \cdot (1 - f_{\text{ice}} \cdot \kappa) \cdot I_{\text{ast}}. \quad (1.1)$$

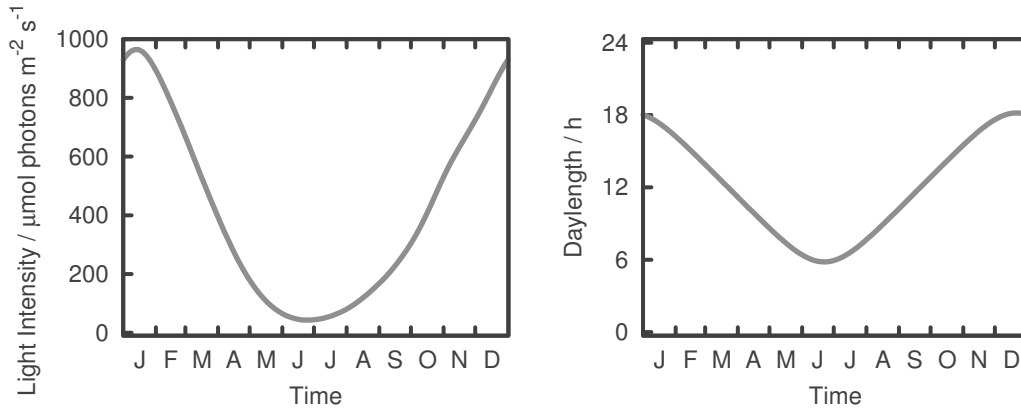


FIGURE 1.3.: Temporal dynamics of the daily averaged light intensity at the sea surface (left) and the daylength (right) over the course of one year for 59°S.

Irradiance in the water column: The irradiance in the water column decreases exponentially with the depth z and depends on the attenuation coefficient σ :

$$I(z) = I_{\text{net}} \cdot e^{-\sigma z}. \quad (1.2)$$

The attenuation depends on the absorption by suspended organic and inorganic particles. The absorption by inorganic particles can be neglected due to relatively low terrestrial influence in the Southern Ocean. Organic particles such as phytoplankton, however, absorb certain wavelengths. The constant σ in this model might therefore overestimate the light in the water column when phytoplankton concentrations are high.

Daylength: In higher latitudes, the daylength (or more precisely: length of the photoperiod) shows strong variations over the course of a year (Figure 1.3, right), which has a strong influence on primary production. The daylength b as a fraction of the total day can be calculated from the times of sunrise and sunset (see Appendix A.2).

1.2.1.3. Mixed Layer Depth

The depth of the mixed layer marks the lower boundary of the water column considered in this model and plays an important role in governing the average light intensity and the nutrient concentrations experienced by the pelagic phytoplankton (Sakshaug and Slagstad, 1991). Taylor et al. (2013) suggest that the shallowing of the mixed layer in spring is important for the development of a phytoplankton bloom and that the deepening of the mixed layer in autumn/winter leads to a break up of the bloom.

Monthly data for the mixed layer depth D (C. Voelker, personal communication, Nov. 2013) were approximated by the following function (Figure 1.4):

$$D = 81.36 - 27.66 \cdot \cos\left(\frac{2\pi t}{365}\right) - 23.18 \cdot \sin\left(\frac{2\pi t}{365}\right). \quad (1.3)$$

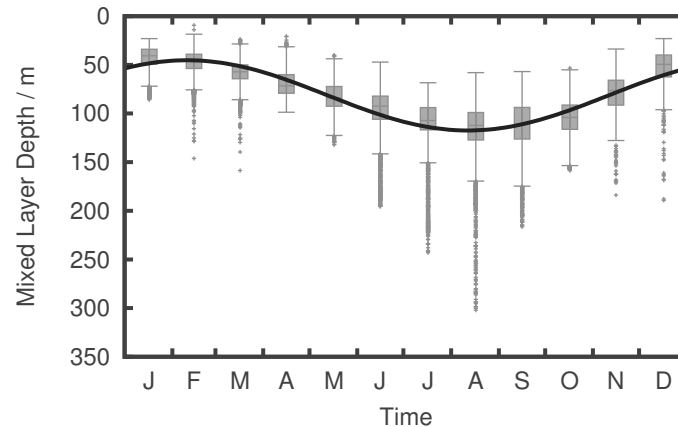


FIGURE 1.4.: Temporal dynamics of the mixed layer depth over the course of one year. The data for the area 65°W to 5°E, 53 to 65°S (C. Voelker, pers. comm., Nov. 2013) are shown as a box-whisker plot. The black line shows the function $D(t)$ used as forcing for the model.

1.2.2. NUTRIENT

Large areas of the Southern Ocean are so called HNLC (high nutrient - low chlorophyll) areas. In these areas, macronutrients such as nitrate and phosphate are usually not limiting phytoplankton growth. Instead, the micronutrient iron was shown to be responsible for the low primary production (Martin, 1990, 1991). For this reason, only the dynamics of the iron concentrations N are considered in this model.

The iron dynamics in the model are driven by two processes: iron uptake by pelagic phytoplankton and input of iron to the surface waters:

$$\dot{N} = \underbrace{-q_R \cdot \mu_P \cdot \min(e_{PN}, e_{PI}) \cdot P}_{\text{Uptake by Pelagic Phytoplankton}} + \underbrace{\frac{m_r + h^+}{D} \cdot (N_{\text{deep}} - N)}_{\text{Input into the Mixed Layer}}$$

Uptake by Pelagic Phytoplankton: The amount of iron taken up by pelagic phytoplankton depends on the Redfield-Ratio q_R and the growth rate of the pelagic phytoplankton. The Redfield-Ratio describes the stoichiometric ratio of elements in phytoplankton. Originally found by Redfield (1934) for carbon, nitrogen and phosphate, this ratio has been extended to other elements including iron (de Baar, 1994). The parameter q_R therefore describes how many μmol of iron are taken up per mg of carbon by phytoplankton growth:

$$\begin{aligned} \text{uptake by phytoplankton} &= -q_R \cdot \text{growth} \\ &= -q_R \cdot \mu_P \cdot \min(e_{PN}, e_{PI}) \cdot P. \end{aligned} \quad (1.4)$$

The growth of the pelagic phytoplankton will be explained in detail in Section 1.2.3.

Input into the Mixed Layer: Iron input into the mixed layer can be attributed mainly to four sources: (1) vertical input from below the mixed layer; (2) horizontal input from the sediment at continental margins; (3) atmospheric input and (4) input from melting icebergs (Löscher et al., 1997). The Antarctic ocean is known to receive very little dust input and input from icebergs are too small and localized to sustain the iron concentration in the surface waters (Tagliabue et al., 2014). Horizontal input might play a role in coastal areas. However, the major source of iron to surface waters is vertical input from below the mixed layer by upwelling and mixing (de Baar et al., 1995; Löscher et al., 1997; Klunder et al., 2011). This process is modelled similarly to the nitrogen and iron input in a model by Weber et al. (2005). Two processes determine the rate of input: mixing at the bottom of the mixed layer D with the mixing rate m_r and entrainment of water during mixed layer deepening:

$$\text{input to surface waters} = \frac{m_r + h^+}{D} \cdot (N_{\text{deep}} - N), \quad (1.5)$$

where N_{deep} is the iron concentration below the mixed layer and the deepening rate h^+ is defined as:

$$h^+ = \max\left(\frac{dD}{dt}, 0\right). \quad (1.6)$$

1.2.3. PELAGIC PHYTOPLANKTON

It has been intensely discussed, which environmental factors influence the primary production in the Southern Ocean (e.g. El-Sayed, 1988; Löscher et al., 1997; Arrigo et al., 1998; Boyd, 2002). Of the possible factors, light conditions and iron supply as bottom-up processes and predation by zooplankton as a top-down process are considered to be the most important ones. In the model, the dynamics of the pelagic phytoplankton concentration P are therefore determined by light- and nutrient-dependent growth and loss through predation. In addition, phytoplankton is lost from the mixed layer through mixing processes and through natural mortality.

$$\dot{P} = \underbrace{\mu_P \cdot \min(e_{PN}, e_{PI}) \cdot P}_{\text{Growth}} - \underbrace{\frac{m_r + h^+}{D} \cdot P}_{\text{Loss from the Mixed Layer}} - \underbrace{m_P \cdot P^2}_{\text{Mortality}} - \underbrace{\eta_J \cdot \frac{P}{H_J + P + \frac{S}{D}} \cdot J - \eta_A \cdot \frac{P}{H_A + P} \cdot A}_{\text{Predation}}$$

Growth: The growth of pelagic phytoplankton depends on the availability of light and the micronutrient iron. How to model co-limitation of resources is in general not trivial. Saito et al. (2008) have discussed this topic for several types of resources and came to the conclusion that iron and light co-limitation is especially difficult. The most commonly used form of co-limitation is Liebig's law of the minimum, which assumes that growth is only limited by the resource available at the lowest concentrations. In terms of this model, this means that the growth of the pelagic phytoplankton is either limited by a light-dependent growth factor e_{PI} or a nutrient-dependent growth factor e_{PN} :

$$\text{growth} = \mu_P \cdot \min(e_{PN}, e_{PI}) \cdot P \quad (1.7)$$

The dimensionless nutrient-dependent growth factor is modelled using a Monod function:

$$e_{PN} = \frac{N}{H_{PN} + N}, \quad (1.8)$$

where H_{PN} is the half-saturation constant and N the nutrient (iron) concentration. Since the nutrient concentration is assumed to be homogeneous in the mixed layer, an integration over depth is neglected.

Gilstad and Sakshaug (1990) have shown for ten arctic diatom species that daylength has a significant impact on the growth rates especially at moderate to high light intensities. Since the light environment in the Arctic and Antarctic are comparable, it can be assumed that this will be similar for Antarctic phytoplankton species. It is therefore necessary to not only average over the depth of the mixed layer D but also over the length of the day b to obtain

the light-dependent growth factor e_{PI} for each day (Ebenhöh et al., 1997):

$$e_{PI} = \frac{1}{b} \int_{\text{photoperiod}} \frac{1}{D} \int_{\text{depth}} p(I(\text{time of day, depth}))$$

$$\approx \frac{b}{6\sigma D} \cdot \left[\ln \left(\frac{H_{PI} + I_n}{H_{PI} + I_n e^{-\sigma D}} \right) + 4 \cdot \ln \left(\frac{H_{PI} + I_a}{H_{PI} + I_a e^{-\sigma D}} \right) \right]. \quad (1.9)$$

For simplicity, the integral has been approximated using Simpson's rule. Consequently, e_{PI} depends only on the noon irradiance I_n and the afternoon I_a irradiance – the irradiance at the temporal midpoint between noon and sunset. These are defined according to Ebenhöh et al. (1997) as:

$$I_n = I_{\text{net}} \cdot 1.7596 \quad (1.10)$$

$$I_a = I_{\text{net}} \cdot 1.0620.$$

The dimensionless growth factor is calculated using a Monod-type productivity-irradiance function $p(I)$:

$$p(I) = p_0 \frac{I}{H_{PI} + I}, \quad (1.11)$$

where H_{PI} is the light-dependent half-saturation constant for phytoplankton growth and p_0 the maximum productivity. It is not necessary to choose a function that does allow for photoinhibition, because persistent cloud cover over open ocean areas of the Southern Ocean sufficiently reduces the irradiance so that photoinhibition is rare (Sakshaug and Slagstad, 1991; Knox, 2006). A detailed calculation of e_{PI} can be found in Appendix A.3.

Predation: It is assumed that juvenile and adult krill both feed on pelagic phytoplankton according to a Holling Type II functional response with a half-saturation constant H_x (where x is either J or A) and the maximum food uptake rate η_x :

$$\begin{aligned} \text{predation} &= -\text{feeding by juvenile krill} - \text{feeding by adult krill} \\ &= -\eta_J \cdot \frac{P}{H_J + P + \frac{S}{D}} \cdot J - \eta_A \cdot \frac{P}{H_A + P} \cdot A. \end{aligned} \quad (1.12)$$

These feeding terms of juvenile and adult krill will be described in detail in Section 1.2.5 and Section 1.2.6.

Loss from the mixed layer: Pelagic phytoplankton concentrations in the mixed layer are strongly influenced by the mixed layer depth. Mixing at the bottom of the mixed layer with the rate m_r and entrainment of water during mixed layer deepening both lead to an input of water from below the mixed layer. In the Southern Ocean, the euphotic zone is often confined to the mixed layer (Sunda and Huntsman, 1997) and the water below the mixed layer depth is therefore free of pelagic phytoplankton cells. Mixing processes and entrainment of water effectively dilute the phytoplankton concentration in the mixed layer leading to a loss of pelagic phytoplankton from the model domain:

$$\text{loss from the mixed layer} = -\frac{m_r + h^+}{D} \cdot P. \quad (1.13)$$

Mortality: Mortality of pelagic phytoplankton includes all processes that lead to the death of a phytoplankton cell, which are not included in this model. Examples for such processes are lysis of phytoplankton cells, competition with other phytoplankton species and predation by species other than krill. The mortality is modelled using a quadratic mortality with the mortality rate m_P :

$$\text{mortality} = -m_P \cdot P^2. \quad (1.14)$$

1.2.4. SEA ICE PHYTOPLANKTON

Although sea ice phytoplankton contributes only little to the total primary production in the Southern Ocean, it is often the most important food source in ice covered waters (Arrigo and Thomas, 2004). The important processes for the modelling of sea ice phytoplankton densities S are growth, natural mortality and loss through predation by juvenile krill.

$$\dot{S} = \underbrace{f_{\text{ice}} \cdot \mu_S \cdot e_{\text{SI}} \cdot S}_{\text{Growth}} - \underbrace{m_S \cdot S^2}_{\text{Mortality}} - \underbrace{\eta_J \cdot \frac{\frac{S}{D}}{H_J + P + \frac{S}{D}} \cdot J \cdot D}_{\text{Predation}}$$

Growth: Micronutrients (such as iron) are usually available in high concentrations in sea ice (Arrigo, 2014). Although limitation by macronutrients in sea ice is occasionally possible, their concentrations in sea ice are often higher than in the water column (Arrigo and Thomas, 2004; Arrigo, 2014) and are thus not limiting sea ice phytoplankton growth. In contrast to the nutrients, light intensities are very low in winter and thus light is considered to be the most important factor limiting sea ice phytoplankton growth (Cota et al., 1991; Cota and Smith, 1991). The light-dependent growth factor is modelled similar to the one for pelagic phytoplankton except that it is only averaged over the photoperiod and not the depth since no depth profile of the sea ice is considered in this model. In this model, neglecting photoinhibition is reasonable for sea ice phytoplankton, because light intensities in ice covered water are not that high that they inhibit growth. Since the majority of the sea ice community grows in the bottom 20 cm of the ice (Arrigo and Thomas, 2004), it is reasonable to use the light intensity at the sea surface (i.e. at the bottom of the sea ice) to calculate the growth factor e_{SI} for each day:

$$e_{\text{SI}} = \frac{1}{b} \int_{\text{photoperiod}} p(I(\text{time of day})) \approx \frac{b}{6} \cdot \left[\frac{I_n}{H_{\text{SI}} + I_n} + 4 \cdot \frac{I_a}{H_{\text{SI}} + I_a} \right]. \quad (1.15)$$

Analogous to Equation 1.9, the integral was approximated using Simpson's rule (see Appendix A.3 for details).

Because sea ice phytoplankton can only grow when there is sea ice available, the ice forcing factor f_{ice} has to be included in the growth equation together with the maximum growth rate μ_S :

$$\text{growth} = f_{ice} \cdot \mu_S \cdot e_{SI} \cdot S. \quad (1.16)$$

Predation: In contrast to the pelagic phytoplankton, the sea ice phytoplankton is only eaten by the juvenile krill. The predation is assumed to be a Holling Type II functional response with a maximum food uptake rate η_J and a half-saturation constant H_J .

$$\begin{aligned} \text{predation} &= -\text{feeding by juvenile krill} \\ &= -\eta_J \cdot \frac{\frac{S}{D}}{H_J + P + \frac{S}{D}} \cdot J \cdot D. \end{aligned} \quad (1.17)$$

A detailed description of this process can be found in Section 1.2.5.

Mortality: The mortality of sea ice phytoplankton is modelled in the same way as the pelagic phytoplankton mortality by using a quadratic mortality with the mortality rate m_S :

$$\text{mortality} = -m_S \cdot S^2. \quad (1.18)$$

The mortality rate m_S includes all processes that lead to the death of a phytoplankton cell which are not directly included in this model, such as lysis of phytoplankton cells, competition with other phytoplankton species, predation by species other than krill and sinking of sea ice phytoplankton cells out of the mixed layer when the sea ice melts.

1.2.5. JUVENILE KRILL

The dynamics of the juvenile krill density J are governed by two main processes: reproduction and maturation. In addition, a natural mortality is added to the equation to account for different processes leading to the death of juvenile krill.

$$\dot{J} = \underbrace{q_{\text{rep}0} \cdot \frac{P}{H_A + P} \cdot A}_{\text{Reproduction}} - \underbrace{q_{\text{mat}} \cdot \frac{P + \frac{S}{D}}{H_J + P + \frac{S}{D}} \cdot J}_{\text{Maturation}} - \underbrace{m_J \cdot J}_{\text{Mortality}}$$

Since the maturation depends on the feeding of juvenile krill on pelagic and sea ice phytoplankton, the feeding equations are discussed below before discussing the maturation. In contrast, the reproduction term will be explained in the section on adult krill processes (Section 1.2.6), since this process depends on the abundance of adult krill.

Feeding: Juvenile krill are known to feed mostly on pelagic phytoplankton during times when it is abundant. In winter, however, phytoplankton concentrations in the water column are very low but the energy demand of juvenile krill is still high. Since they have very few lipid reserves, they need to feed on a food source other than the pelagic phytoplankton to survive the winter: the sea ice phytoplankton (e.g. Torres et al., 1994; Quetin et al., 1996; Meyer, 2012). The functional response of krill feeding on different food sources has rarely been measured and the results, especially the values of the obtained rates, differ greatly (Atkinson et al., 2012). The feeding of juvenile krill on both – pelagic and sea ice phytoplankton – is assumed to be proportional to a Holling Type II functional response that depends on the total amount of food available:

$$\text{feeding} \sim \frac{P + \frac{S}{D}}{H_j + P + \frac{S}{D}} \cdot J, \quad (1.19)$$

where H_j is the half-saturation constant and $P + \frac{S}{D}$ is the total concentration of food available for juvenile krill. The division of S by the mixed layer depth D is necessary because the pelagic phytoplankton (given in $\mu\text{mol m}^{-3}$) is distributed in the water column and the sea ice phytoplankton (given in $\mu\text{mol m}^{-2}$) occurs at the bottom of the sea ice.

Maturation: Juvenile krill grow and mature to become adults. This process usually takes 2-3 years depending on the sex (Siegel and Loeb, 1994) and strongly depends on the amount of food that juvenile krill can assimilate (Ross et al., 2000; Meyer et al., 2003). From the total amount of food taken up by juvenile krill, a certain amount is used for maturation:

$$\begin{aligned} \text{maturation} &= q_{\text{mat}} \cdot \text{feeding} \\ &= q_{\text{mat}} \cdot \frac{P + \frac{S}{D}}{H_j + P + \frac{S}{D}} \cdot J. \end{aligned} \quad (1.20)$$

If the maximum maturation rate q_{mat} is a constant, every day a certain fraction of the food taken up by juvenile krill would be invested into maturation. This strategy would probably lead to a collapse of the population, because krill would invest into maturation even if the amount of food available is not high enough to sustain its metabolism. Buchholz (1991) suggests that juvenile krill can prolong their development until the food conditions are more suitable. This strategy is modelled by using a Naka-Rushton equation (i.e. a Holling-type function with exponent n):

$$q_{\text{mat}} = q_{\text{mat}0} \cdot \frac{\left(\frac{P + \frac{S}{D}}{J}\right)^n}{\left(\frac{P + \frac{S}{D}}{J}\right)^n + F_{\text{crit}}^n}. \quad (1.21)$$

In this equation, $q_{\text{mat}0}$ is the maximum maturation rate and F_{crit}^n the critical amount of food per krill needed to reach half of the maximum maturation rate. Especially important is that that this function does not depend on the absolute food concentration but on the ratio between this concentration and the juvenile krill density. High food concentrations can

thus lead to low maturation rates when the density of juvenile krill is very high at the same time. Figure 1.5 shows the maturation function for different values of the exponent n . This exponent determines the slope of the function at F_{crit} , which can be understood as a measure for how good juvenile krill can mature under suboptimal food conditions. A low value of n allows for small maturation rates when there is little food available, while a large value of n leads to a very steep function that only allows for maturation when the amount of food available is close to the critical value.

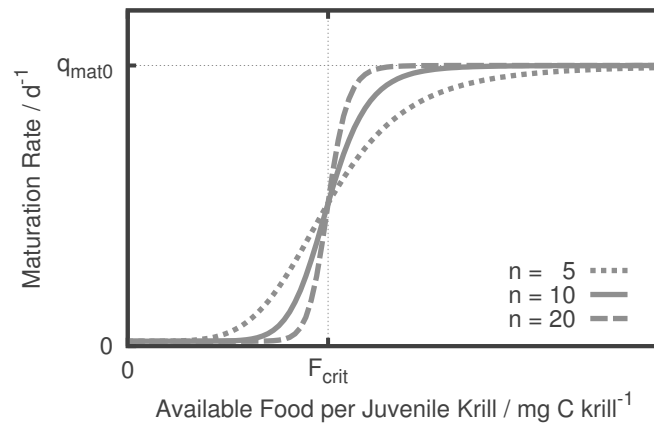


FIGURE 1.5.: Dependence of the maturation function q_{mat} on the food per juvenile krill for different values of the steepness of the maturation function n . The thick line marks the value used in the reference run ($n=10$), while the dashed line marks a higher value ($n=20$) and the dotted line marks a lower value ($n=5$).

Mortality: Mechanisms and magnitudes of krill mortality are rather poorly understood (Atkinson et al., 2012). Since so little is known, the mortality is modelled as a simple linear process:

$$\text{mortality} = -m_J \cdot J. \quad (1.22)$$

The mortality rate m_J is thought to include all processes that add to a loss of krill from the system including natural death, predation by higher trophic levels, harvesting of krill by the fishery and advective transport to other regions.

1.2.6. ADULT KRILL

The dynamics of the adult krill density A are governed by two processes: maturation and mortality.

$$\dot{A} = \underbrace{q_{\text{mat}} \cdot \frac{P + \frac{S}{D}}{H_J + P + \frac{S}{D}} \cdot J}_{\text{Maturation}} - \underbrace{m_A \cdot A}_{\text{Mortality}}$$

Reproduction does not lead to a loss of adult individuals and thus does not show up in the differential equation for adult krill. Since the reproduction depends on the feeding of adult krill on pelagic phytoplankton, the feeding functions are discussed first before discussing the reproduction. As maturation is the growth of juvenile krill to become adults, this processes has been described in Section 1.2.5.

Feeding: In contrast to juvenile krill, adult krill can survive the winter with very little feeding. They have adopted different strategies to survive the winter among which the reduction of their metabolism is the most widely agreed on (Quetin and Ross, 1991; Meyer, 2012). Several studies have shown, that adult krill seem to overwinter in deeper layers of the water column and are rarely attached to the sea ice (Quetin and Ross, 1991; Quetin et al., 1996; Meyer, 2012; Schaafsma et al., 2016). Thus, adult krill do not feed on sea ice phytoplankton in this model but only on pelagic phytoplankton:

$$\text{feeding} \sim \frac{P}{H_A + P} \cdot A. \quad (1.23)$$

In this equation, H_A is the half-saturation rate for feeding on pelagic phytoplankton. Nicol (2006) has suggested that the juvenile and adult krill stages are geographically separated during most of the year, which means that competition for food between juvenile and adult krill does not need to be considered.

Reproduction: Reproduction is strongly influenced by food availability (Quetin et al., 1996). From the total food taken up by adult krill, a fraction is used for reproduction:

$$\begin{aligned} \text{reproduction} &= q_{\text{rep}0} \cdot \text{feeding} \\ &= q_{\text{rep}0} \cdot \frac{P}{H_A + P} \cdot A. \end{aligned} \quad (1.24)$$

In this equation, the reproduction rate $q_{\text{rep}0}$ is constant over the year. In nature, adult krill most likely reduce their investment into reproduction when food is scarce. In the model, pelagic phytoplankton concentrations are very low in winter and reproduction at that time of the year is therefore so small that a constant reproduction rate gives reasonable results.

Mortality: As for juveniles, little is known about mechanisms and magnitude of adult krill mortality. Thus, it is modelled as a linear process:

$$\text{mortality} = -m_A \cdot A, \quad (1.25)$$

where the mortality rate m_A includes all processes leading to a loss of adult krill from the system such as natural death, predation by higher trophic levels, harvesting by the fishery and advective transport to other regions.

1.2.7. IMPLEMENTATION

The model was implemented in CEMoS (C Environment for Model Simulation, Hamberg (1996)). The differential equations are solved using a classical 4th order Runge-Kutta method with time step adaptation and a maximum time step of one day. The forcing is not included in this integration routine but is calculated separately at the beginning of each day and assumed to be constant over the whole day. This approach is sufficiently accurate for the model output and saves computational time, but it is problematic when using a Runge-Kutta integration scheme, because it introduces step functions in the differential equations. The Runge-Kutta method, however, can only be used for differential equations with continuously differentiable terms. This problem is avoided in CEMoS by restarting the integration routine for every day, i.e. at the time points at which the discontinuous steps occur. That way, it is possible to include daily-averaged forcing or data without running into problems with the numerics.

All simulations were initialized with the following values: $N_0=1.3 \mu\text{mol m}^{-3}$, $P_0=50 \text{ mg C m}^{-3}$, $S_0=1.0 \text{ mg C m}^{-2}$, $J_0=0.005 \text{ krill m}^{-3}$ and $A_0=0.01 \text{ krill m}^{-3}$. All results shown are from the steady-state phase of the model, which is typically reached after running the simulation for five to ten years.

1.2.8. PARAMETRIZATION

Parametrization of a model with a relatively high number of parameters is always difficult. Most parameter values have been chosen using values taken from the literature. However, for some parameters no literature values exist or their ranges span over multiple orders of magnitude. Table 1.1 lists all parameters, their units and their respective value used in the reference run. If available, a range of literature values is given depicting the lowest and highest values found in the respective literature.

Forcing: Abiotic parameters are often easier to measure than biotic ones and thus the ranges of values found in the literature are smaller for the forcing parameters. One forcing parameter that stands out is the loss factor q_{loss} , which describes how much of the atmospheric irradiance reaches the sea surface. A value larger than one implies that the irradiance reaching the sea surface is higher than the atmospheric irradiance. Locally, increased reflection from the ice during sunny weather conditions could lead to such high values (Moline and Prézelin, 1997). On a larger spatial scale, however, the irradiance reaching the sea surface will be much

lower than the atmospheric irradiance. A persistent cloud cover during winter also suggests a large loss of irradiance on a larger temporal scale. A moderate value of q_{loss} is thus the best choice for an annual and spatial average.

Nutrient: The values found in the literature for the Redfield parameter q_R correspond to an extended Redfield Ratio of approximately C:Fe 106:(0.0003 - 0.1). The value of the reference run corresponds to a ratio of C:Fe 106:0.001 and thus lies on the lower end of that range. To get a visible depletion of iron during summer, the mixing rate m_r was also chosen to be relatively low to prevent instantaneous renewal of iron in the mixed layer.

Phytoplankton: Although the ranges for the half-saturation constants for light of pelagic and sea ice phytoplankton (H_{PI}, H_{SI}) overlap, the chosen parameter value has to be smaller for sea ice phytoplankton than for pelagic phytoplankton. In winter, the irradiance reaching the ocean surface is very low. For sea ice phytoplankton to be able to grow it needs to be more shade-adapted than pelagic phytoplankton. In contrast, the mortality rate (m_P, m_S) was chosen to be larger for sea ice phytoplankton to be able to account for their high mortality rates when the sea ice melts.

Krill: Krill population parameters are especially difficult to measure due to the remoteness of their habitat and the difficulty in culturing them in an aquarium. Krill half-saturation constants (H_J, H_A) found in the literature usually correlate growth in size or weight to the food concentration. In this model, however, the half-saturation constant relates the food concentration to the maturation and reproduction. Both – the growth-based and uptake-based – half-saturation rates don't have to be the same, but it is reasonable to assume that they are similar. An additional uncertainty is added because the values for the half-saturation constants as well as the maximum food uptake rate of adult krill (η_A) were converted from chl *a*-based to carbon-based units. The problem with this conversion is, that the ratio between chl *a* and carbon varies between phytoplankton species and between different times of the year. For the mentioned calculations, a constant chl *a* : C ratio of 1 : 50 (Atkinson et al., 2002) was used.

Values for krill mortality are poorly known and thus the values differ greatly (Atkinson et al., 2012). From the values in Table 1.1 the mortality rate seems to be the same for juvenile and adult krill. However, it is known that the mortality of juvenile krill is higher than for adult krill, because juvenile krill don't have the ability to survive long periods of starvation (Pakhomov, 1995).

Juvenile krill mature in their third or fourth year depending on the sex (Siegel and Loeb, 1994). Converting this time to a daily rate provides an estimate for the maximum maturation rate (q_{mat0}). The parameter n defines the slope of the maturation function and is a purely artificial parameter. A moderate value – as was chosen for the reference run – means that some krill can mature under suboptimal food conditions with the trade-off that the food conditions need to be very good to reach the maximum maturation rate. The feeding conditions where half of the maximum maturation rate is reached are determined by F_{crit} . This

value can be estimated from the minimum amount of food that juvenile krill need every day to maintain their metabolism. Holm-Hansen and Huntley (1984) calculated this maintenance carbon concentration to be between 72 to 208 mg C m⁻³ depending on the developmental stage. Considering that this value does not include costs for development, the value of F_{crit} has to be higher to include the maturation costs.

To estimate the maximum reproduction rate of the adult krill q_{rep0} the fecundity of a population needs to be taken into account as well as the proportion of the food that is allocated to reproduction. The fecundity of a population depends on the abundance of reproducing females, how often they spawn per season and how many eggs they release per spawning event (Everson, 2000). The number of spawning events and eggs released per event is highly variable. Ross and Quetin (1983), for example, estimated that a female krill releases on average 500 to 8000 eggs per spawning event and spawns 9 to 10 times per season thus releasing a total number of 4500 to 80 000 eggs per year. Assuming that half the population is female, the percentage of the total population that reproduce can vary between 10% and almost 50% (Everson, 2000). From the total amount of food ingested, only 13.6% are invested into reproduction (Ross and Quetin, 1986). The maximum reproduction rate was estimated by combining these values.

TABLE 1.1.: Overview of the parameter values used in the reference run and the corresponding values found in the literature. The range of values marks the lowest and highest values found in the literature. The units of the literature values were converted to fit the units of the model.

Parameter	Meaning	Unit	Reference Run	Values found in the Literature
I_{solar}	mean solar irradiance	W m^{-2}	1360	1360 ¹
q_{PAR}	photosynthetically active fraction of the irradiance	–	0.42	0.42 ²
q_{w2P}	unit conversion factor	$\mu\text{mol W}^{-1} \text{s}^{-1}$	4.57	4.57 ³
q_{loss}	fraction of the irradiance that reaches the sea surface	–	0.5	0.28 – 1.4 ⁴
ϕ	latitude	°	59	
σ	attenuation of light in sea water	m^{-1}	0.11	0.05 – 0.66 ⁵
κ	attenuation of light in sea ice (fraction of total light)	–	0.9	>0.81 ⁶
m_{r}	mixing rate at the bottom of the mixed layer	m d^{-1}	0.15	0.13 – 0.26 ⁷
N_{deep}	iron concentration below the mixed layer	$\mu\text{mol m}^{-3}$	1.5	0.4 – 2.8 ⁸
q_{R}	Redfield-Ratio Fe:C	$\mu\text{mol mg}^{-1}$	0.00079	0.0002 – 0.08 ⁹
μ_{P}	maximum growth rate of pelagic phytoplankton	d^{-1}	0.7	0.08 – 0.71 ¹⁰
H_{PN}	half-saturation constant of pelagic phytoplankton for iron	$\mu\text{mol m}^{-3}$	0.25	0.0006 – 1.2 ¹¹

TABLE 1.1.: continued

Parameter	Meaning	Unit	Reference Run	Values found in the Literature
H_{PI}	half-saturation constant of pelagic phytoplankton for light	$\mu\text{mol m}^{-2} \text{s}^{-1}$	30	$27 - 57$ ¹²
m_P	mortality rate of pelagic phytoplankton	d^{-1}	0.0035	
μ_S	maximum growth rate of sea ice phytoplankton	d^{-1}	0.8	$0.01 - 0.8$ ¹³
H_{SI}	half-saturation constant of sea ice phytoplankton for light	$\mu\text{mol m}^{-2} \text{s}^{-1}$	8	12 ¹⁴
m_S	mortality rate of sea ice phytoplankton	d^{-1}	0.01	
η_J	maximum food uptake rate of juvenile krill	$\text{mg krill}^{-1} \text{d}^{-1}$	0.05	$0.02 - 0.033$ ¹⁵
H_J	half-saturation constant of juvenile krill for food uptake	mg m^{-3}	30	$5.5 - 38^\Delta$ ¹⁶
m_J	mortality rate of juvenile krill	d^{-1}	0.01	$0.001 - 0.01$ ¹⁷
F_{crit}	typical amount of food per krill needed for maturation	mg krill^{-1}	100	$>72 - 208$ ¹⁸
$q_{\text{mat}0}$	maximum maturation rate	d^{-1}	0.001	$0.0007 - 0.001^\Delta$ ¹⁹
n	steepness of the maturation function	-	10	
η_A	maximum food uptake rate of adult krill	$\text{mg krill}^{-1} \text{d}^{-1}$	0.25	$0.05 - 16.3^\Delta$ ²⁰
H_A	half-saturation constant of adult krill for food uptake	mg m^{-3}	200	$14.85 - 16^\Delta$ ²¹

TABLE 1.1.: continued

Parameter	Meaning	Unit	Reference Run	Values found in the Literature
m_A	mortality rate of adult krill	d^{-1}	0.001	0.001 – 0.01 ²²
q_{rep0}	maximum reproduction rate	d^{-1}	10	0.03 – 29.8 ^{Δ 23}

^Δ Converted to the units of the model using a C : chl *a* ratio of 50 : 1 (Atkinson et al., 2002)

¹ Kopp and Lean (2011) ² Thimijan and Heins (1983) ³ Thimijan and Heins (1983) ⁴ Moline and Prézelin (1997) ⁵ Fenton et al. (1994)
⁶ Palmisano et al. (1985, 1987a,b); McMinn et al. (1999) ⁷ de Baar et al. (1995); Löscher et al. (1997) ⁸ de Baar et al. (1995); Löscher et al. (1997)
⁹ Martin (1990); de Baar (1994); Lancelot et al. (2000); Holm-Hansen et al. (2004) ¹⁰ Sommer (1989); Sakshaug and Slagstad (1991); Coale et al. (2003)
¹¹ Lancelot et al. (2000); Timmermans et al. (2001); Coale et al. (2003); Taylor et al. (2013) ¹² Stambler (2003) ¹³ Palmisano et al. (1985); Cota and Smith (1991); Knox (2006) ¹⁴ Knox (2006) ¹⁵ Meyer et al. (2003) ¹⁶ Atkinson et al. (2006); Meyer et al. (2009) ¹⁷ Pakhomov (1995); Everson (2000) ¹⁸ Holm-Hansen and Huntley (1984) ¹⁹ Siegel and Loeb (1994) ²⁰ Ross and Quetin (1988); Nicol et al. (1995) ²¹ Atkinson et al. (2006)
²² Pakhomov (1995); Everson (2000) ²³ Ross and Quetin (1983, 1986); Nicol et al. (1995); Everson (2000); Tarling et al. (2007)

1.2.9. SENSITIVITY ANALYSIS

To determine the sensitivity of the model concerning the chosen parametrization, two different methods are used: the Morris method and Taylor and Target diagrams. The first method is a qualitative method to gain insight into the overall importance of a parameter on the model, while the second one graphically displays the influence of individual parameters on the annual dynamics.

1.2.9.1. Morris Screening Design

The Morris screening (Morris, 1991) is a method to determine the importance of parameters for certain model outputs. The advantage compared to other methods is that it takes relatively little computation time. Although this method can be classified as a “one-factor-at-a-time”-method (OAT), it has the advantage of a global sensitivity analysis, because for each parameter a large number of independent parameter sets is sampled from the whole parameter space. It is important to note here that the Morris method can only rank the parameters in order of importance and cannot give a quantitative sensitivity value. Nevertheless, it provides a good tool to identify the parameters which substantially influence the model output.

The method is based on the estimation of so-called elementary effects E_i for each parameter x_i :

$$E_i = \frac{y(x_1, \dots, x_{i-1}, x_i + \Delta, x_{i+1}, \dots, x_k) - y(x_1, \dots, x_k)}{\Delta}. \quad (1.26)$$

In this equation, $y(x_1, \dots, x_{i-1}, x_i + \Delta, x_{i+1}, \dots, x_k)$ and $y(x_1, \dots, x_k)$ are model outputs obtained from two parameter sets which only differ in the i -th parameter. Δ is the difference between two parameter values and can be calculated from the number of possible parameter values p . According to Morris, a convenient choice for this relationship is:

$$\Delta = \frac{p}{2(p-1)}. \quad (1.27)$$

For each of the k parameters, r elementary effects are calculated using the sampling design proposed by Morris (1991). With this sampling design, a number of $2rk$ model runs are needed. For a detailed description of the sampling routine see Morris (1991) or Saltelli et al. (2004).

Morris proposed to use the mean μ_i and the standard deviation σ_i of the distribution of the elementary effects as sensitivity measures:

$$\mu_i = \frac{1}{r} \sum_{k=1}^r E_i, \quad (1.28)$$

$$\sigma_i = \frac{1}{r} \sqrt{\sum_{k=1}^r (E_i - \mu_i)^2}. \quad (1.29)$$

The mean μ_i is a measure of overall influence on the model, while the standard deviation σ_i is a measure for the dependence of the parameter on other parameters or for nonlinear

effects of the parameter on the model. A small mean in combination with a small standard deviation thus implies that the parameter has only a small overall influence on the model output.

Campolongo et al. (2007) proposed a revised measure μ^* , which uses the absolute values of the elementary effects to avoid cancellation effects when the elementary effects of one parameter have different signs:

$$\mu_i^* = \frac{1}{r} \sum_{k=1}^r |E_i|. \quad (1.30)$$

For the sensitivity analysis of this model, $p = 4$ different levels in the $\pm 50\%$ -range around the reference value are sampled 500 times for each parameter. The elementary effects are calculated for the mean juvenile and adult krill density. To make the results comparable, the respective mean is normalized by dividing it by the respective mean of the reference run.

1.2.9.2. Taylor and Target Diagrams

Although the Morris screening is a good method to determine the overall influence of a parameter on the model output, one problem remains: it only determines the influence on one single model output and does not give any information about the influence on the annual dynamics of the model. To solve this problem, Taylor and Target diagrams provide a useful graphical method to assess the sensitivity of the entire dynamics (Taylor, 2001; Jolliff et al., 2009). While visual comparison of two model runs can be difficult in a time series diagram, the Taylor and Target diagrams make this comparison much easier.

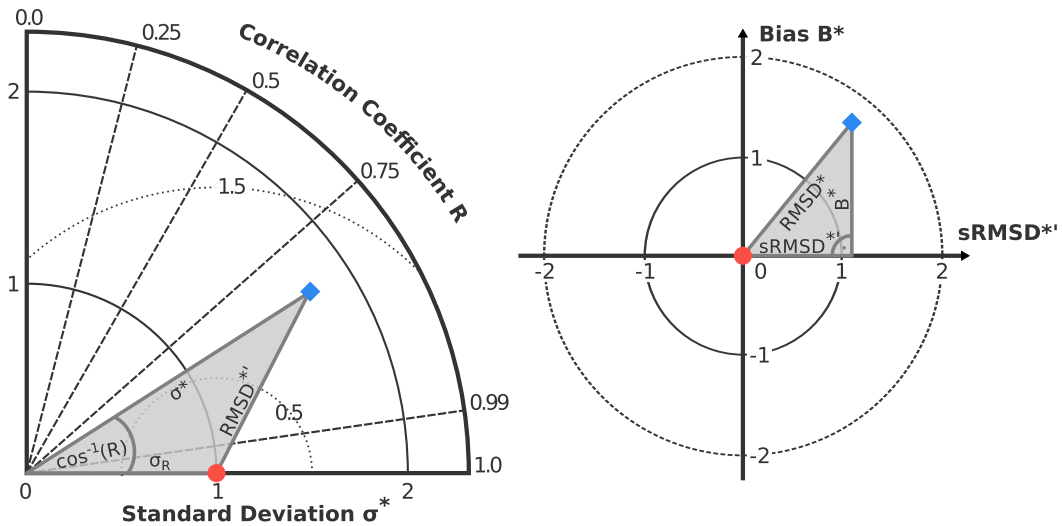


FIGURE 1.6.: Example of a Taylor diagram (left) and a Target diagram (right). The red dot marks the reference run and the blue diamond is an example of a model run. The grey triangles illustrate the relationships between the different statistical properties.

Taylor Diagrams: The Taylor diagram combines three statistical properties in a single point in a polar diagram: correlation, standard deviation and unbiased root-mean-square difference (Taylor, 2001). The correlation between two time series is defined as:

$$R = \frac{\frac{1}{N} \sum_{n=1}^N (m_n - \bar{m})(r_n - \bar{r})}{\sigma_m \sigma_r}, \quad (1.31)$$

where r is the reference run and m another model run, \bar{r} and \bar{m} are the mean values of the respective time series, σ_r and σ_m are the standard deviations and N is the length of the time series. For this model, n corresponds to the time t , because the model output is given in discrete time steps of one day. The correlation is a measure for the difference in phase compared to the reference run.

The second statistical property – the standard deviation σ – is a measure for the difference in amplitude which can be normalized to allow for easier comparison of different graphs:

$$\sigma^* = \frac{\sigma_m}{\sigma_r}. \quad (1.32)$$

The third property is the unbiased root-mean-square difference, which is a measure for the overall agreement between two time series:

$$\text{RMSD}' = \sqrt{\frac{1}{N} \sum_{n=1}^N [(m_n - \bar{m}) - (r_n - \bar{r})]^2}. \quad (1.33)$$

Because these three properties are related to each other by the following relationship

$$\text{RMSD}'^2 = \sigma_r^2 + \sigma_m^2 - 2\sigma_m \sigma_r R, \quad (1.34)$$

it is possible to combine them in one single point in a polar diagram using the law of cosines (Figure 1.6, left). The normalized, unbiased root-mean-square distance is then:

$$\text{RMSD}^{*'} = \sqrt{1 + \sigma^{*2} - 2\sigma^* R}. \quad (1.35)$$

Summarizing the above, the Taylor diagram is helpful to compare one or more model runs to a reference in terms of difference in phase (R) and amplitude (σ^*) and overall agreement of the dynamics ($\text{RMSD}^{*'}$) between the amplitude and phase.

Target Diagrams: While the information from the Taylor diagram already helps to understand the dynamics, it lacks information about the bias, i.e. the difference in mean between the model run and the reference. The Target diagram combines the normalized, unbiased root-mean-square difference and the normalized bias in one diagram and thus provides a useful addition to the Taylor diagram. The normalized, unbiased root-mean-square difference has already been described above (Equation 1.35); the normalized bias is defined as:

$$B^* = \frac{\bar{m} - \bar{r}}{\sigma_r}. \quad (1.36)$$

The Target diagram (Figure 1.6, right) can then be constructed using the following relationship between the normalized, unbiased root-mean-square difference ($\text{RMSD}^{*'}$), the normalized bias (B^*) and the normalized, total root-mean-square difference (RMSD^*):

$$\text{RMSD}^{*2} = B^{*2} + \text{RMSD}^{*'}^2. \quad (1.37)$$

By using the signed normalized, unbiased root-mean-square difference

$$\text{sRMSD}^{*'} = \text{RMSD}^{*'} \cdot \text{sign}(\sigma_m - \sigma_r), \quad (1.38)$$

the difference in standard deviation between the model run and the reference can be added to the plot.

In summary, the Target diagram provides information about the difference in mean between one or more model runs and a reference (B^*), the general agreement between the model runs and the reference ($\text{sRMSD}^{*'}$) and whether the standard deviation of a model run is smaller or larger than the standard deviation of the reference run (sign of the $\text{sRMSD}^{*'}$).

1.3. RESULTS

The results discussed in this section form the basis of the whole thesis. All results in later chapters will be compared to this so-called reference run. Unless otherwise stated, the results are from simulations using the reference parametrization stated in Table 1.1.

1.3.1. ANNUAL DYNAMICS

From a krill perspective, the year can be divided into two parts: the three months of the year when food concentrations are sufficiently high for maturation and reproduction and the other nine months when they are not (Figure 1.7).

The period of the year with very low food concentrations spans from Mid-March to the end of November (i.e. autumn, winter and early spring). Consequently, juvenile and adult krill densities are declining during this period. Pelagic phytoplankton concentrations are very low due to the low light intensities and short days. Sea ice phytoplankton is better adapted to these conditions and thus their densities start to increase in June even though the light intensity is at its minimum. Their maximum density of 17.7 mg C m^{-2} is reached at the beginning of October when the sea ice coverage is almost maximal and the light intensity is quite high for these low-light adapted species. Sea ice phytoplankton densities remain high until the beginning of December when the sea ice melts more rapidly.

From this description and Figure 1.7, it might not be obvious at first why there is not enough food available for juvenile krill to mature. It becomes clearer when remembering that krill can only feed on the sea ice phytoplankton at the bottom of the ice, i.e. it can only feed on a surface and not a volume. Projecting all the juvenile krill from the volume of the mixed layer onto this surface it becomes clear that there is by far not enough food available for juvenile krill to mature. Even the maximum amount of sea ice phytoplankton per juvenile krill of $1.85 \text{ mg C krill}^{-1}$ is well below the typical amount of food needed for maturation of $100 \text{ mg C krill}^{-1}$.

The period of the year with high food concentrations spans from December to Mid-March (i.e. late spring and summer). These months are characterized by low sea ice concentrations, high light intensities and long days with 14 to 18 h of light. Under these conditions, pelagic phytoplankton can grow well up to a maximum concentration of 61.7 mg C m^{-3} at the end of January. As a result of the strong pelagic phytoplankton growth, the nutrient concentrations decrease. They are replenished again shortly after the breakup of the phytoplankton bloom by mixed layer deepening. Fueled by the high food concentrations, adult krill starts to reproduce at the onset of the phytoplankton bloom in December. Due to the high reproduction rates, juvenile krill concentrations show a strong increase from the minimum of $123 \text{ krill } 1000 \text{ m}^{-3}$ at the end of November to a maximum of $1602 \text{ krill } 1000 \text{ m}^{-3}$ at the beginning of March. Shortly after the adult krill starts to reproduce, the juvenile krill also has enough food to mature which leads to an increase in adult krill until they reach the maximum of $15 \text{ krill } 1000 \text{ m}^{-3}$ in January.

Sampling in the Southern Ocean is both sparse and very infrequent. Combined with

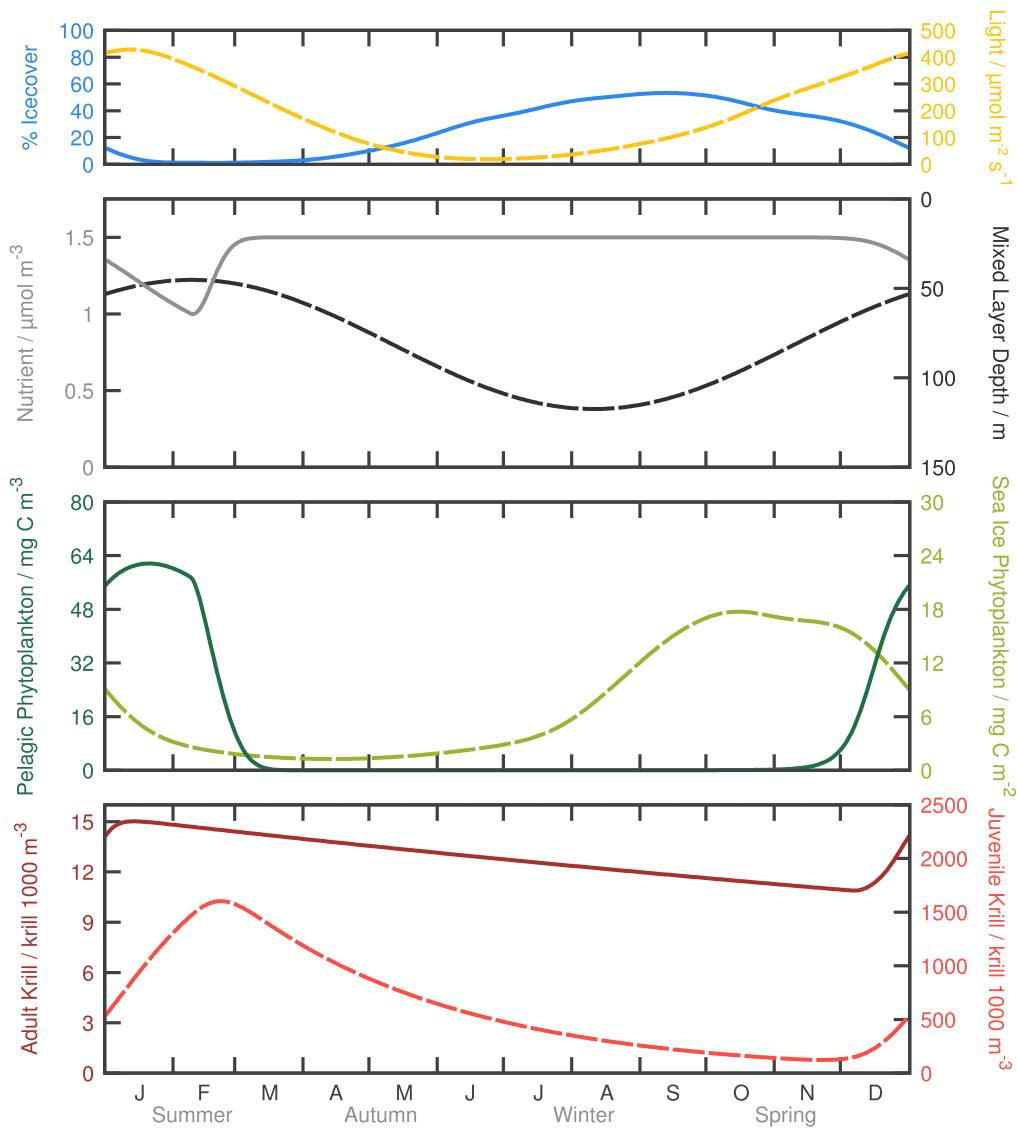


FIGURE 1.7.: Annual dynamics of the reference run. Shown are the results for the five state variables iron (second from top, solid line), pelagic phytoplankton (third from top, solid line), sea ice phytoplankton (third from top, dashed line), juvenile krill (bottom, dashed line) and adult krill (bottom, solid line). The three forcing functions light intensity (top, dashed line), sea ice coverage (top, solid line) and mixed layer depth (second from top, dashed line) are included for better interpretation of the results.

the strong spatial and temporal variability of the environment, empirical data are subject to a lot of variation. Nevertheless, empirical data show certain characteristics which are also reproduced by the model. High pelagic phytoplankton biomass coincides with the high light intensities in December and January and is very small during winter (Smith Jr

and Sakshaug, 1990). Although sea ice phytoplankton can grow with very little light, their primary production is highest in November when the sea ice coverage is still fairly high and the light intensities are increasing (Arrigo, 2014; Cota and Smith, 1991). According to the concept proposed by Siegel (2000), krill densities show a strong increase in November and a strong decrease in March. This general pattern is also reflected in the model as well as the large variability between the minimum and maximum densities described by Siegel.

Bottom-Up vs. Top-Down Control on Pelagic Phytoplankton: It is often debated whether phytoplankton in the Southern Ocean is top-down or bottom-up controlled. Figure 1.8 shows the annual mean fluxes of the four processes influencing pelagic phytoplankton in the model: growth, mixing, mortality as bottom-up processes and predation by juvenile and adult krill as top-down process. It is obvious that the growth process is the most important flux whereas the predation flux is by far the smallest. Although the distribution looks slightly different at specific times of the year, the predation flux is always the smallest one. This result agrees well with the observations by Miller et al. (1985) that only a small portion of the phytoplankton is consumed by krill. Within a krill swarm, this will not be true because “krill in large swarms are capable of sweeping the water clean” (Nicol, 2006). On a larger spatial scale, however, it is reasonable to assume that pelagic phytoplankton is bottom-up controlled.

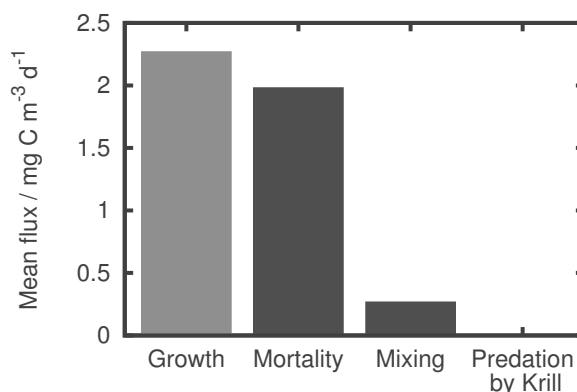


FIGURE 1.8.: Mean values of the fluxes describing pelagic phytoplankton. For the negative fluxes (dark grey), the absolute values are plotted for better comparison with the positive flux (light grey).

Light vs. Iron Limitation of Pelagic Phytoplankton: Having shown in the previous paragraph that pelagic phytoplankton is bottom-up controlled, the question is whether light or iron is the limiting factor. In the model, the pelagic phytoplankton is always limited by light and never by iron (Figure 1.9). This contradicts the common believe that the primary production in the Southern Ocean is mostly iron limited. However, several studies have also suggested that light might be the most important environmental factor for primary production in the Southern Ocean (Arrigo et al., 1998; Taylor et al., 2013; Arteaga et al., 2014).

In addition, krill densities in the most likely iron-limited HNLC areas are low (Atkinson et al., 2008) suggesting perhaps that krill is predominantly distributed in areas where limitation by light (or other environmental factors) is stronger than by iron.

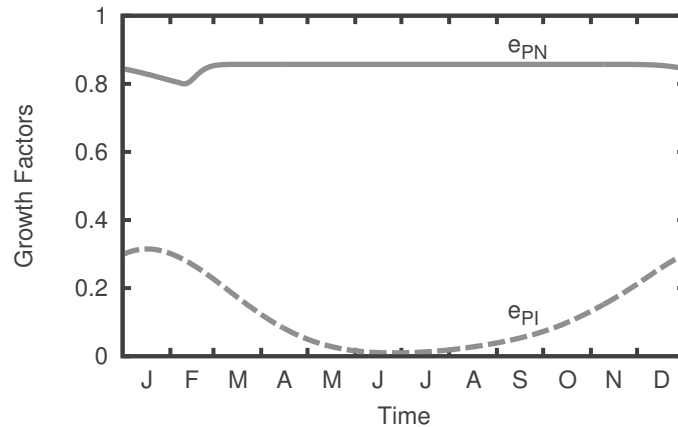


FIGURE 1.9.: Factors limiting pelagic phytoplankton growth. Shown are the annual dynamics of the nutrient-dependent limitation factor (solid line) and the light-dependent limitation factor (dashed line).

Bottom-Up vs. Top-Down Control on Sea Ice Phytoplankton: Similar to pelagic phytoplankton, sea ice phytoplankton is also bottom-up controlled (not shown). From the three fluxes influencing sea ice phytoplankton – growth, mortality and feeding by juvenile krill – the feeding flux is by far the smallest. Again, this is realistic only on a larger spatial scale. When a swarm of krill finds a patch with a high sea ice phytoplankton density, most of the phytoplankton will be consumed quickly.

Timing and Duration of Reproduction: Reproduction of Antarctic krill requires a high amount of energy and thus is only possible under good feeding conditions (Ross and Quetin, 1986; Quetin and Ross, 1991; Nicol et al., 1995; Quetin and Ross, 2001). Depending on the food conditions and the geographical location, the reproductive season can span from December to March (Ross and Quetin, 1986; Quetin and Ross, 1991; Siegel, 2005). As can be seen in Figure 1.10 (top), both the timing and duration are reproduced by the model with maximum reproduction coinciding with the times of maximum phytoplankton concentrations in January. In winter, there is no reproduction due to the very low phytoplankton concentrations. This is in good agreement with observations of sexual regression to an immature stage occurring in autumn and winter (Quetin and Ross, 2001; Kawaguchi et al., 2007).

Considering that the reproduction in the model is directly coupled to the feeding of adult krill on pelagic phytoplankton, the close agreement between the reproduction and pelagic phytoplankton is not surprising. The dependence of the reproduction on the adult krill

feeding – described in Section 1.2.6 – is an important mechanism in the model, which is needed to produce annual cycles. A simplified version of the model with a constant, food-independent reproduction rate produced only cycles that spanned over several years instead of one year (C. Kohlmeier, personal communication).

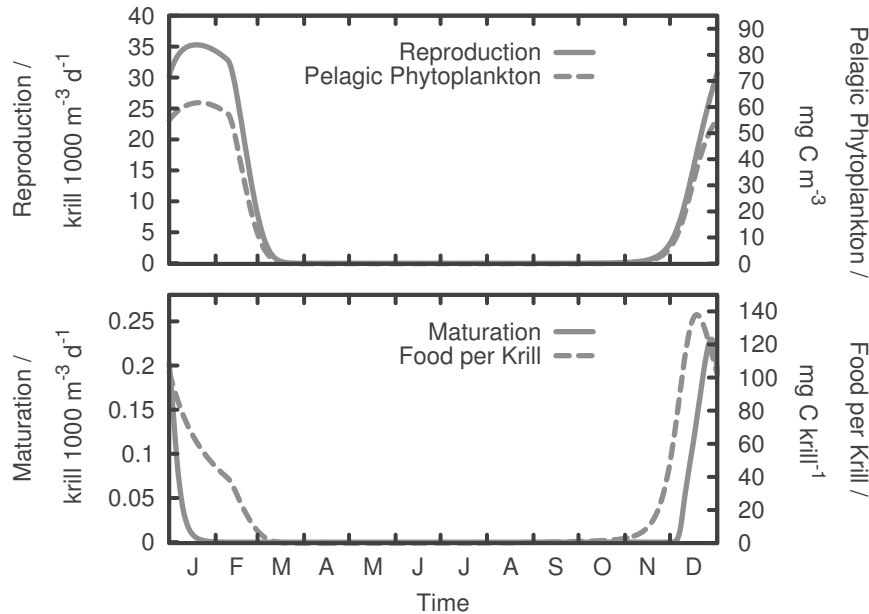


FIGURE 1.10.: Annual dynamics of the reproduction of adult krill (top) and the maturation of juvenile krill (bottom) and their dependence on the food. The daily fluxes of reproduction and maturation are plotted as dashed lines. The concentrations of pelagic phytoplankton (top) and the food per juvenile krill (bottom) are plotted as solid lines.

Timing and Duration of Maturation: Maturation in the model can be understood as the point in time where krill is able to reproduce for the first time. Thus, the requirement for good feeding conditions as described above for the reproduction applies to the maturation as well. Due to the ratio-dependence of the maturation rate, the timing and duration of the maturation is not as strongly coupled to the food concentrations as the reproduction (Figure 1.10, bottom). Maturation starts once the available food per krill exceeds the critical value at the beginning of December and peaks at the end of the month. The following decrease in maturation is connected to the reproduction, because the high reproduction rates lead to a strong increase in juvenile krill density. Consequently, each juvenile krill has less food available to mature. Through this effect, the maturation season is confined to less than a month compared to the more than three months of reproduction. In addition, the maximum maturation flux is two orders of magnitude smaller than the reproduction rate. This is not surprising considering that a female krill takes two years to reach maturity but produces thousands of offspring per year (Siegel and Loeb, 1994).

Changes in the parametrization of the maturation function can lead to multi-annual cycles. This topic will be discussed in more detail in Section 1.3.3.

1.3.2. SENSITIVITY ANALYSIS

1.3.2.1. Morris Screening

The Morris Screening provides a good tool to identify which parameters have a high influence on the model results. Figure 1.11 shows the effects of the different parameters on the normalized mean juvenile and adult krill density. A high mean μ^* means that the parameter has a high overall influence on the model, while a high standard deviation σ means that the parameter is strongly dependent on the values of other parameters or it has a nonlinear effect on the output.

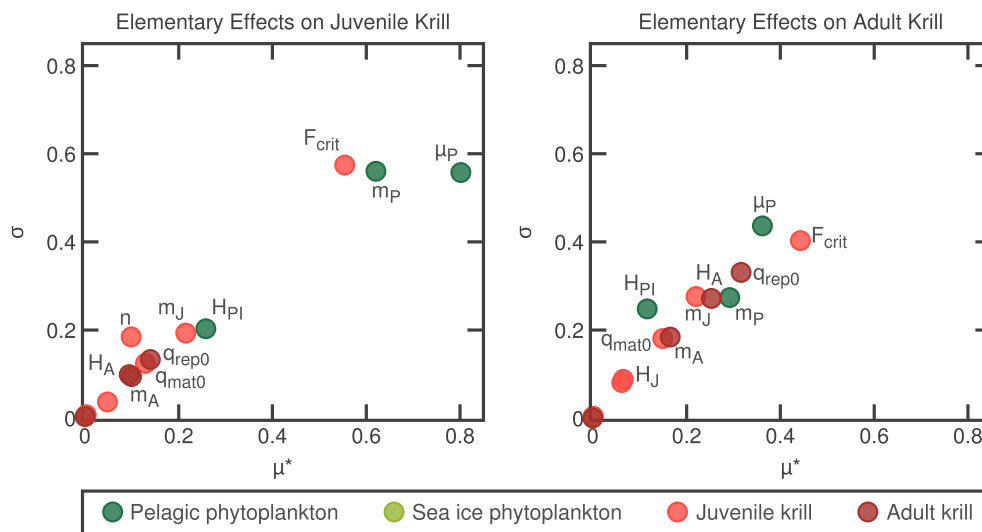


FIGURE 1.11.: Results of the Morris Screening for the abiotic parameters. Shown are the estimated means μ^* and standard deviations σ of the distributions of elementary effects for the annual mean of juvenile krill (left) and adult krill (right). For each graph, only the ten parameters with the highest influence on the model (i.e. the highest μ^* -value) are labelled. The colours indicate which state variable the parameter belongs to.

It can be seen at first glance that the sea ice phytoplankton parameters (μ_S , H_{SI} and m_S) are not visible, i.e. the mean and standard deviation are close to zero and thus, the parameters have no effect on the model results. In contrast to that are the pelagic phytoplankton parameters: only the half-saturation constant for iron uptake H_{PN} is considered uninfluential, while the other three parameters are all ranked under the ten most influential ones. Ranked as the parameter with the highest influence on juvenile krill densities and the second highest on adult krill densities, the growth rate of pelagic phytoplankton μ_P is especially important for the model output. Only slightly lower are the influences of the mortality rate of pelagic

phytoplankton m_p and the typical amount of food per krill needed for maturation F_{crit} . These three parameters have an especially high influence on juvenile krill. The high standard deviation suggests that this influence is nonlinear or dependent on other parameters.

The distribution of the parameters is more evenly spread for the effect on the adult krill. None of the parameters has an especially high mean or standard deviation. Surprisingly, the maximum reproduction rate q_{rep} is the parameter with the third highest influence on the mean adult krill density, but does not have such a strong effect on juvenile. Adult krill parameters, in general, do not have a very high influence on the juvenile krill density even though they are directly coupled through reproduction.

1.3.2.2. Taylor and Target Diagrams

Using the Morris screening design, it was possible to determine the ten parameters with the highest influence on the mean juvenile and adult krill density. So far, however, it is not known how exactly each parameter influences the krill. This information can be obtained from the Taylor and Target diagrams of 20 model simulations where each parameter was varied separately $\pm 50\%$ around the reference value. The results from the Taylor and Target diagrams suggest that the effect of parameter changes is smaller on juvenile krill than on adult krill. Even parameters with a low rank in the Morris screening can have a strong effect on the adult krill dynamics, while the strong effect on juvenile krill is mostly refined to the three parameters which were separated from the other parameters in the Morris diagram. The exact effects of the ten most influential parameters will be discussed below. In this context, only the most interesting figures will be shown.

Maximum Growth Rate of Pelagic Phytoplankton: Of all the parameters, the maximum growth rate of pelagic phytoplankton μ_p has the strongest effect on juvenile and adult krill (Figure 1.12). A decrease in the parameter value leads to a strong decrease in the standard deviation σ^* of juvenile and adult krill (Figure 1.12, left). This indicates a lower amplitude of the dynamics compared to the reference run. An increase in the parameter leads to an increase in the standard deviation of juvenile krill but not of adult krill. Most importantly, an increase and decrease of the maximum growth rate of pelagic phytoplankton strongly decrease the correlation R for adult krill densities and slightly decrease it for juvenile krill. This indicates a shift in the phase of the dynamics, which is also clearly visible in the time diagram (Figure 1.12, bottom right).

An increased growth rate leads to an earlier onset of reproduction of krill due to the faster growth of pelagic phytoplankton in spring. This leads to an earlier increase in juvenile krill density. Consequently, krill mature earlier in the year which leads to a shift in adult krill densities. The maximum of juvenile krill changes less in phase, because the end of the reproductive period is due to light-limitation of phytoplankton which is independent of the growth rate.

Typical Amount of Food per Krill Needed for Maturation: The typical amount of food per krill needed for maturation F_{crit} has a strong effect on adult krill (Figure 1.13)

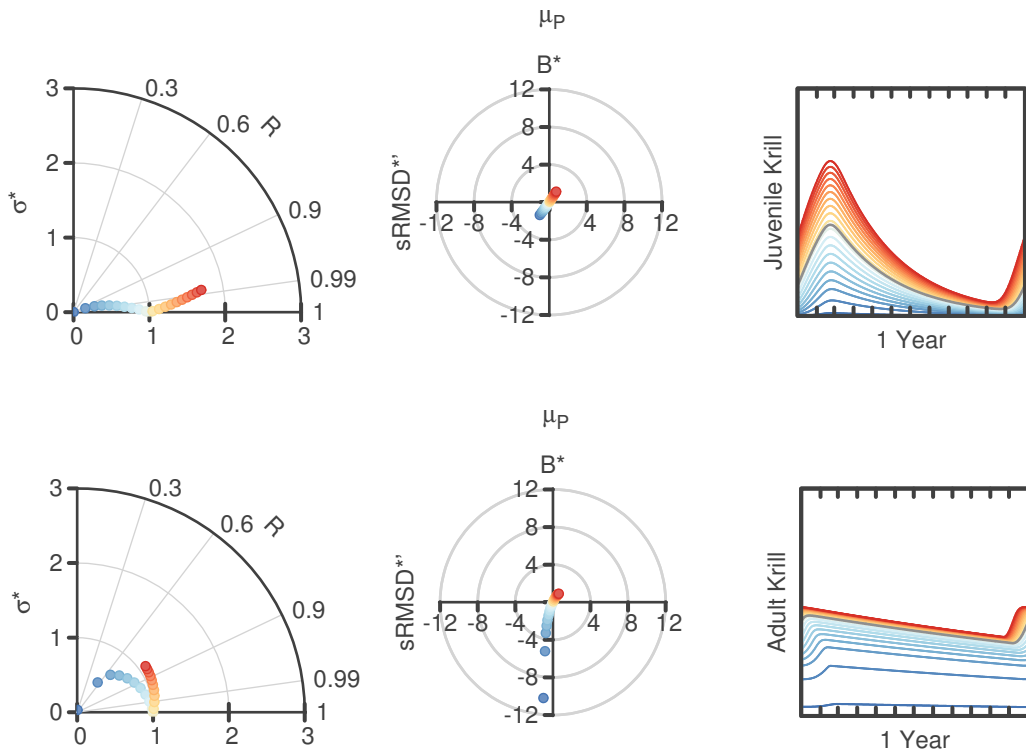


FIGURE 1.12.: Taylor (left), Target (centre) and Time diagram (right) showing the effect of the maximum growth rate of pelagic phytoplankton μ_P on juvenile krill (top) and adult krill (bottom). A red point or line means that the parameter has been increased by up to 50%, while a blue point or line denotes a decrease by up to 50% around the reference value. The reference run is shown in grey.

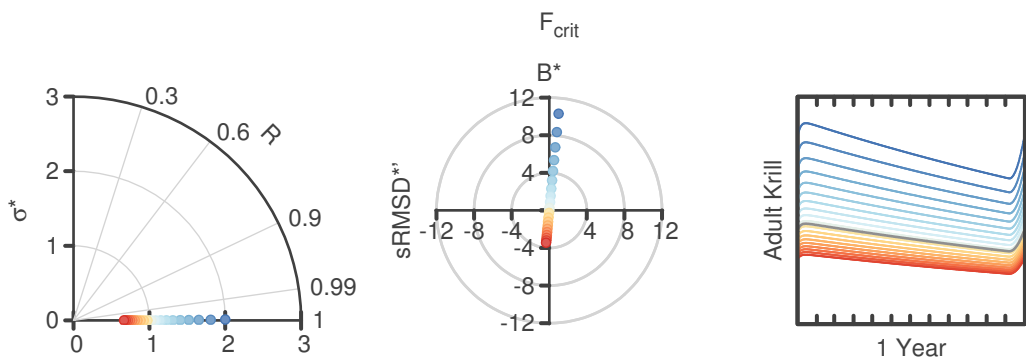


FIGURE 1.13.: Taylor (left), Target (centre) and Time diagram (right) showing the effect of the typical amount of food per krill needed for maturation F_{crit} on adult krill. See Figure 1.12 for details.

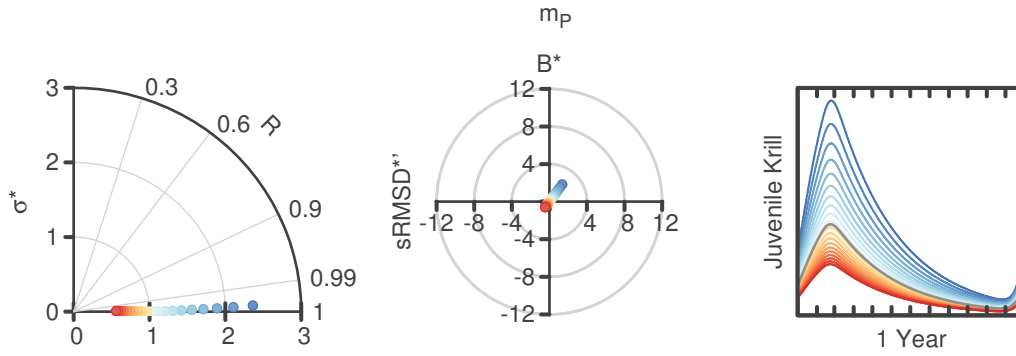


FIGURE 1.14.: Taylor (left), Target (centre) and Time diagram (right) showing the effect of the mortality rate of pelagic phytoplankton m_P on juvenile krill. See Figure 1.12 for details.

and juvenile krill (not shown). A decrease in the parameter value leads to a strong increase in the standard deviation σ^* (Figure 1.13, left) and the bias B^* (Figure 1.13, centre). This indicates an increased amplitude and an increased mean of the annual dynamics compared to the reference run. An increased value of the parameter leads to the opposite behaviour, but the effect is not as strong.

With a higher value of F_{crit} , juvenile krill need more food to start the maturation. This shortens the maturation period, which consequently leads to lower overall krill densities.

Mortality Rate of Pelagic Phytoplankton: The mortality rate of pelagic phytoplankton m_P has a strong effect on the standard deviation σ^* of the juvenile krill dynamics (Figure 1.14, left). A decrease in the parameter value leads to an increase in standard deviation. The effect on the standard deviation of the adult krill is not very strong, but the bias shows a strong increase with decreasing parameter values (not shown). The correlation R does not change for juvenile or adult krill. These results indicate that a decrease in the mortality rate of pelagic phytoplankton increase the amplitude of the juvenile dynamics and the mean of of the adult krill dynamics, but does not change the phase of the dynamics.

A decrease in the mortality rate leads to higher concentrations of pelagic phytoplankton. However, the concentrations in winter are still very small. Thus, the reproduction flux and consequently the juvenile krill densities at the end of the year are similar to the reference run (Figure 1.14, right). In summer, the decreased mortality rate of phytoplankton has a much larger positive effect on pelagic phytoplankton concentrations and with that on the reproduction. As a consequence, juvenile krill dynamics are increased in summer with decreasing mortality rates.

Maximum Reproduction Rate: A decrease in the value of the maximum reproduction rate q_{rep0} leads to an increase in the standard deviation σ^* , the correlation R (Figure 1.15, left) and the bias B^* (Figure 1.15, centre). This indicates an increase in amplitude and mean and a shift of the adult krill dynamics. An increase in the reproduction rate has a much smaller

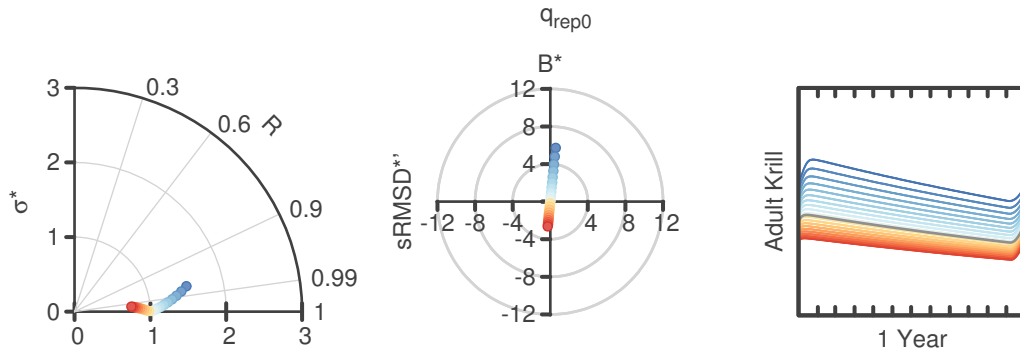


FIGURE 1.15.: Taylor (left), Target (centre) and Time diagram (right) showing the effect of the maximum reproduction rate $q_{\text{rep}0}$ on adult krill. See Figure 1.12 for details.

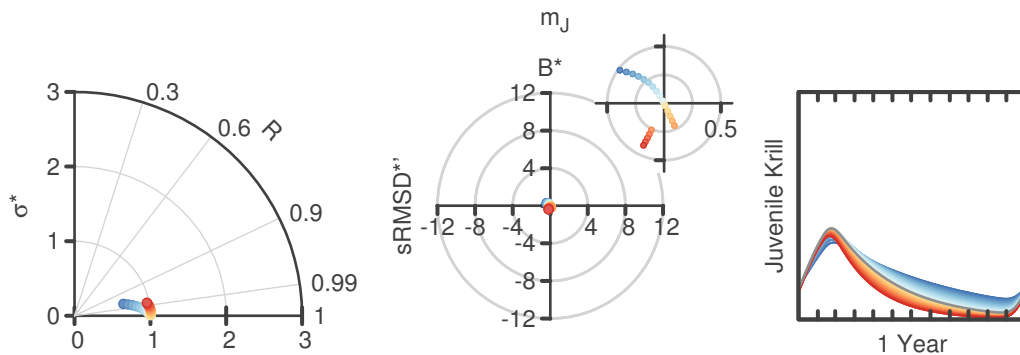


FIGURE 1.16.: Taylor (left), Target (centre) and Time diagram (right) showing the effect of the mortality rate of juvenile krill m_j on juvenile krill. See Figure 1.12 for details. The Target diagram includes a magnified version in the top right corner.

effect on the dynamics than a decrease. In contrast to the adult dynamics, the juvenile krill dynamics show only a very small change in standard deviation and bias (not shown).

The reason for the decrease in adult krill densities is coupled to the maturation process. Increased juvenile krill numbers mean that each krill has less food. This leads to a lower maturation flux and thus lower adult krill densities. A decrease in reproduction rate, on the other hand, means that juvenile krill exceed the critical food concentration earlier in the year and can thus mature earlier. This leads to a shift in the adult krill maximum.

Mortality Rate of Juvenile Krill: The juvenile krill mortality rate m_j has an interesting effect on the juvenile krill dynamics. A decrease in the parameter value leads to a small decrease in the standard deviation σ^* , but an increase in the parameter value does not lead to a change in standard deviation (Figure 1.16, left). This suggests that the amplitude decreases when decreasing the mortality rate, but does not change for an increased parameter value.

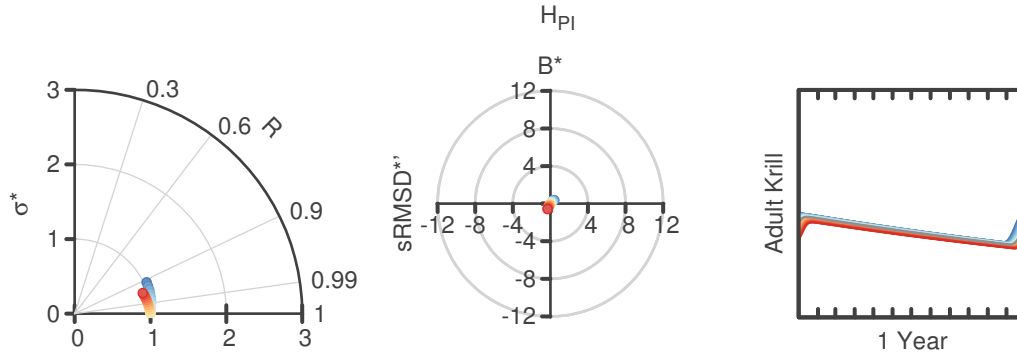


FIGURE 1.17.: Taylor (left), Target (centre) and Time diagram (right) showing the effect of the half-saturation constant of pelagic phytoplankton for light H_{PI} on adult krill. See Figure 1.12 for details.

In contrast to other parameters, a decrease in the mortality rate leads to a slightly negative $sRMSD^*$ (Figure 1.16, centre), i.e. the standard deviation of the reference run is larger than the standard deviation of these sensitivity runs. An increase in the mortality rate at first leads to a positive $sRMSD^*$ but then it suddenly becomes negative. This means that the standard deviation of the sensitivity runs is at first larger but then becomes smaller than the standard deviation of the reference run. The time diagram shows that an increase as well as a decrease in the mortality rate leads to a decrease in juvenile krill densities in summer compared to the reference run (Figure 1.16, right). In winter, in contrast, an increased mortality leads to a decrease in density compared to the reference run while a decreased mortality leads to an increase in density.

For adult krill, the effect of a change in the juvenile krill mortality is much more straightforward: a decrease in the mortality rate leads to a decrease in amplitude and mean of the adult krill dynamics and a small change in phase (not shown). An increased mortality rate leads to only a small increase in amplitude and mean.

The reason for the observed effect on the dynamics is related to the maturation. A decrease in mortality rate leads to higher juvenile densities after winter and thus less food for each krill to mature. The lower maturation rates then lead to lower adult krill densities which in turn lead to lower reproduction rates and consequently lower juvenile krill densities in summer.

Half-Saturation Constant of Pelagic Phytoplankton for Light: Either change in the half-saturation constant of pelagic phytoplankton for light H_{PI} leads to a strong decrease in the correlation R for the adult krill dynamics (Figure 1.17, left). The effect on the standard deviation σ^* and the bias B^* is small. This suggests a shift in adult krill dynamics but only a small change on the mean and amplitude. With a decrease of the parameter value, the mean and amplitude of the juvenile krill dynamics increase and the dynamics are shifted (not shown). An increased parameter value leads to a decrease in mean and amplitude, but the change is much smaller than for the decrease of the parameter value.

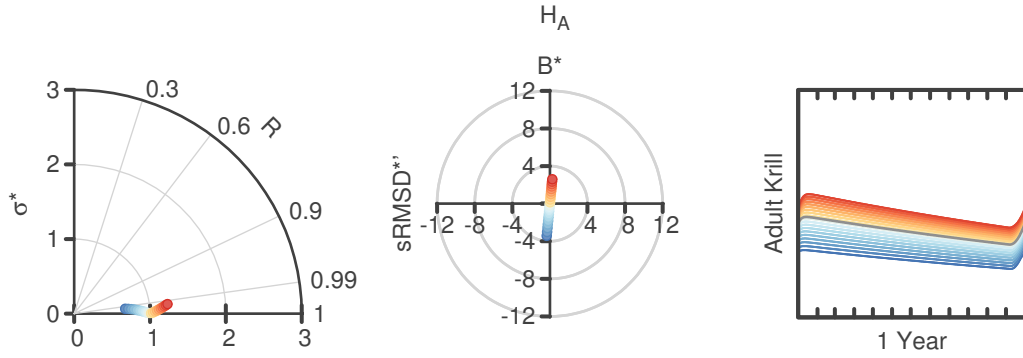


FIGURE 1.18.: Taylor (left), Target (centre) and Time diagram (right) showing the effect of the half-saturation constant of adult krill for food uptake H_A on adult krill. See Figure 1.12 for details.

A decrease in the half-saturation constant leads to earlier growth of the phytoplankton after winter. This leads to an earlier maturation and reproduction, which shifts the maximum of the juvenile and adult krill dynamics. The lower half-saturation constant also leads to increased phytoplankton concentrations. This leads to an increase in reproduction rates and consequently to higher juvenile krill densities. The higher juvenile krill densities and higher phytoplankton concentrations balance each other so that the food per krill remains almost the same as in the reference run. As a consequence, maturation rates remain almost the same and the adult krill densities change only very little.

Half-Saturation Constant of Adult Krill for Food Uptake: An increase in the half-saturation constant of adult krill H_A leads to a small increase in the standard deviation σ^* (Figure 1.18, left) and the bias B^* (Figure 1.18, centre). The standard deviation and the mean of the juvenile krill dynamics decrease slightly with an increase in the parameter value (not shown).

An increased half-saturation constant leads to a lower reproduction and consequently lower juvenile krill densities. Because each juvenile krill has more food available, the maturation rate increases and with that the adult krill densities.

Maximum Maturation Rate: An decrease in the maximum maturation rate q_{mat0} leads to a decrease in amplitude of the juvenile and adult krill dynamics and a decrease in the mean of the adult krill dynamics (not shown). In addition, the adult krill dynamics are shifted.

A decrease in the maximum maturation leads to lower and later maturation in spring. This leads to a shift in phase and a lower maximum of the adult krill dynamics.

Mortality Rate of Adult Krill: An increase in the adult krill mortality rate m_A leads to an increase in the standard deviation σ^* of the adult krill dynamics (Figure 1.19, left) but a decrease of the bias B^* and a positive RMSD^* (Figure 1.19, centre). This indicates that an increase in the mortality rate leads to a higher amplitude than the reference run but at

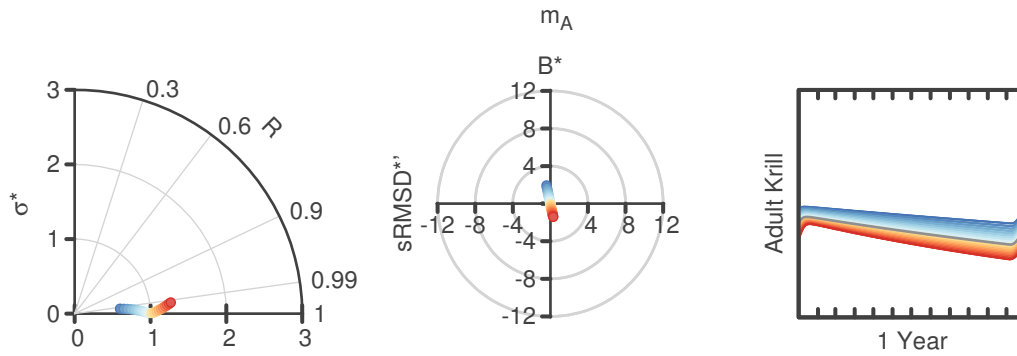


FIGURE 1.19.: Taylor (left), Target (centre) and Time diagram (right) showing the effect of the mortality rate of adult krill m_A on adult krill. See Figure 1.12 for details.

the same time a lower mean. A change in adult krill mortality has almost no effect on the juvenile krill dynamics (not shown).

Steepness of the Maturation Function: The steepness of the maturation function n has a small effect on juvenile and adult krill (not shown). A decrease in the parameter value leads to an increase in krill densities and a slight shift in the adult maximum. The shift in the maximum is due to the longer maturation period as a result of the less steep maturation curve.

Half-Saturation Constant of Juvenile Krill for Food Uptake: The effect of the half-saturation constant of juvenile krill H_j for food uptake is small (not shown). An increase in the parameter value leads to a decrease in krill densities due to lower maturation.

1.3.3. MULTI-ANNUAL DYNAMICS

With the parametrization of the reference run, the model exhibits annual dynamics – i.e. all the dynamics are exactly the same each year. However, multi-annual dynamics can emerge in this model depending on the parametrization of the maturation function. Whether multi-annual cycles emerge depends on the combination of two parameters: the maximum maturation rate q_{mat0} and the steepness of the maturation function n . The most crucial factor for the emergence, however, is the dependence of the maturation function on the food per juvenile krill (ratio-dependence). With a density-dependent maturation function, the multi-annual dynamics would not occur but at the same time it would not be possible to parametrize the model in a way that krill survives.

Figure 1.20 (left) shows the results from a parametrization that leads to annual cycles in krill dynamics. Compared to the reference parametrization, the maximum maturation rate q_{mat0} has been increased, but all the points discussed above for the reference parametrization still hold true. In contrast to that is Figure 1.20 (right) which shows an example of a two-year

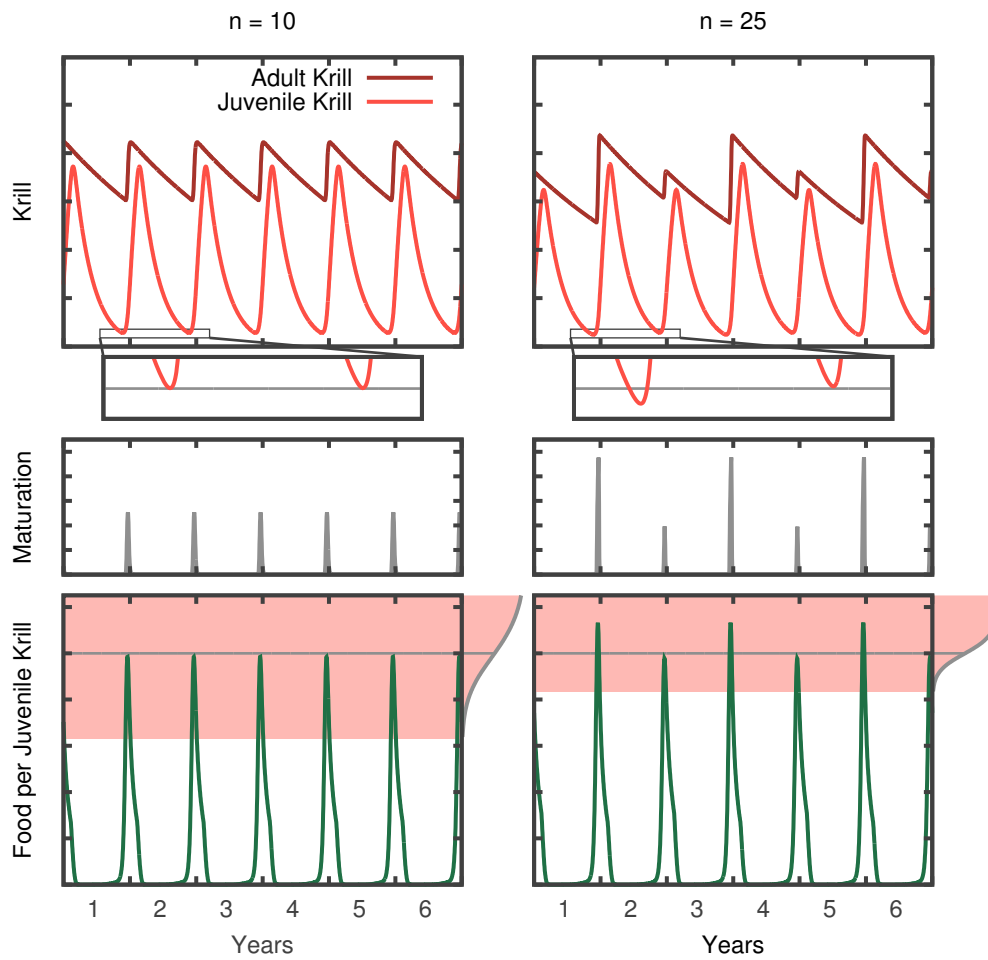


FIGURE 1.20.: Qualitative comparison of an annual and a multi-annual cycle in krill dynamics. Shown are the dynamics of juvenile and adult krill (top), the maturation flux (middle) and the food per juvenile krill (bottom) for two different values of the steepness of the maturation function n (left: $n = 10$; right: $n = 25$). The red area in the bottom plot marks the range of food per krill where at least 1% of the maximum maturation rate is reached. The maturation function is shown on the right of the bottom plot as illustration. Values on the y-axis have been omitted for simplicity, but all y-axes start at zero and are the same for the left and right hand side of the figure. All units are the same as previously described for the reference run.

cycle. The two parametrizations only differ in one parameter: the steepness of the maturation function n , which is larger for the right hand side of the figure ($n=25$ compared to $n=10$).

An increase of the steepness of the maturation function has the effect that it makes the maturation more sensitive to changes in the food per juvenile krill. The consequence of this is the emergence of the multi-annual cycles. Since the pelagic phytoplankton is the same for both figures (not shown), the ratio-dependence is very crucial for the dynamics. A low juvenile krill density in winter leads to high values of food per juvenile krill in the following summer, which in turn leads to a high maturation rate and consequently to an increase in adult krill density. The increased adult krill density leads to a higher reproduction and thus higher juvenile krill densities in summer. Since the mortality is proportional to the juvenile krill density, the minimum krill density in winter is slightly higher than in the year before. Because the absolute amount of food remains the same, there is less food available for each individual juvenile krill which then leads to a lower maturation in that season. The low maturation consequently leads to a lower adult krill density compared to the previous year and with that lower reproduction. Due to the lower reproduction, the maximum juvenile krill density is lower than the previous year and the minimum in winter naturally will be lower as well. From that minimum in juvenile krill density, the described two-year cycle starts again. This examples shows that high juvenile krill densities can lead to lower krill densities in the next year, because the ratio-dependence effectively introduces a competition for food between the juvenile krill. In the worst case, juvenile krill might not mature for one or even more years.

Characteristic for the multi-annual cycles is that the general juvenile krill dynamics within one year remain the same: there is always one juvenile krill maximum at the beginning of the year and one minimum at the end of the year. What changes is only the height of the maximum. In the following, this height – the annual maximum in juvenile krill – is used to analyze the dependence of the multi-annual cycles on changes in the maximum maturation rate q_{mat0} and the steepness of the maturation function n . Using the annual maximum is similar to using a Pointcaré map as long as the maxima occur on the same day each year, which is the case in the analyzed parameter range. To get an overview, the two maturation parameters were varied over a large range and the number of different maxima within 100 years of simulation were counted (Figure 1.21).

For $n \leq 10$ and $q_{mat0} \leq 0.004$, the model always exhibits annual cycles independent of the value for the other parameter. As we have already seen in the example above, an increase in n can lead to cycles with longer periods. For high values of n , the length of the period also increases when increasing q_{mat0} . Although cycles with periods up to 15 years can be found in the analyzed parameter range, periods of 7 years or less prevail. In between the regions with defined periods, regions with chaotic behaviour exist.

Figure 1.22 shows a cross-section of the diagram at $q_{mat0} = 0.6$. In this bifurcation diagram, the steepness of the maturation function n is increased while the maximum maturation rate q_{mat0} is held constant. This diagram shows typical period-doubling cascades into chaotic regions. At first, the annual cycle branches into a cycle with a period of two years, followed by period four and so on. After a region of chaos, a periodic window opens and a period three cycle emerges which again doubles to a period six cycle and eventually leads to chaos again.

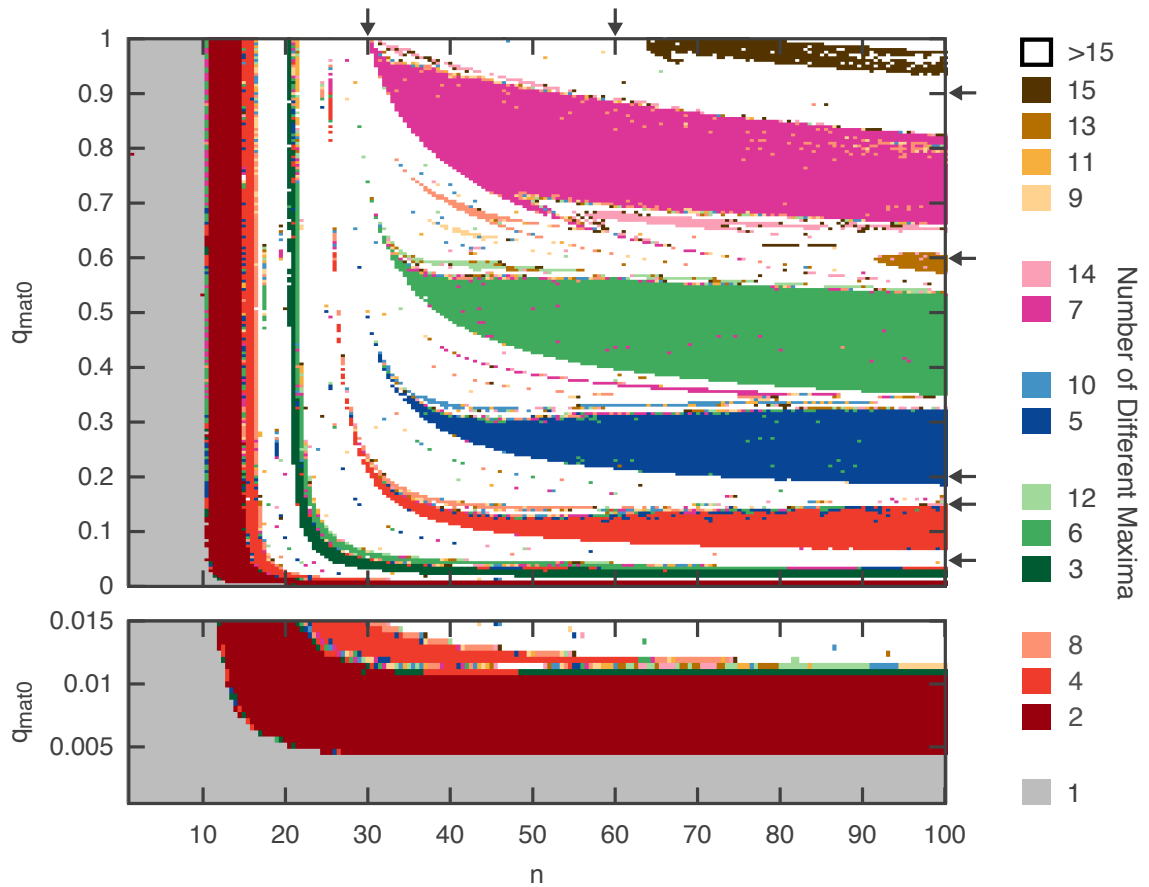


FIGURE 1.21.: Dependence of the number of different maxima in juvenile krill density on the maximum maturation rate $q_{\text{mat}0}$ and the steepness of the maturation function n . Two maxima are defined as being different, when their difference is larger than $0.01 \text{ krill m}^{-3}$. The simulations with more than 15 different maxima seem to be chaotic. The arrows mark the locations of cross-sections shown in Figures 1.22 – 1.24.

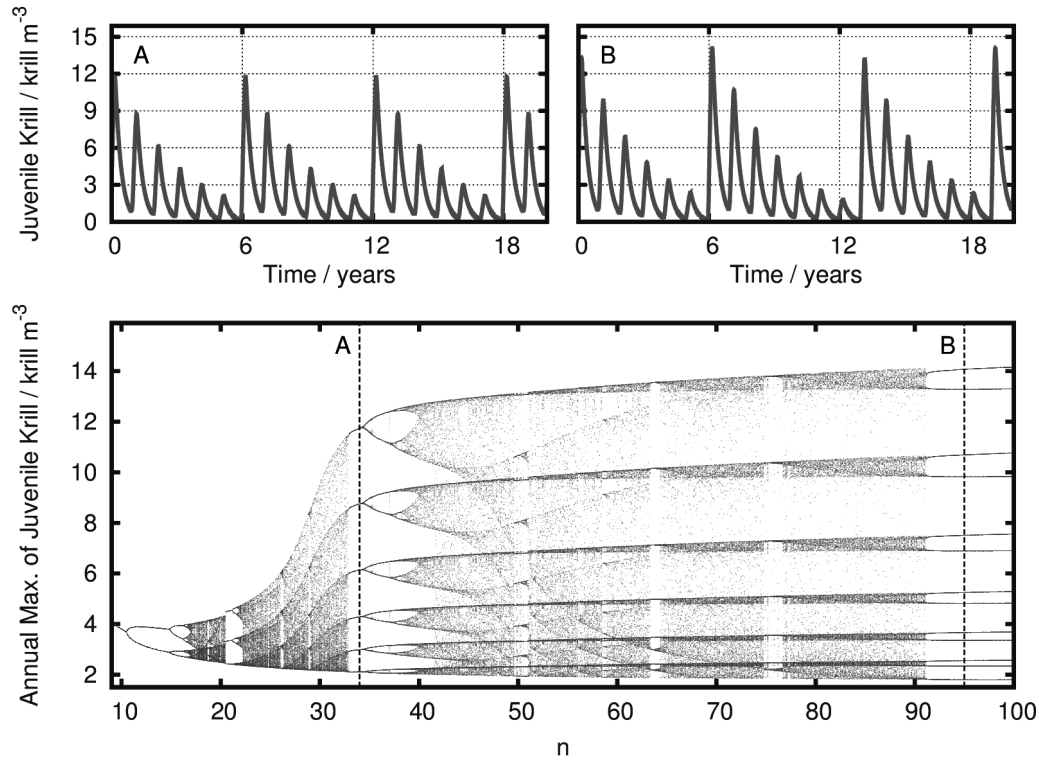


FIGURE 1.22.: Bifurcation diagram of the annual maxima of juvenile krill as a function of the steepness of the maturation function n for $q_{\text{mat}0} = 0.6$ and the corresponding time series at $n = 34$ (A) and $n = 95$ (B).

For very high values of n , a cycle with a period of 13 years emerges. Looking at the time diagrams of a cycle with a period of six years and this cycle with period 13 (Figure 1.22, top), it can be seen that the 13 year cycle consists of a six year period of decreasing maxima followed by a seven year period of decreasing maxima. Although cycles with up to 15 different maxima could be detected in the whole analyzed parameter space (Figure 1.21), an eight year period of decreasing maxima was the longest period that could be observed. All longer cycles seem to consist of more than one shorter cycle with different maxima.

Although the period-doubling for low values of n can be found for all parameter values that lead to multi-annual cycles, bifurcation diagrams for different values of $q_{\text{mat}0}$ can look very different to the example described above (Figure 1.23). For large values of n , stable multi-annual cycles can emerge (Figure 1.23, top right and bottom left) but chaotic behaviour is also possible (Figure 1.23, top left and bottom right). In addition, behaviour such as intermittency (Figure 1.23, top left) or period-halving (Figure 1.23, top right) can be observed.

Cross-sections in the other direction – i.e. changing $q_{\text{mat}0}$ while keeping n constant – shows a simpler behaviour (Figure 1.24). The number of maxima and also the height of the large maxima increase towards higher values of $q_{\text{mat}0}$, while the smallest maximum remains almost constant. The stable cycles are interrupted by regions of chaos. For higher values of n ,

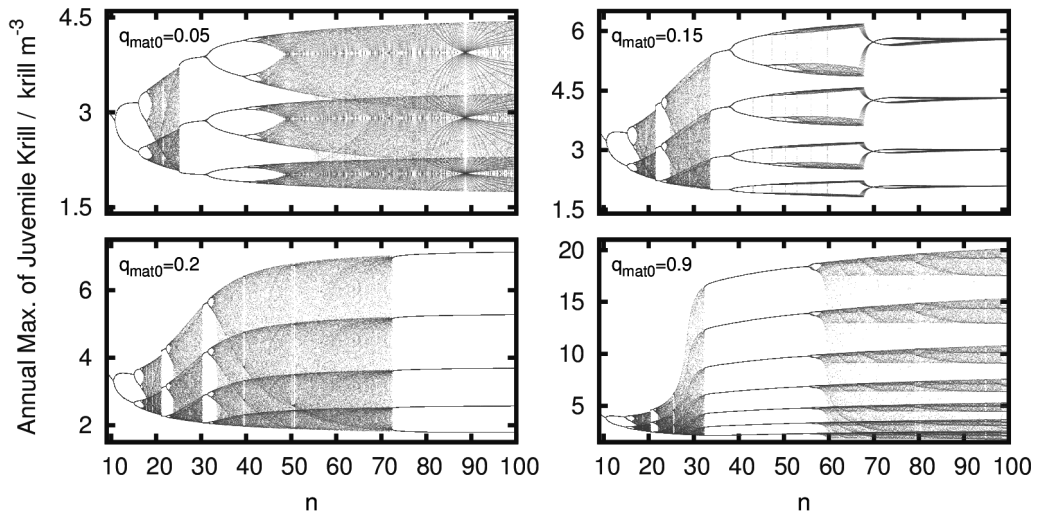


FIGURE 1.23.: Bifurcation diagrams of the annual maxima of juvenile krill as a function of the steepness of the maturation function n for $q_{mat0} = 0.05$ (top left), $q_{mat0} = 0.15$ (top right), $q_{mat0} = 0.2$ (bottom left) and $q_{mat0} = 0.9$ (bottom right).

the system changes from a mostly chaotic system with small periodic windows (Figure 1.24, left) to a more periodic system with small regions of chaos (Figure 1.24, right).

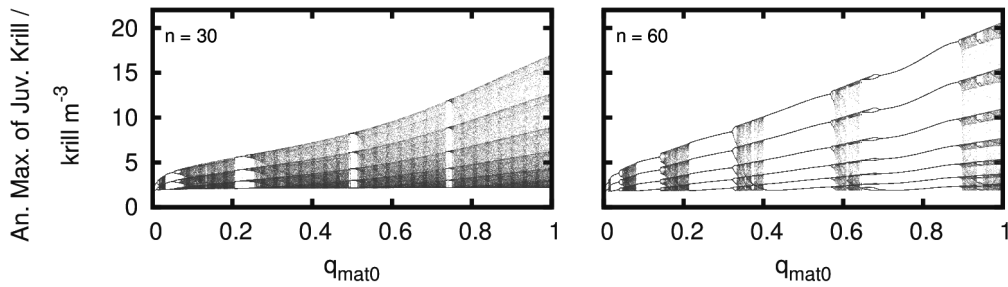


FIGURE 1.24.: Bifurcation diagrams of the annual maxima of juvenile krill as a function of the maximum maturation rate q_{mat0} for $n = 30$ (left) and $n = 60$ (right).

The bifurcation diagrams give an idea about the complexity of the dynamics. A detailed theoretical analysis, however, would be beyond the scope of this thesis. Summarizing the above, it can be concluded that the maturation function gives rise to very complex dynamics. From a more biological point of view it is interesting to note that multi-annual cycles in krill density can occur even under stable environmental conditions.

1.4. SHORT SUMMARY

In this chapter, a new model describing the population dynamics of juvenile and adult krill, their food sources – pelagic and sea ice phytoplankton – and the micronutrient iron was presented. The model is able to reproduce the annual cycles of these variables observed in nature. The model shows that pelagic phytoplankton is bottom-up controlled by the availability of light. Neither the iron availability nor the top-down control through predation of krill on phytoplankton play a significant role. Krill strongly depends on the availability of phytoplankton for maturation and reproduction, which is available in sufficiently high concentrations for only a short period of the year. The most important process in the whole life cycle is the maturation from juveniles into adults, which limits the size of the whole krill population. Changes in the parametrization of the maturation function can even lead to multi-annual cycles of the krill population or chaotic behaviour.

2

THE INFLUENCE OF A BIOLOGICAL CLOCK ON KRILL REPRODUCTION

2.1. INTRODUCTION

A reduction of the metabolic activity in winter has been described as the most effective over-wintering mechanism for adult krill (Quetin and Ross, 1991). Now, there is increasing evidence that this reduction is not only a reaction to decreasing food concentrations, but that it might be an inherent physiological process to cope with the unfavourable conditions in winter (Teschke et al., 2007, 2008; Brown et al., 2011; Meyer, 2012). Many organisms in seasonally changing environments have developed rhythms to cope with unfavourable conditions or time their reproduction to maximize the survival of their offspring (Gwinner, 1986). The changes in the environment are particularly pronounced in polar regions, which makes a synchronization of the rhythm to favourable conditions essential for survival of the species living in these regions. Before discussing the mechanisms of synchronization that krill has developed, it is useful to introduce some terms according to the definitions by Gwinner (1986).

2.1.1. TYPES OF ANNUAL RHYTHMS

Two different types of environmental factors control the annual (and also daily) rhythms: *ultimate factors* and *proximate factors*. Ultimate factors are “those environmental variables that, in the course of evolution, exert selection pressure to restrict an activity to a particular time of the year”(Gwinner, 1986). Proximate factors are those factors which give the organism

a cue to initiate a certain physiological process, i.e. they allow the organism to predict the upcoming favourable conditions. This is essential for processes such as reproduction, which need to be initiated before the conditions become optimal.

If the annual change in the environmental conditions is fairly predictable it might also be advantageous to develop an *endogenous circannual rhythm* (or often called: endogenous clock) instead of relying on proximate factors. A rhythm is called endogenous if it “continues in conditions that provide no external information about the period it normally assumes” (Gwinner, 1986). Without any external information, the period might not be exactly one year but only circannual i.e. a bit longer or shorter than 12 months. To prevent the endogenous rhythm and the environment from desynchronizing, so-called *zeitgebers* exist: “seasonally varying environmental factors that are capable of synchronizing (entraining) circannual rhythms with the yearly cycle of the seasons” (Gwinner, 1986). With this definition, the term *zeitgeber* is a special case of a proximate factor. It is important to stress here that an endogenous rhythm continues with its normal period if the *zeitgeber* is missing. An *exogenous rhythm*, in contrast, is entirely dependent on the proximate factor and thus the physiological process will be skipped if the cue for its initialization is missing (Aschoff, 1981).

2.1.2. TIMING OF KRILL REPRODUCTION

Adult krill have a very high energy demand to develop their reproductive organs (Ross and Quetin, 1986; Kawaguchi et al., 2007). In addition, the survival of their offspring is strongly dependent on the food availability during their first year (see Section 1.1.2). Thus, it can be assumed that in the course of evolution, food availability has served as an ultimate factor to restrict the reproduction to a time of the year when food availability is high.

How the reproduction cycle is influenced each year by environmental factors is a difficult question, which has not been conclusively answered. Experimentally proving that a rhythm is truly endogenous – i.e. it runs without any external information – is especially difficult for annual rhythms, because experiments have to be long enough to rule out any other influence on the rhythm. Almost 30 years ago, Thomas and Ikeda (1987) first proposed that krill possesses an endogenous clock. Like Kawaguchi et al. (2007) and Yoshida (2009) 20 years later, Thomas and Ikeda noticed that mature female krill kept under constant darkness and constant food in the laboratory underwent a regression of their external sexual organs in winter before they re-matured in spring.

Kawaguchi et al. (2007) proposed a division of the annual maturity cycle into two parts: the regression cycle and the ovarian cycle (Figure 2.1). The regression cycle is important for krill to restore their ovaries after a reproductive season and save energy during the winter months with low food availability. Kawaguchi et al. (2007) suggest that this regression cycle might be driven by an endogenous clock. The ovarian cycle marks the reproductive period during which multiple spawning events can happen depending on the environmental conditions. The onset and the termination of this ovarian cycle – the actual spawning season – could be dependent on some proximate environmental factor (Kawaguchi et al., 2007).

The results of Teschke et al. (2008) are somewhat contrary to the previous experiments. In

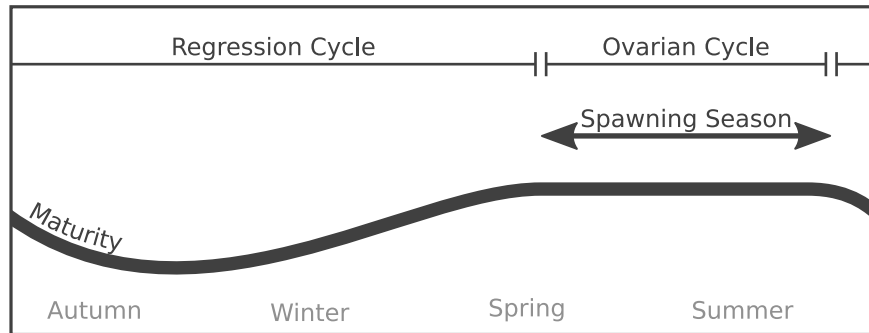


FIGURE 2.1.: Overview of the krill maturity cycle proposed by Kawaguchi et al. (2007). [modified after Kawaguchi et al. (2007)]

a 12-week experiment, they found that krill exposed to light (continuous or 12 h light/12 h dark) showed a development of maturity compared to those krill kept in continuous darkness who showed no development at all. At a first glance, this might seem as evidence that krill does not possess an endogenous clock, but Teschke et al. pointed out that all the krill in their experiment had already undergone at least part of the re-maturation before they were subjected to the different light conditions. That part of the development before the start of the experiment might have been due to the endogenous clock which was then synchronized with the light conditions in the experiment. Despite the faster development, Teschke et al. did not observe any signs of onset of the ovarian cycle. The authors are not sure whether this is due to the short experimental period or whether it supports the hypothesis of Kawaguchi et al. (2007) that the onset of the ovarian cycle depends on some environmental cue.

An experimental study by Brown et al. (2011) suggests that the termination of the ovarian cycle might be affected by light as well. In that experiment, krill subjected to an advanced winter light regime (4 months earlier in darkness) started the regression earlier than those subjected to a prolonged winter or spring light regime. Under all three light regimes, the regression cycle was 3 months long, i.e. the timing of re-maturation was not affected by the light regime. The authors suggest that these results indicate that krill maturation is driven by an endogenous rhythm which can be altered by a light cue.

Considering all the mentioned studies, it is likely that light plays an important role in the annual reproduction cycle. However, other studies have suggested that food availability might play some role as well. Under low food or starved conditions, krill can develop their external sexual organs but they don't start their ovarian development (Kawaguchi et al., 2007; Yoshida, 2009). Hence, food availability seems to have an influence on the start of the reproductive season. In addition, Kawaguchi et al. (2007) suggested that the termination of the reproductive season could be due to insufficient food to sustain the ovarian cycle.

2.2. MODEL CHANGES

Despite the numerous studies mentioned in the previous section, the exact role environmental factors play in the reproductive cycle remains unclear. To gain more understanding of this role, the model described in the previous chapter is extended by a biological clock. Using this model, many different potential setups of this biological clock can be analyzed with relatively little effort and few costs compared to a lab experiment. The metabolism and maturity state of krill are not considered in this model. Therefore, the start and the termination of the ovarian cycle are the two times of the year that are determined by the clock in this model.

Compared to the model described in Chapter 1, only the equation describing the reproduction of adult krill (Equation 1.24) is changed:

$$\text{reproduction} = q_{\text{rep}0} \cdot \mathbf{clock} \cdot \text{feeding}. \quad (2.1)$$

The reproduction is still dependent on how much adult krill feeds on pelagic phytoplankton. In addition, the reproduction is switched on and off by a so-called clock. This clock depends on the state of two environmental factors $ON(t)$ and $OFF(t)$ (Figure 2.2):

$$\text{clock}(t) = \begin{cases} 1 & \text{for } ON(t) \geq \text{crit}_{ON} \text{ and } \text{clock}(t - \Delta t) = 0 \\ 0 & \text{for } OFF(t) < \text{crit}_{OFF} \text{ and } \text{clock}(t - \Delta t) = 1 \\ \text{clock}(t - \Delta t) & \text{otherwise.} \end{cases} \quad (2.2)$$

In this equation, ON is an environmental factor which is responsible for switching the clock on if it is above a critical value crit_{ON} . The clock is switched off if the environmental factor OFF falls below a critical value crit_{OFF} . The clock is switched on and off only once per year. The environmental factors ON and OFF can be the same but they can also be different.

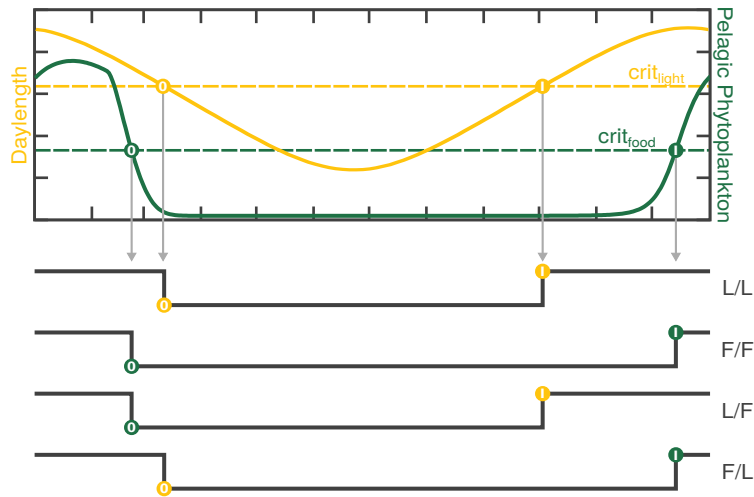


FIGURE 2.2.: Illustration of the biological clock, which regulates the reproduction. The clock is switched on and off depending on the state of the environmental factors daylength and pelagic phytoplankton.

As discussed in the previous section, two different environmental factors have been suggested to play a role in the reproduction cycle of krill: daylength and food availability for adult krill – in this model the pelagic phytoplankton concentration (Kawaguchi et al., 2007; Teschke, 2007; Yoshida, 2009; Brown, 2010). The model was set up with all four possible combinations of these two environmental factors as on- and off-switches of the clock (Table 2.1). The clock setups used in this thesis are the same as the trigger scenarios used by Groeneveld et al. (2015). However, in that study, a clock that influences the metabolic activity was studied instead of a clock that influences the ovarian cycle (this study).

TABLE 2.1.: Overview of the four different clock setups.

<i>ON(t)</i> \ <i>OFF(t)</i>	Daylength	Pelagic Phytoplankton
Daylength	Light/Light (L/L)	Light/Food (L/F)
Pelagic Phytoplankton	Food/Light (F/L)	Food/Food (F/F)

Although Teschke et al. (2008) have suggested that light intensity could potentially control the reproductive cycle, it is neglected here as an environmental factor. Light intensity at the sea surface can vary strongly from year to year and even within one year depending on the weather and ice and snow conditions. Photoperiod is much more stable and thus a better predictor for upcoming environmental conditions. In addition, it is known that many seasonal processes in plants and animals are controlled by changes in the daylength (Gwinner, 1986, and references within). It is likely that krill has also adapted its annual cycle to this environmental factor.

2.3. RESULTS

The aim of this section is to characterize the effect of the different clock setups on the krill density compared to the reference run described in Chapter 1. Therefore, only relative changes in density compared to the reference run instead of absolute values are considered in this section.

Even less than about the general clock mechanism is known about the actual value of the critical daylength or critical food availability which starts or terminates the reproduction. Hence, all clock setups are analyzed for a large range of possible critical values, i.e. 0 to 24 hours of daylength and 0 to 65 mg C m⁻³ of food.

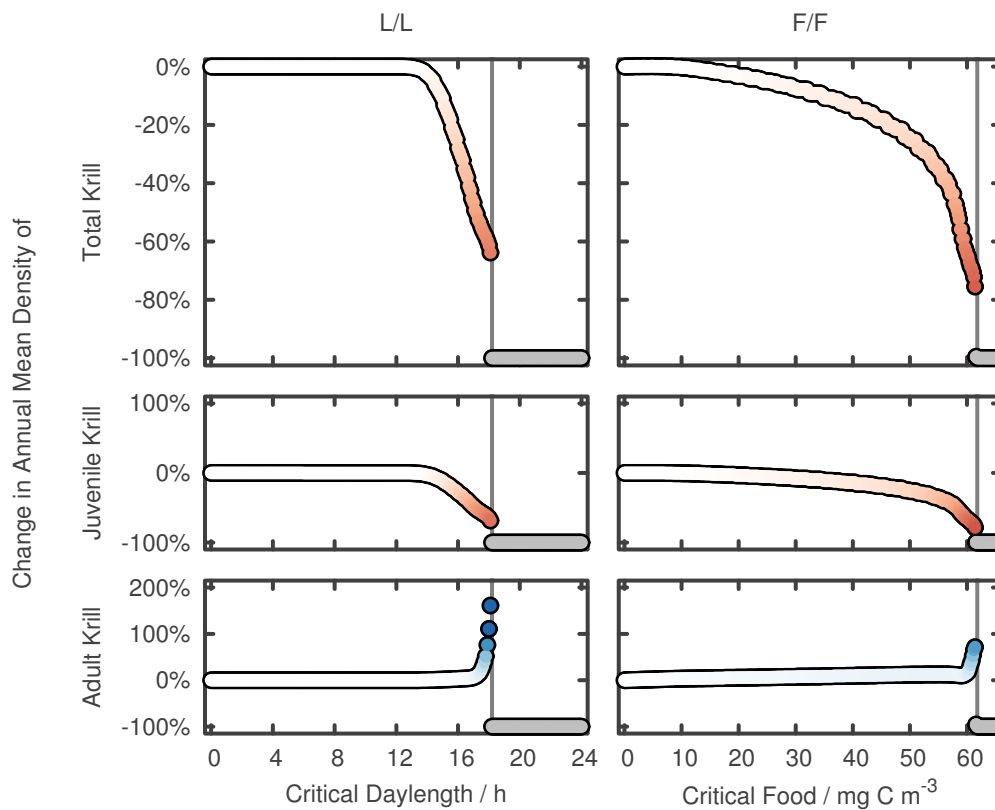


FIGURE 2.3.: Relative change in annual mean krill density in dependence on the critical values of the light/light clock setup (left) and the food/food clock setup (right). Shown are the relative changes in annual mean density of total krill (sum of adult and juvenile krill, top), juvenile krill (middle) and adult krill (bottom). The changes in density were calculated for each critical value relative to the reference run. Circles are coloured according to their y-value for easier comparison with Figure 2.6. The grey line marks the maximum daylength and the maximum food concentration of the reference run, respectively. The grey circles denote critical values for which krill dies out.

2.3.1. DEPENDENCE OF THE KRILL DENSITY ON THE CRITICAL VALUES

Light/Light Clock: Up to a critical daylength of 12.6 hours, the light/light clock has no effect on the krill density (Figure 2.3, top left). When the critical value exceeds the maximum daylength of 18.2 hours, krill does not experience the light cue and dies out because the reproduction is never switched on. In between those two critical values, the total krill density declines almost linearly by more than 60% compared to the reference run. This decline is driven by a decline in juvenile krill density (Figure 2.3, middle left). The adult krill density even strongly increases for critical daylengths above 16.9 hours (Figure 2.3, bottom left). However, this does not influence the total density, because the adult krill density is much smaller than the juvenile krill density.

The explanation for the behaviour in the first part is simple: the clock does not significantly shorten the food-dependent reproductive season for critical daylengths below 12.6 hours (Figure 2.4, solid line). Above this value, an increase in the critical daylength shortens the reproductive season which in turn leads to a decreasing juvenile krill abundance. However, up to a critical daylength of 16.9 hours, only the end of the reproductive season is significantly affected (Figure 2.4, dotted line). For higher values, the beginning of the reproductive season in spring is affected as well. This strongly reduces the length of the reproductive season and the maximum is reached earlier in the season. Although the maximum reproduction flux is higher for shorter reproductive seasons, the total reproduction within one year decreases. This has the same effect as a decrease in the maximum reproduction rate described in Section 1.3.2.2: The decreasing reproduction leads to lower juvenile krill densities. Due to the ratio-dependence, each juvenile krill has more food available and the maturation is therefore stronger. This in turn leads to a shift in the population structure towards adult krill. For a critical daylength of 18.1 hours, the reproductive season is so short (Figure 2.4, dashed line) that the fraction of adult krill in the total population increases to 15% compared to the 2% in the reference run (not shown).

Food/Food Clock: Whereas the light/light clock only has an effect on the krill density for relatively high critical values, any changes in the critical food concentration directly affect krill (Figure 2.3, top right). For small critical values, the decrease in density is very small. For higher critical values, the density strongly decreases compared to the reference run without a clock. Similar to the light/light clock, adult krill densities increase strongly when juvenile krill densities decrease (Figure 2.3, middle and right bottom), which is again a result of the ratio-dependent maturation function. For critical food concentrations above 61.8 mg C m^{-3} (i.e. the maximum pelagic phytoplankton concentration), krill dies out because they never receive the cue to start the reproduction.

Although the reproductive season is shortened by a few days even for small critical values, the effect on the densities for low values is weak. This is because the shortening of the reproductive season only affects times in winter when the reproduction is already low (Figure 2.5, solid line). For higher critical food concentrations, the effect is much stronger

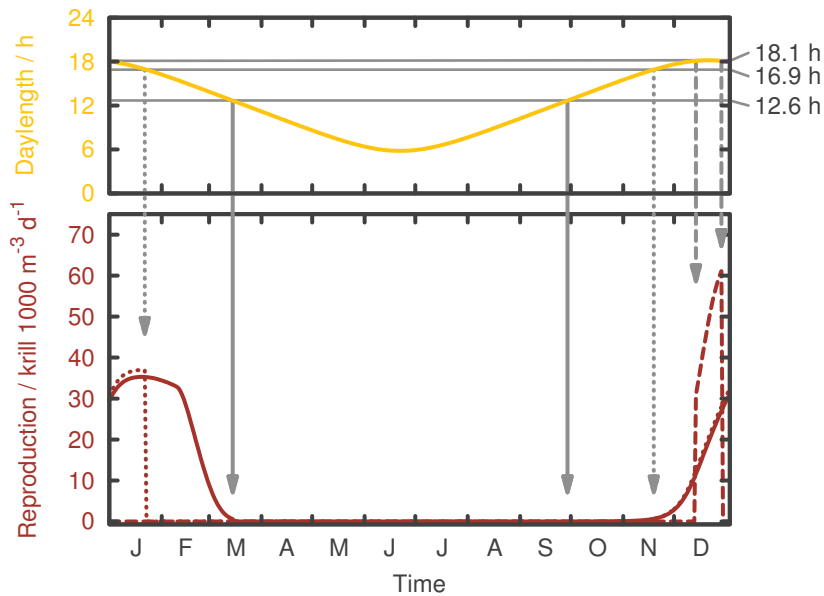


FIGURE 2.4.: Temporal dynamics of the reproduction over the course of one year for the light/light clock setup. The reproduction flux (bottom) is shown exemplarily for three different values of the critical daylength: $\text{crit}_{\text{light}} = 12.6$ hours (solid), $\text{crit}_{\text{light}} = 16.9$ hours (dotted) and $\text{crit}_{\text{light}} = 18.1$ hours (dashed). The arrows mark the day of the year where the daylength (top) falls below or exceeds the critical daylength.

because it prevents adult krill from reproducing during times with high food abundances and thus potentially high reproduction rates (Figure 2.5, dashed and dotted line). In contrast to the light/light clock, the timing of the maximum reproduction flux is less shifted.

Light/Food Clock: When the daylength acts as a cue to start reproducing and food availability terminates the reproduction, the effect of the clock is small compared to the other clocks (Figure 2.6, left). For values of the critical daylength below 6 hours, there is no change in krill density because the critical value is below the minimum daylength. Thus, the reproduction is always switched on, which is equivalent to the reference run. For values higher than 18.1 hours, krill never receives the cue to start reproducing and therefore dies out. The values in between have very little effect on the krill density, which is not surprising when remembering the results from the light/light clock. As shown in Figure 2.4, daylength as a cue to start reproducing has only an effect on the reproductive season when the critical value is above 16.9 hours. Even with a critical daylength of 18.1 hours, the start of the reproductive season is not significantly shifted to later days.

More important is the effect of the critical food concentration – the cue to terminate the reproduction. With higher critical food concentrations, the krill density decreases. This can be understood when looking at the results from the food/food clock. Even low critical

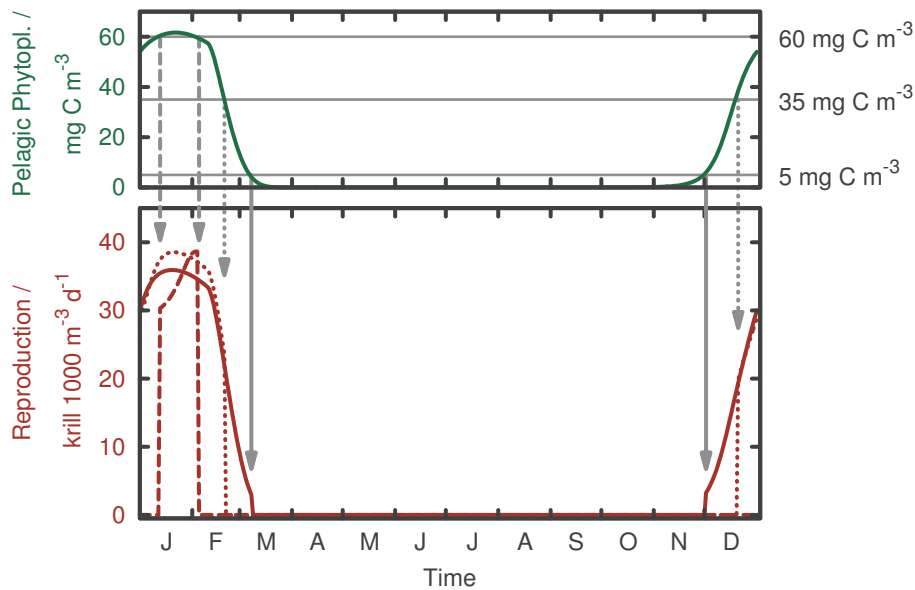


FIGURE 2.5.: Temporal dynamics of the reproduction over the course of one year for the food/food clock setup. The reproduction flux (bottom) is shown exemplarily for three different values of the critical food concentration: $\text{crit}_{\text{food}} = 5 \text{ mg C m}^{-3}$ (solid), $\text{crit}_{\text{food}} = 35 \text{ mg C m}^{-3}$ (dotted) and $\text{crit}_{\text{food}} = 60 \text{ mg C m}^{-3}$ (dashed). The arrows mark the day of the year where the pelagic phytoplankton concentration (top) falls below or exceeds the critical food concentration.

food concentrations significantly shorten the reproductive season (Figure 2.5). Especially important is that they prohibit reproduction during times when the pelagic phytoplankton concentrations are still very high. For critical values above the pelagic phytoplankton maximum of $61.66 \text{ mg C m}^{-3}$, the krill density does not change compared to the reference run because krill never receives a cue to switch off the reproduction. It is questionable whether this behaviour is biologically reasonable, but it is in any case very unlikely that krill has adapted to such a high critical value.

Food/Light Clock: The food/light clock looks the most complex of the four clocks, because both – food as the on-switch and daylength as the off-switch – affect the density (Figure 2.6, right). Increasing the critical food concentration decreases the krill density. For critical food concentrations above the pelagic phytoplankton maximum of $61.66 \text{ mg C m}^{-3}$ krill dies out because the reproduction is never switched on.

For values of the critical daylength below 6 hours, the reproduction is always switched on which is equivalent to the reference run. For values above the maximum daylength of 18.18 hours, the clock is never switched off. Again, it is questionable whether this is biologically reasonable, but critical values that high are in any case very unlikely. For

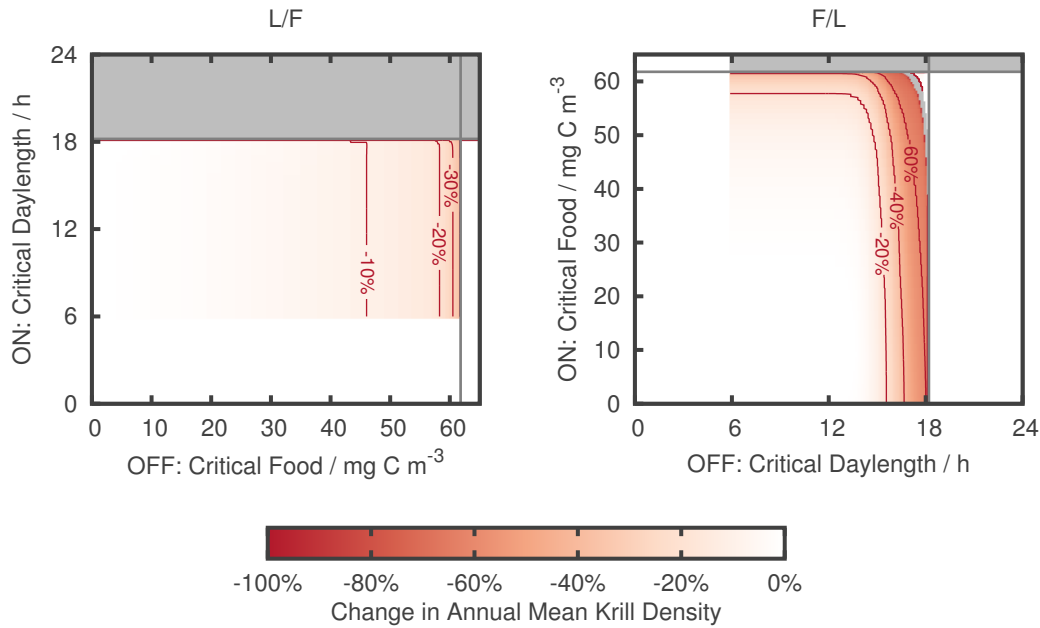


FIGURE 2.6.: Relative change in annual mean krill density in dependence on the critical values of the light/food clock setup (left) and the food/light clock setup (right). The changes in density were calculated for each critical value relative to the reference run. The grey line marks the maximum daylength and the maximum food concentration, respectively. The grey areas denote critical values for which krill dies out.

moderate values of the critical daylength, an increase in the critical value leads to a decrease in krill density. This effect is stronger than the effect of the critical food concentration because times with a normally high reproduction rate are cut off.

If both of the parameters are high but still below the maximum possible value, krill dies out because the reproductive season becomes too short. When the parameters are increased even further, it seems that krill densities increase again. The high values in food concentration needed to switch on the clock occur later in the year than the daylength that switches the clock off. That means that the clock is turned on for almost the whole year. From a biological point of view, this behaviour would have no advantage compared to the reference run and is thus very unlikely.

2.3.2. COMPARISON OF THE DIFFERENT CLOCKS

From the figures above, it is difficult to compare how much the effects of the different clocks differ – especially for the combined food and light clocks. Figure 2.7 shows the relative frequencies of different effect strengths independent of the actual critical values. In this representation, it is clearly visible that the clocks where the daylength acts as a cue to terminate the reproduction show a different behaviour compared to those where the

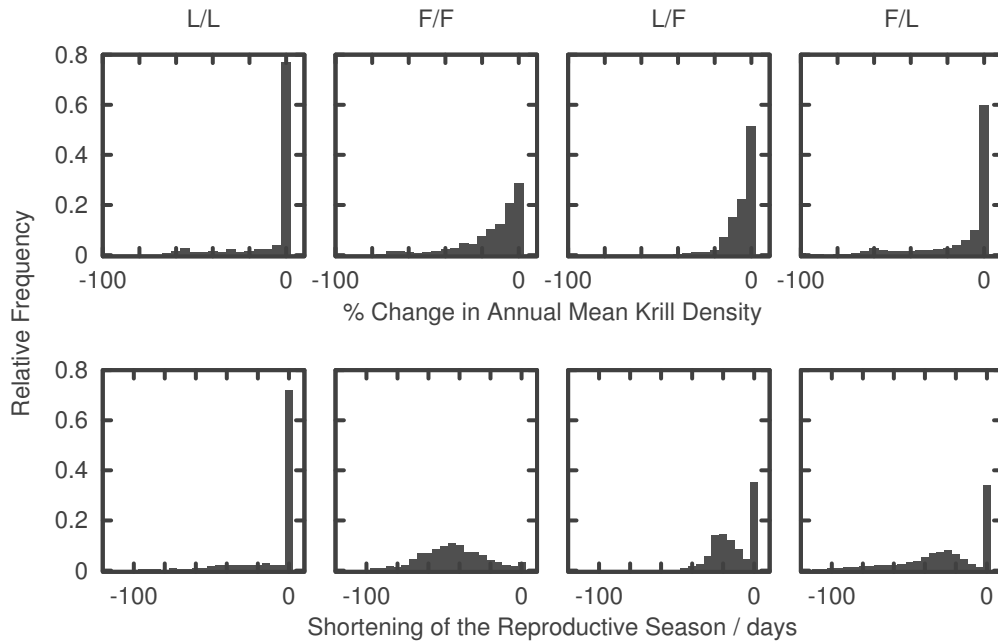


FIGURE 2.7.: Relative frequencies of the relative changes in mean krill density (top) and and the shortening of the reproductive season (bottom) for the four different clock setups. Considered are only relative changes for critical values below the maximum daylength and food concentration, respectively.

reproduction is terminated by the food availability. For the light-terminated clocks (L/L and F/L), most critical value combinations have no effect on the mean krill density (Figure 2.7, top). In contrast to that are the food-terminated clocks (F/F and L/F), where the distribution of the decrease in mean density is broader. This means that more critical value combinations have an effect on the density.

The reason for the difference between the clocks becomes clear when looking at the relative frequency histogram of the shortening of the reproductive season (Figure 2.7, bottom). For the light/light clock, almost 80% of the critical values do not lead to a shortening of the reproductive season. For the food/light clock the effect is less pronounced – only approximately 40% of the critical values do not change the length of the reproductive season. In addition, there is a second peak in the histogram around -20 days. The reproductive season of the food/food clock is shortened much stronger for all critical values and distributed around -45 days. This is a decrease of 6 weeks compared to the reference run. The light/food clock is somewhere in-between the food/food and food/light clock: approximately 40% of the critical values have no effect on the length of the reproductive season, but there is also a large proportion of critical values that shortens the reproductive season by about one month.

2.4. SHORT SUMMARY

One essential adaptation of krill to the seasonal environment is the timing of the reproduction to times with high food availability. This timing is thought to be controlled by a biological clock, which is triggered by some environmental factor. Despite many experimental studies, it is not clear how exactly this timing system works and which environmental factors are responsible for triggering the reproduction. To study this role of the environment, the model described in Chapter 1 was extended by a biological clock. The clock initiates and terminates the reproductive season depending on the state of an environmental cue. To examine the implications of different possible trigger factors, the clock was set up with all four combinations of daylength and food availability as a cue to start and/or terminate the reproduction. All of these four clock scenarios lead to a decrease in krill density compared to the reference run without a clock described in Chapter 1. The clock setups with daylength as an environmental factor have only a significant impact if the critical daylength triggering the clock is high. In contrast, the clock setups with food availability as an environmental factor shorten the reproductive season even for low critical food concentrations and thus lead to a stronger decline in krill densities.

3

THE IMPACT OF CLIMATE CHANGE ON KRILL

3.1. INTRODUCTION

Sea ice decline, temperature rise, ocean acidification and changes in the circulation patterns are some of the environmental changes that krill is already facing or expected to face in the future (Flores et al., 2012a). In addition, the krill fishery in the Atlantic sector of the Southern Ocean is already operating for a longer part of the year than in the past and is projected to increase even more in the future (Nicol et al., 2012). These environmental and social factors are likely to increase the pressure on the krill population, but how krill will react is so far unknown.

The annual extent of sea ice in the Antarctic is highly variable on a temporal scale as well as a spatial scale. Overall, the sea ice cover has increased from 1979 to 2012 by 1.5% per decade (Vaughan et al., 2013). On a regional scale, however, the picture looks very different. While sea ice extent is increasing in the Ross Sea, it is decreasing in the adjacent Amundsen and Bellingshausen Seas. In the Atlantic sector of the Southern Ocean – the area with the highest krill densities –, sea ice extent is particularly decreasing in winter and spring (Vaughan et al., 2013). Simulations for the end of the century predict a further decrease in sea ice extent of 33% (Bracegirdle et al., 2008).

Maybe even more crucial for krill than the spatial extent is the temporal shortening of sea ice season. From 1979 to 2011, there has been a continuous trend of later sea ice advance and earlier sea ice retreat in the Scotia Sea and the Amundsen and Bellingshausen Seas with a shortening of the sea ice duration of 3 months within that period (Stammerjohn et al., 2008,

2012). Considering the expected strong decrease in sea ice extent, a further shortening of the sea ice season is likely. The life-cycle of krill is strongly tied to the sea ice dynamics. A change in the extend of the sea ice and timing of the advance and retreat could have a profound effect on the recruitment and the survival when the sea ice biota as a food source and the ice itself as a shelter vanish.

Although the temperature rise in the water column is projected to be small compared to the surface air temperature, surface water temperatures around Antarctica are increasing (Flores et al., 2012a). Around South Georgia – a major distribution area of krill – summer temperatures have increased by 0.9 °C and winter temperatures by 2.3 °C from 1925 to 2006 (Whitehouse et al., 2008). This trend of increasing temperatures is projected to continue for the rest of the century (Bracegirdle et al., 2008). The seemingly small increase in temperature could have a significant impact on krill considering that the temperature difference in his whole distributional range is only around 7 °C (Flores et al., 2012a). However, it is not clear yet whether that impact will be positive or negative. On the one hand, it has been found that krill reduce their growth above 0.5 °C, but on the other hand, increasing metabolic rates at higher temperatures might favour krill growth and survival (Atkinson et al., 2006; Tarling et al., 2006).

The Southern Ocean is predicted to be a major sink of the increasing atmospheric CO₂ during the remainder of this century (Turner et al., 2014). As a consequence, many organisms will probably be severely affected by ocean acidification. Krill embryo development has already been shown to be negatively affected by elevated pCO₂ (Kawaguchi et al., 2011, 2013). Adult krill increase their metabolic activity when exposed to elevated pCO₂ (Saba et al., 2012). The resulting higher energetic demand might be especially difficult to maintain in winter when food is scarce. Besides these direct effects on krill, the phytoplankton community might change due to ocean acidification, which would pose an additional stress on the krill population (Constable et al., 2014).

How the circulation patterns will change in the future is largely unknown. Upwelling of nutrient rich waters might increase through increased wind stress, but this might be counteracted by increased stratification due to increasing temperatures and decreasing salinity of the upper ocean (Turner et al., 2014). As a consequence, food availability for krill might be enhanced by the increased nutrient input, but it is also possible that the phytoplankton composition or productivity changes to the disadvantage of krill (Flores et al., 2012a).

There are still many uncertainties in the projections of future environmental conditions, but Hill et al. (2013) projected that the krill habitat in the Atlantic sector of the Southern Ocean could be significantly reduced. As a consequence, krill might be forced to move further south, where the conditions might be similar to the ones it experiences now (Siegel, 2005; Atkinson et al., 2012; Flores et al., 2012a; Mackey et al., 2012). Although the sea ice conditions could remain the same, other environmental conditions are likely to be different at higher latitudes. Especially with regard to a possible light-mediated biological clock, the different light regime could have profound effects on the krill population. If krill does not change its distribution area, it is questionable whether krill can adapt to future conditions (Flores et al., 2012a). If they cannot sustain their current densities, a decline would severely affect krill's

predators and likely change the whole Southern Ocean Ecosystem (Fraser and Hofmann, 2003; Trivelpiece et al., 2011).

3.2. MODEL CHANGES

As discussed in the previous section, the environment of the Southern Ocean is undergoing a multitude of changes. Especially the sea ice cover – which is very important in the krill life cycle – is projected to continue to decrease (Bracegirdle et al., 2008). Two possible scenarios have been suggested as a mechanism for krill to cope with the changes in its environment: (1) Moving southward to areas where the sea ice conditions are the same as they are now in the current distribution area of krill (Siegel, 2005; Atkinson et al., 2012; Flores et al., 2012a; Mackey et al., 2012); or (2) Adapting to the changing sea ice conditions in the current distribution area (Flores et al., 2012a). Using the model developed in this thesis, it is possible to simulate both of these scenarios and analyze how krill will react to the changes in its environment – particularly with regard to the different clock setups described in Chapter 2.

3.2.1. SCENARIO 1: KRILL MOVES SOUTH

Simulating a southward shift in krill distribution does not require any modifications in the model. Merely the latitude in the calculation of the astronomical irradiance and the daylength has to be varied (see Section 1.2.1.2 for details).

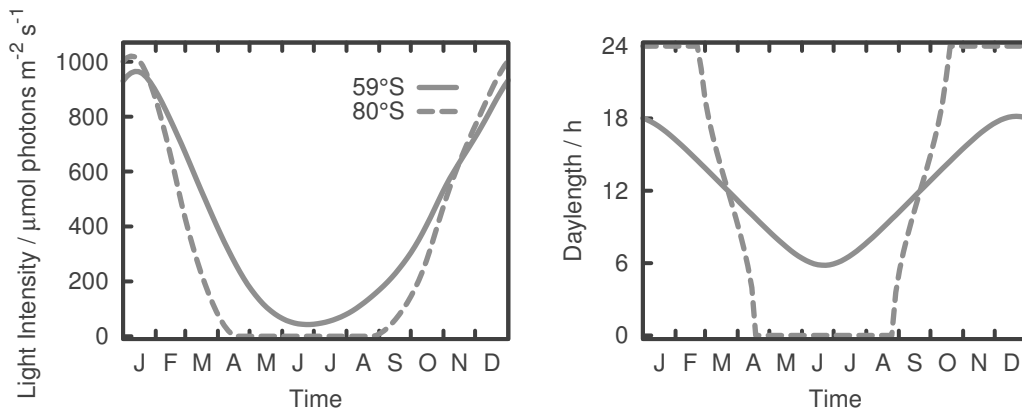


FIGURE 3.1.: Temporal dynamics of the daily averaged light intensity at the sea surface (left) and the daylength (right) over the course of one year for 59°S (solid line) and 80°S (dashed line).

Krill moving towards higher latitudes will experience a very different light regime. Moving from the current area at 59°S (the latitude of the reference run) to the extreme of 80°S will lead to an increase in daylength by 6 hours and more in summer, but also 4 months of total darkness in winter compared to the current 6 hours of light (Figure 1.3). In addition, the minimum light intensity is lower and the period of low intensities in winter last longer further south, but the maximum light intensity in summer is not much higher than it currently is.

3.2.2. SCENARIO 2: KRILL EXPERIENCES A SHORTER SEA ICE SEASON

If krill will remain in their current distribution area, they will probably face a shorter sea ice season. To simulate a shortening of the sea ice season, a simple sea ice function was fitted to the sea ice function used in reference run (Figure 3.2).

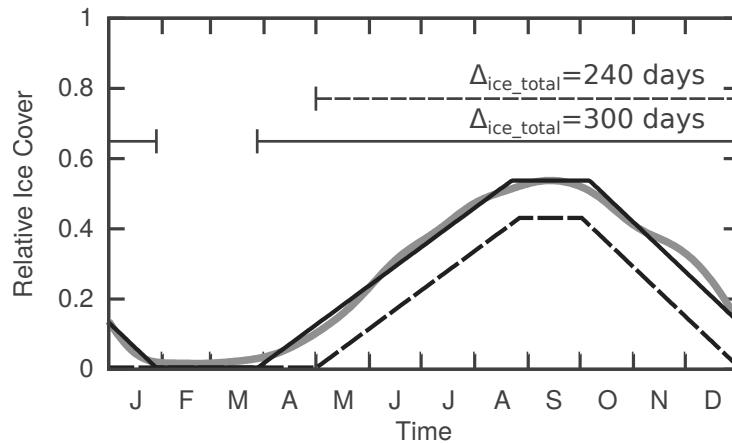


FIGURE 3.2.: Temporal dynamics of the simple ice cover over the course of one year. The dark grey line shows the function $f_{ice}(t)$ used in the reference run. The solid black line shows the simple ice function with the same length of the ice season ($\Delta_{ice_total} = 300$ days). The dashed line shows an example of a shorter ice season ($\Delta_{ice_total} = 240$ days).

The simple function has only the total length of the sea ice season Δ_{ice_total} as a free parameter (see Section A.4 for details). The relative times the sea ice needs to freeze and melt and the time of the sea ice maximum remain the same. This results in a decrease of the maximum for shorter sea ice seasons.

3.3. RESULTS

The aim of this section is to characterize how krill will react to the two different climate change scenarios described in the previous section. For the first scenario – krill moves south – all latitudes between the current 59 °S and 80 °S are considered. For the second scenario – krill experiences a shorter sea ice season – the sea ice season can be shortened by up to 300 days, which is equivalent to an ice free environment. Krill living at 80 °S or in a completely ice free environment is probably unrealistic, because it would involve a drastic melting of the sea ice and for the 80 °S even a disintegration of part of the shelf ice. These two values should rather represent a worst case scenario.

For both scenarios, the reference model (i.e. the setup without a clock) and the four different clock scenarios are analyzed respectively. The interesting question is whether krill with a certain clock setup currently living at 59 °S would be able to live at a different latitude or under different ice conditions. Therefore, the annual mean densities under climate change are given relative to the density at 59 °S with the same clock setup and parametrization. For the clock parametrization, only critical values for which krill survives under the current conditions – at 59 °S and 300 days of sea ice – are considered. In addition, the combined clock setups (i.e. light/food and food/light) are reduced to two cross sections in the parameter space at 12 hours and 35 mg C m⁻³ respectively.

3.3.1. SCENARIO 1: KRILL MOVES SOUTH

Following the retreating ice edge and moving further south has an overall positive effect on krill density (Figure 3.3). Compared to the annual mean krill density at 59 °S, the density slowly increases until a steep increase at the polar circle (66.5 °S) and again a slow increase afterwards. Without a clock (grey lines), the mean krill density at 80 °S is 65% larger than the krill density at 59 °S.

The reason for the overall increase in krill density with latitude – and especially the strong increase at the polar circle – is the increase in phytoplankton during summer due to the longer days. Figure 3.4 (left) shows the light-dependent limitation factor for phytoplankton growth over one year for different latitudes. This growth factor depends on the sea ice coverage, light intensity, daylength and mixed layer depth. Since it combines all environmental factors, it is a good proxy for the growth potential of pelagic phytoplankton. With increasing latitude, pelagic phytoplankton can start to grow earlier in the year. In addition, growth in summer is strongly enhanced south of the polar circle.

The effect of the increased growth on the krill can be seen in Figure 3.5, which shows the annual dynamics of phytoplankton and krill for 80 °S (dashed line) compared to the reference run at 59 °S (solid line) for krill without a clock. At 80 °S, the pelagic and the sea ice phytoplankton concentrations are much higher in spring and summer due to the longer days and higher light intensities. Due to these increased concentrations, krill has more food available to mature and reproduce. In addition, the reproductive season starts earlier at 80 °S, because the pelagic phytoplankton has sufficient light to grow earlier in the year. This earlier

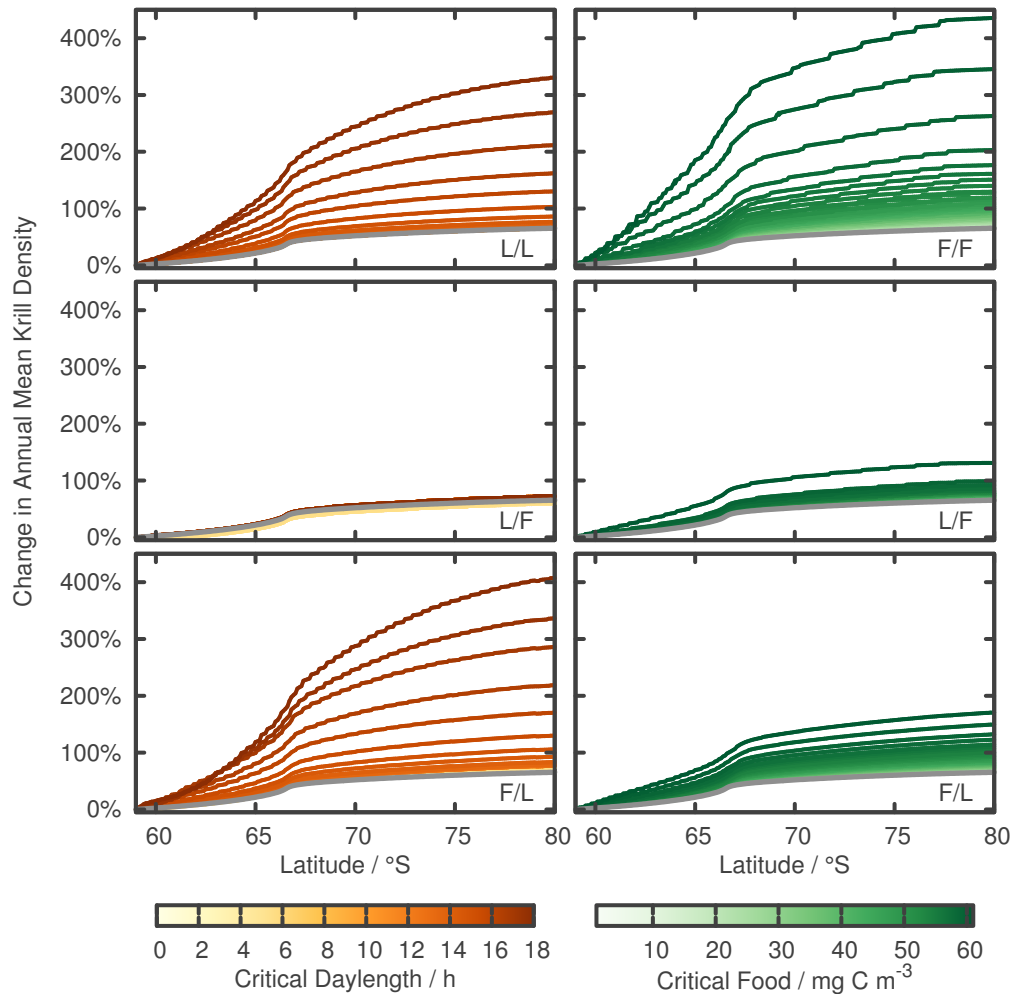


FIGURE 3.3.: Relative change in annual mean krill density in dependence on the latitude. Shown are the results for the light/light clock (top left), the food/food clock (top right), the light/food clock (middle) and the food/light clock (bottom) for different values of the critical daylength and critical food concentration. The grey line shows the results of the reference model (i.e. without a clock). The changes in density were calculated for each critical value relative to the density at 59°S with the same critical value. For the variation in critical daylength of the light/food and food/light clock, the critical food concentration was kept constant at 35 mg C m⁻³. For the variation in critical food of these two clocks, the critical daylength was kept constant at 12 hours.

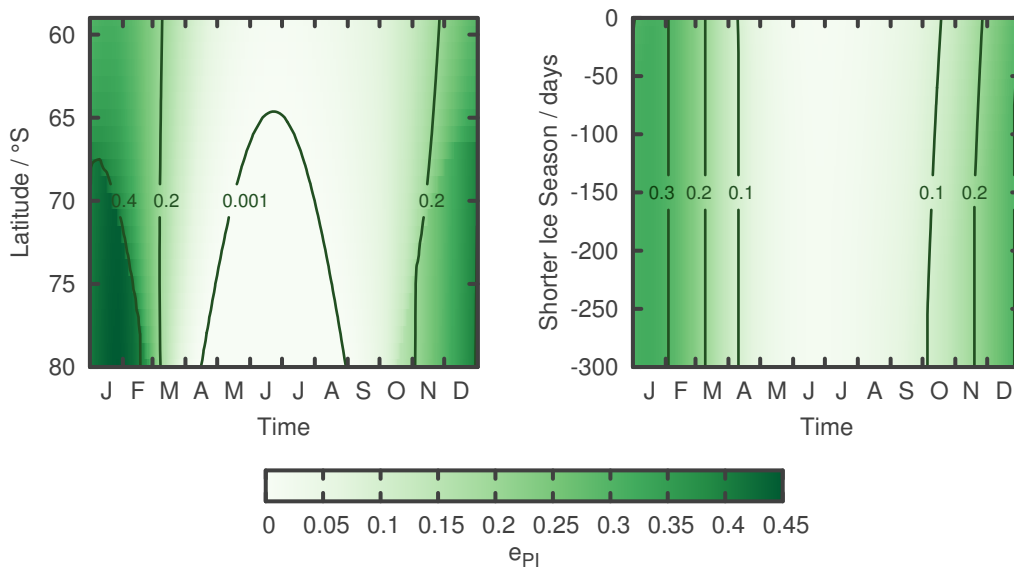


FIGURE 3.4.: Dependence of the light-dependent growth factor for pelagic phytoplankton e_{PI} on the time of the year for the two climate change scenarios. Shown are the dependence on the latitude (left) and the dependence on the length of the sea ice season (right).

growth also leads to an earlier increase in maturation and thus an earlier increase in adult krill and consequently an increase in juvenile krill.

If krill has a light/light clock and a critical daylength below 13 hours, the dependence on the latitude is the same as without a clock (Figure 3.3, top left). For higher critical daylengths, moving south leads to a strong increase in krill density up to 330% for a critical daylength of 18 hours at 80 °S. It might seem that possessing a clock with a high critical daylength is an advantage under climate change. However, it is important to remember that the change in krill density was calculated relative to the density at 59 °S with the respective critical daylength and that the analyses in the previous chapter have shown that krill with high critical daylengths have lower densities at 59 °S than without a clock (Figure 2.3). The high increase in relative density at 80 °S is thus only a compensation of the lower densities at 59 °S. In fact, the absolute densities at 80 °S are the same for all critical daylengths and the reference model (Appendix A.5).

The food/food clock leads to the strongest increase in density with latitude of 435% for a critical food concentration of 60 mg C m⁻³ (Figure 3.3, top right). The increase in density is less strong for lower critical values, but stronger than for the reference model. Again, the strong increase is due to the lower absolute densities at 59 °S for high critical values (Figure 2.3). At 80 °S, the difference in absolute density between different critical values has almost vanished (Appendix A.5). South of the polar circle, low critical values even lead to slightly higher absolute densities than for the reference model, which is due to the earlier growth of pelagic phytoplankton.

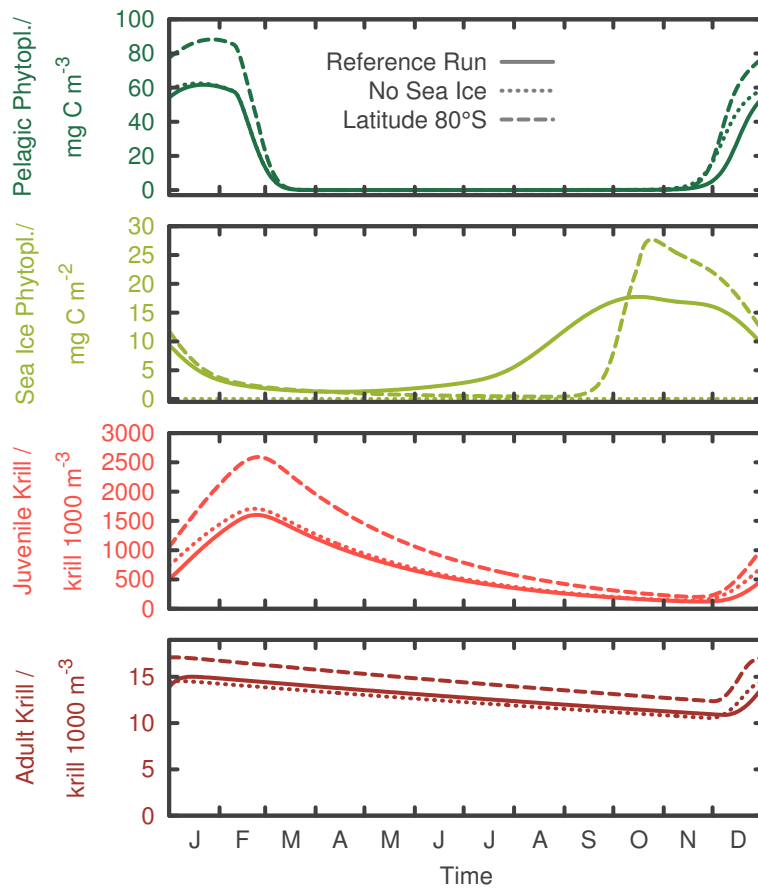


FIGURE 3.5.: Temporal dynamics of the state variables over the course of one year for the two climate change scenarios. Shown are the dynamics of pelagic phytoplankton (top), sea ice phytoplankton (second from top), juvenile krill (third from top) and adult krill (bottom) for the reference run without a clock (solid line) and the worst case of the two scenarios without a clock, respectively. Iron is not shown because it is not limiting phytoplankton growth in any of the scenarios.

The light/food clock shows the smallest change in annual mean density (Figure 3.3, middle). Different critical daylengths – which trigger the start of the reproduction – have no effect compared to the reference model (Figure 3.3, middle left). For high critical food concentrations – which trigger the termination of the reproduction –, the increase in density with latitude is stronger than for the reference model (Figure 3.3, middle right), but the absolute density is always lower (Appendix A.5).

For the food/light clock, an increase in the critical daylength – which triggers the termination of the reproduction – leads to a similar behaviour as for the light/light clock, but the increase with latitude is even stronger (up to 400%) (Figure 3.3, bottom left). A critical daylength above 13 hours even leads to higher absolute densities south of the polar circle compared to the reference model (Appendix A.5). The same is true for an increase in the critical food – which triggers the start of the reproduction –, even though the change in krill density compared to 59°S is less strong (Figure 3.3, bottom right).

To summarize the above, moving south leads to an increase in density compared to 59°S for all critical values. Except for the light/food clock, critical daylengths above 13 hours lead to a stronger increase in relative density compared to the reference model. Higher critical food concentrations also lead to higher increases in relative densities. The food/light clock is the clock setup which also leads to higher absolute densities compared to the reference model for latitudes south of the polar circle. Therefore, this clock setup would actually be advantageous for krill under climate change.

3.3.2. SCENARIO 2: KRILL EXPERIENCES A SHORTER SEA ICE SEASON

Similar to moving further south, a shorter sea ice season at 59°S has a positive effect on the krill density (Figure 3.6). However, the magnitude of the increase in density is an order of magnitude smaller. Even under totally ice free conditions (i.e. –300 days), the maximum increase in annual mean krill density is less than 45%. Without a clock (grey lines), the maximum increase is even less than 10% under totally ice free conditions. In general, only the first 50 to 100 days of shortening of the sea ice season lead to an increase. For a stronger shortening of the sea ice season, the annual mean krill density approaches saturation.

For the food/food, food/light and light/food clocks, the level of saturation generally increases with increasing critical food concentrations (Figure 3.6, right). The effect is highest for the food/food clock and lowest for the light/food clock. The critical daylength has a much smaller effect on the krill density (Figure 3.6, left). For the food/light clock, a change in the critical daylength – which triggers the termination of the reproduction – has no effect at all compared to the reference model (Figure 3.6, bottom left). For the light/food clock where light triggers the start of the reproduction, high values of the critical daylength lead to a slight increase in annual mean krill densities compared to the reference model for a shortening of the sea ice season of more than 100 days. For the light/light clock and a critical daylength below 13 hours, there is no difference in the change in density compared to the reference model (Figure 3.6, top left). The change in krill density for –300 days of sea ice generally

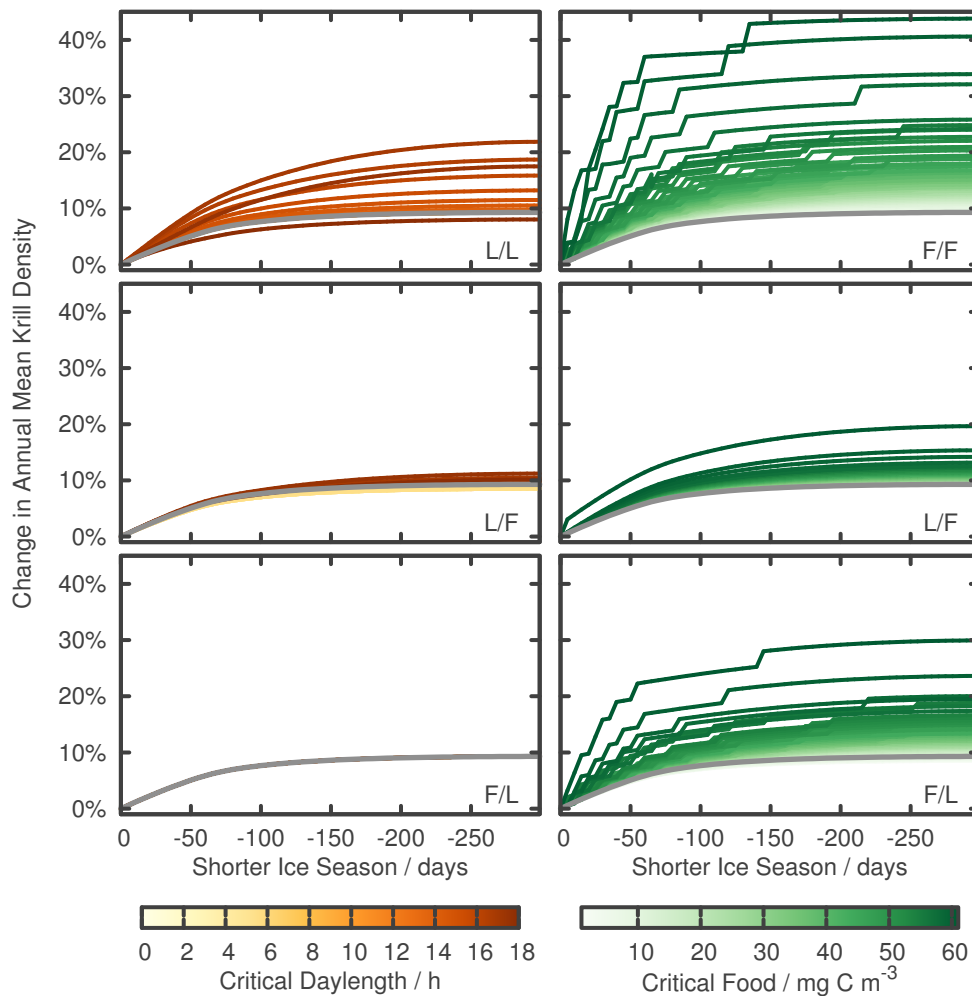


FIGURE 3.6.: Relative change in annual mean krill density in dependence on the length of the sea ice season. Shown are the results for the light/light clock (top left), the food/food clock (top right), the light/food clock (middle) and the food/light clock (bottom) for different values of the critical daylength and critical food concentration. The grey line shows the results of the reference model (i.e. without a clock). The changes in density were calculated for each critical value relative to the density at 59°S with the same critical value. For the variation in critical daylength of the light/food and food/light clock, the critical food concentration was kept constant at 35 mg C m⁻³. For the variation in critical food of these two clocks, the critical daylength was kept constant at 12 hours.

increases for higher critical values, but for critical values above 17 hours it decreases again.

The reason for the relatively small impact of the shortening of the sea ice season is again connected to the phytoplankton. In the model, krill is coupled to the sea ice only indirectly via the phytoplankton. The sea ice phytoplankton has only a very minor effect on the krill dynamics in the model and the effect of its absence in an ice free ocean is negligible (Figure 3.5, dotted line). The pelagic phytoplankton, in contrast, is very important for the reproduction and maturation of krill. Pelagic phytoplankton growth strongly depends on the light intensity which in turn depends on the sea ice coverage. However, the sea ice is strongest during the winter when the light intensity is in any case insufficient for phytoplankton growth. For this reason, the effect of a shorter ice season on the light-dependent growth factor of pelagic phytoplankton e_{PI} is very small (Figure 3.4, right). As a result, pelagic phytoplankton under ice free conditions starts to grow a few days earlier in spring but the concentrations during the rest of the year are the same as in the reference run (Figure 3.5, dotted line). This leads to a slightly earlier maturation and reproduction and consequently an earlier increase in juvenile and adult krill densities, but does not significantly change the dynamics.

It might seem that possessing a clock is an advantage under climate change although the effect is less strong than for the first climate change scenario. It is again important to remember that the change in krill density was calculated relative to the density with the current sea ice conditions and with the respective critical value. As described in the previous chapter, higher critical values lead to lower krill densities under the current sea ice conditions (Figure 2.3). The absolute krill densities only slightly increase for shorter ice seasons for most critical values (Appendix A.5).

3.4. SHORT SUMMARY

The environment in the Southern Ocean is already undergoing changes. For example, the ice coverage in the Atlantic sector of the Southern Ocean – the main distribution area of krill – is already declining and projected to further decline in the future. As a consequence, krill might be forced to move further south to escape the bad conditions in his current distribution area. At higher latitudes, krill will experience different light conditions, which could have profound effects especially with regard to a biological clock. A second possible scenario is that krill stays in its current distribution area, where it will likely experience a later advance and earlier retreat of the sea ice. For both scenarios, the results of the model suggest that independent of the clock, krill densities will increase due to increased phytoplankton growth. The reasons for the increased growth are the increased light intensities and longer days at higher latitudes in summer in the first scenario and the increased light in the water column due to the shorter sea ice seasons in the second scenario. The latter affects only the low light intensities in winter and early spring when phytoplankton growth is strongly limited by light. Thus, the increase in krill density due to the shorter sea ice season in the second scenario is not as strong as the increase due to the change in latitude in the first scenario.

4

DISCUSSION AND CONCLUSIONS

The aim of this thesis was to examine the role of a biological clock in krill reproduction and the effect of climate change on the krill dynamics. The basis for these studies forms a new krill model, which was developed in this thesis (**Chapter 1**). The model is a mechanistic NPZ-model describing the dynamics of iron, pelagic and sea ice phytoplankton and juvenile and adult krill. It was developed based on knowledge about key processes in the krill life cycle and parametrized with values obtained from literature. There is evidence that the model provides a good description of the krill population dynamics observed in nature.

First of all, the results of the reference simulations without clock or climate change have shown that the developed model can reproduce the qualitative seasonal dynamics of Antarctic krill previously described by Siegel (2000) (and recently summarized in Siegel (2016)). In addition, the average krill abundance per area (i.e. krill density \times mixed layer depth) of 44 krill m^{-2} obtained with the model agrees very well with recently published, measured averages for the Atlantic sector of the Southern Ocean of 35 to 75 krill m^{-2} (Siegel and Watkins, 2016). Secondly, the krill population in the model is controlled by the ability to successfully mature from juveniles into adults. This has also been suggested by Meyer (2012) as the key process for the development of the krill population.

Although the sensitivity analysis has shown that the model is not very sensitive to changes in the maturation parameters, the model reacts sensitive to the maturation process as a whole. An increased reproduction, for example, does not necessarily lead to an increase but to a decrease in adult krill densities. Higher reproduction decreases the amount of food per juvenile krill, which can lead to less maturation and hence less adult krill.

With strongly increased maturation parameters, the krill dynamics change quantitatively and the stable annual cycles can develop into multi-annual cycles or chaotic behaviour. The multi-annual cycles can have periods of up to 15 years but these are combinations of shorter

periods of decreasing density with a maximum length of eight years. Multi-annual cycles in krill densities with periods of up to eight years have also been observed in nature (Hewitt et al., 2003). The interannual variability in krill density has so far been attributed to changing environmental factors such as sea-ice conditions (Siegel and Loeb, 1995; Loeb et al., 1997; Fraser and Hofmann, 2003; Atkinson et al., 2004), primary production (Steinberg et al., 2015), temperature (Fielding et al., 2014) or climatic variability such as Southern Annual Mode (SAM) (Saba et al., 2014) and El Niño-Southern Oscillation (ENSO) (Quetin and Ross, 2003; Loeb et al., 2009; Ross et al., 2014). In the model, in contrast, the cycles emerge even though these environmental factors show either stable annual cycles (phytoplankton and sea ice conditions) or are not included (all others). It is not completely clear how the multi-annual cycles emerge in the model, but it suggests that the emergence of these cycles in nature is also not fully understood. The model shows that the interannual variability is not necessarily a result of changing environmental factors as so far assumed, but can be caused by processes that are inherent in the krill population such as the maturation process.

In contrast to previous krill models, this new model explicitly considers the dynamics of krill's food sources pelagic and sea ice phytoplankton and their dependence on environmental factors. The results have shown that it is very important to know the annual dynamics of the phytoplankton correctly, because it is an important factor for krill maturation and reproduction. On the other hand, pelagic phytoplankton is only bottom-up controlled and not top-down by the krill feeding, i.e. it is barely influenced by the krill. Including phytoplankton as a time series should thus give the same results. These time series could be obtained from measurements or from more detailed phytoplankton models. In addition, the iron dynamics can be completely neglected as long as pelagic phytoplankton growth is always limited by light and never by iron.

It has been observed that mature krill do not start the ovarian cycle under low food conditions although they have already developed their sexual organs (Kawaguchi et al., 2007; Yoshida, 2009). This behaviour suggests that the ovarian cycle – i.e the actual spawning season – is probably not driven by an endogenous clock, because an endogenous clock would continue with its normal period even if the zeitgeber is missing. It is more likely that krill depends on some proximate factor, which tells the organism that the conditions are good enough for spawning or at least will be in the near future. The same or another proximate factor could also tell krill to stop spawning at the end of summer, when the conditions are not good enough anymore for the females to spawn or for the larvae to survive. One aim of this thesis was to test whether daylength or food availability could be used as a proximate factor to start and/or terminate the reproduction. To do so, the effects of four different clock setups on the krill dynamics were investigated (**Chapter 2**): The reproduction is either started and terminated at a certain critical daylength; It is started and terminated at a certain critical food concentration; It is started at a certain critical daylength and terminated at a certain critical food concentration or vice versa.

In general with all four clock setups, the model still exhibits the same qualitative annual cycle as the reference run. Therefore, none of the clock setups can be excluded from the analysis. Depending on the critical daylength or food concentration, the biological clock has

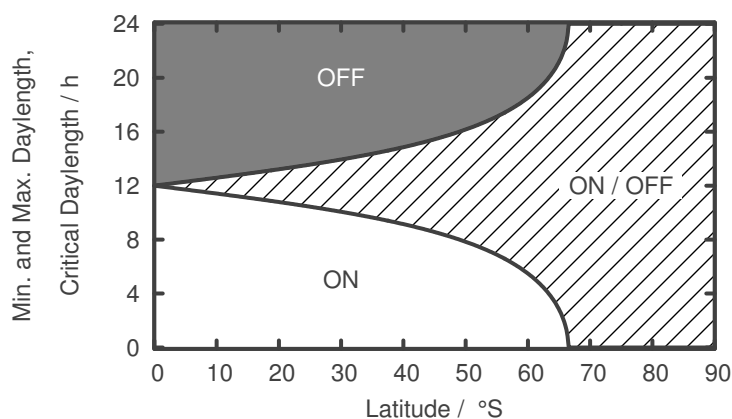


FIGURE 4.1.: Dependence of a light-mediated biological clock on the daylength and the latitude. The minimum and maximum daylength at a certain latitude are shown as grey lines. For critical daylengths below the minimum daylength, the clock is always switched on (white area). For critical daylengths above the maximum daylength, the clock is always switched off (grey area). In-between the clock can be switched on and off (striped area).

either no quantitative influence on the krill density compared to the reference run, it leads to a decrease in density or krill dies out. The latter case applies to very high values of the critical daylength or the critical food concentration, which are above the respective maximum at 59°S (18 hours or 61 mg C m⁻³). These critical values can already be excluded as they are biologically irrelevant. For the critical daylength, values below 16 hours are biologically unfeasible due to the latitudinal distribution of krill. It is known that the distribution of krill is limited by the Polar Front, which can be as far north as 50°S (Atkinson et al., 2004). At this latitude, the maximum daylength is 16 hours and thus the critical daylength has to be below this value for krill to be able to switch on the clock for at least part of the year (Figure 4.1). With a critical value close to 16 hours, krill would be very vulnerable to transport by currents further north. Thus, a realistic critical daylength is probably a few hours lower than the 16 hours. The critical food concentration is more difficult to restrict to a certain range of feasible values. Very high values close to the maximum food concentration are unlikely, because krill would be very vulnerable to interannual changes in primary production. The lowest possible value is probably restricted by the amount of food that krill need to sustain its metabolism, but the exact value is not known and this process is not included in the model.

In the model, none of the four clock setups shows a particularly strong advantage or disadvantage compared to the other setups. However, some of them are more likely from a biological point of view than the others. With the food concentration acting as a cue to start the ovarian cycle the reproductive season is shortened and shifted towards later times in the season. On one hand, this could make sense because krill needs elevated food concentrations to fuel the ovarian cycle (Ross and Quetin, 1986). On the other hand, the shift of the reproductive season might prohibit larval krill to develop sufficiently far to survive

their first winter (Quetin and Ross, 1991). The latter problem can be avoided if the spawning season is terminated by a light cue. This would prevent reproduction at the end of summer when food concentrations are still high, but it would also ensure that the larvae still find enough food to develop before winter. A light cue as a termination of the reproduction would agree with the experimental results from Brown et al. (2011), which found that the regression cycle started earlier when krill were exposed to advanced winter light conditions. If krill possesses this type of clock, only a critical daylength above 12 hours would make a difference and shorten the reproductive period compared to the reference run.

Teschke et al. (2008) have suggested that light could also play a role for the onset of the reproduction. However, the model results show that pelagic phytoplankton grows very late in relation to the daylength cycle. The onset of the growth coincides approximately with the maximum daylength. Since the reproduction strongly depends on the phytoplankton, krill cannot start to reproduce many days before the maximum daylength occurs. If the reproduction would be triggered by the daylength as a proximate factor, the critical daylength would need to be close to 16 hours. However, critical daylengths that high have already been rejected due to the current latitudinal distribution of krill. Teschke et al. (2008) have already speculated that the light in their experiment only acted as a zeitgeber for the regression cycle and did not influence the ovarian cycle. This explanation would be in agreement with the model results.

The environmental conditions in the Southern Ocean are already changing and these changes are expected to continue (Flores et al., 2012a). Due to krill's central role in the Southern Ocean food web, it is crucial to understand how the krill population is affected by these changes. The results from the model simulations suggest an increase in krill densities under the analyzed climate change scenarios (**Chapter 3**). For krill following the retreating sea ice further south, the density increases up to 65% without a clock and up to 435% for certain clock setups compared to the density at 59°S. A more precise knowledge about the biological clock of krill would lead to more accurate predictions for future increases in krill density.

The strong increase in density is due to higher pelagic phytoplankton concentrations at higher latitudes and thus higher reproduction and maturation. Especially south of the polar circle, phytoplankton experiences very long days in summer combined with higher light intensities than at 59°S, which leads to enhanced krill growth. The long months without light do not influence the phytoplankton, because at all latitudes, light intensities are too low in winter for phytoplankton growth. Independent of the exact clock setup, krill can benefit from the changing environmental conditions further south and increase their density relative to 59°S. The absolute densities at high latitudes depend less on the parametrization of the clock, which suggests that the influence of the clock decreases with latitude.

If krill does not move south, they will experience changes in the sea ice conditions. The model results suggest that krill densities increase with decreasing sea ice, because the melting of the sea ice allows for more light to reach the water column. This increases phytoplankton growth, which in turn fuels the reproduction and maturation. However, the effect of the melting is not very strong, because the melting sea ice mainly increases the light in winter when it is insufficient for phytoplankton growth even in a totally ice free ocean. Independent

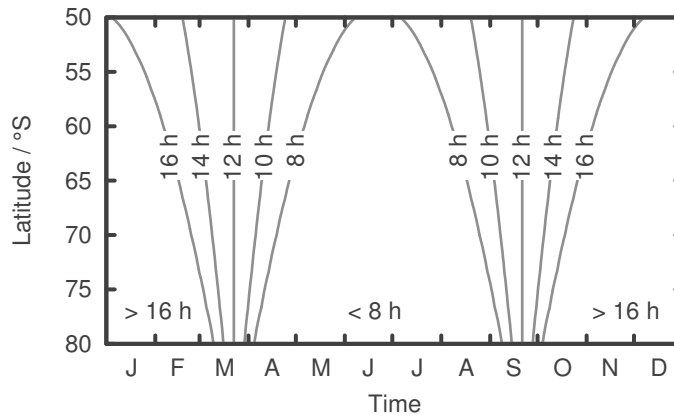


FIGURE 4.2.: Daylength in dependence on the day of the year and the latitude. Shown are only the daylengths that are feasible as a critical daylength for a biological clock.

of the clock setup, the increase in density due to a shortening of the ice season is a magnitude lower than the increase due to moving south.

This enormous increase in krill density in the model is in contrast to the already observed decline in krill density (Atkinson et al., 2004) and the expected continuation of this trend (Flores et al., 2012a). The truth is probably somewhere in-between the extremely optimistic predictions of the model and the pessimistic presumptions of other studies. Some other environmental effects not considered in this model will likely have a negative effect on krill, which could mitigate the positive effects of stronger phytoplankton growth. Increasing temperatures (Hill et al., 2013) and ocean acidification (Kawaguchi et al., 2011, 2013) are expected to reduce the krill habitat. Changes in the phytoplankton composition and competition with salps or other euphausiids could lead to an additional decline in densities (Flores et al., 2012a). In addition, only the positive effect of the melting sea ice – the increase in light in the water column – has been taken into account in the model. The potentially negative effect that the sea ice is missing as a feeding ground and shelter for larval krill in winter is missing. Since larval krill has no energy reserves like adult krill, it is questionable whether this loss can be compensated by the increased primary production in summer. The problem is also that krill will be able to follow the retreating ice only up to a certain extend, because krill need a depth of 700 to 1000 m for the successful completion of the developmental descent/ascent (Nicol, 2006). Hence, the southward movement is restricted by the shelf, which could mean that krill will experience different sea ice conditions in combination with different light conditions. The model developed in this thesis does not include any of these effects and likely favours a strong overestimation of the krill densities.

Meyer (2012) has speculated that the current match between the krill life cycle and their food could go out of phase under climate change. This effect, however, cannot be found in the model. Even as far south as 80°S, the pelagic phytoplankton starts to grow only 10 days earlier and for the ice free conditions the shift is even less. A change as little as 10 days is not expected to desynchronize the krill life cycle. If krill reproduction is started by a food

cue, the life cycle will in any case remain synchronized with the pelagic phytoplankton. If light triggers the reproduction and the critical daylength is biologically feasible (i.e. below 16 hours), the onset of the reproduction can be shifted by up to 30 days when krill moves south (Figure 4.2). For most critical daylengths, the shift will be much shorter and will barely influence the reproduction.

Summarizing the above, the two questions of the Southern Ocean Horizon Scan (Kennicutt II et al., 2015) mentioned in the preface can be addressed as follows:

Q.58 “How will climate change affect existing and future Southern Ocean fisheries, especially krill stocks?”:

The model results suggest an increase in krill density under climate change. This increase in density results from an increased phytoplankton growth due to the longer days in summer at higher latitudes or increased light intensities due to the melting of the sea ice. Earlier studies who predicted a decrease in density under climate change (e.g. Groeneveld et al., 2015) have not taken this change in the light conditions and the resulting effect on phytoplankton into account. This shows how important it is to use a 'bottom-up approach' when studying the effects of climate change, i.e. taking into account the effect of climate change on lower trophic levels. The same holds true for effects on the higher trophic levels and the fishery for which it is essential to understand the effect of climate change on krill. Some of the negative impacts of climate change might in fact be balanced by positive effects on lower trophic levels. The magnitude of the increase in krill density has probably been overestimated by the model, because other – possibly negative – environmental effects such as ocean acidification have not been included in the model. This stresses the importance of experimental and model studies analyzing the impact of multiple stressors to be able to make more precise predictions of the impact of climate change on krill.

Q.60 “What are the impacts of changing seasonality and transitional events on Antarctic and Southern Ocean marine ecology, biogeochemistry and energy flow?”:

The model shows that the seasonality plays – as expected – an important role in the krill life cycle. A particularly important aspect is that the availability of food confines the reproduction and maturation to a very short period of the year. The seasonality experienced by krill will probably change in the future, for example because krill moves further south and experiences a different light regime or because the sea ice conditions change. The model results suggest that the changing seasonality will not negatively impact the krill density and especially not lead to a collapse of the krill population. Since the phytoplankton will experience the changes as well, a mismatch between krill and its food appears unlikely. Even if it is assumed that krill has a biological clock, the model

shows no significant desynchronization between the life cycle of krill and the availability of its food. This again stresses the necessity of a bottom-up approach in modelling of climate change impacts.

REFERENCES

- Arrigo, K.R., 2014. Sea ice ecosystems. *Annual review of marine science* 6, 439–467.
- Arrigo, K.R., Thomas, D.N., 2004. Large scale importance of sea ice biology in the Southern Ocean. *Antarctic Science* 16, 471–486.
- Arrigo, K.R., Worthen, D., Schnell, A., Lizotte, M.P., 1998. Primary production in Southern Ocean waters. *Journal of Geophysical Research* 103, 15587–15600.
- Arrigo, K.R., Worthen, D.L., Lizotte, M.P., Dixon, P., Dieckmann, G.S., 1997. Primary Production in Antarctic Sea Ice. *Science* 276, 394–397.
- Arteaga, L., Pahlow, M., Oschlies, A., 2014. Global patterns of phytoplankton nutrient and light colimitation inferred from an optimality-based model. *Global Biogeochemical Cycles* 28, 648–661.
- Aschoff, J., 1981. A Survey on Biological Rhythms, in: *Biological Rhythms*. Springer US, Boston, pp. 3–10.
- Astheimer, H., 1986. A Length Class Model of the Population Dynamics of the Antarctic Krill *Euphausia superba* DANA. *Polar Biology* 6, 227–232.
- Astheimer, H., Krause, H., Rakusa-Suszczewski, S., 1985. Modelling Individual Growth of the Antarctic Krill *Euphausia superba* DANA. *Polar Biology* 4, 65–73.
- Atkinson, A., Meyer, B., Stübing, D., Hagen, W., Schmidt, K., Bathmann, U.V., 2002. Feeding and energy budgets of Antarctic krill *Euphausia superba* at the onset of winter–II. Juveniles and Adults. *Limnology and Oceanography* 47, 953–966.
- Atkinson, A., Nicol, S., Kawaguchi, S., Pakhomov, E.A., Quetin, L.B., Ross, R.M., Hill, S.L., Reiss, C.S., Siegel, V., Tarling, G.A., 2012. Fitting *Euphausia superba* into Southern Ocean Food-Web Models: A Review of Data Sources and Their Limitations. *CCAMLR Science* 19, 219–245.
- Atkinson, A., Shreeve, R.S., Hirst, A.G., Rothery, P., Tarling, G.A., Pond, D.W., Korb, R.E., Murphy, E.J., Watkins, J.L., 2006. Natural growth rates in Antarctic krill (*Euphausia superba*): II. Predictive models based on food, temperature, body length, sex, and maturity stage. *Limnology and Oceanography* 51, 973–987.

- Atkinson, A., Siegel, V., Pakhomov, E.A., Jessopp, M.J., Loeb, V.J., 2009. A re-appraisal of the total biomass and annual production of Antarctic krill. *Deep-Sea Research Part I* 56, 727–740.
- Atkinson, A., Siegel, V., Pakhomov, E.A., Rothery, P., 2004. Long-term decline in krill stock and increase in salps within the Southern Ocean. *Nature* 432, 100–103.
- Atkinson, A., Siegel, V., Pakhomov, E.A., Rothery, P., Loeb, V.J., Ross, R.M., Quetin, L.B., Schmidt, K., Fretwell, P., Murphy, E.J., Tarling, G.A., Fleming, A.H., 2008. Oceanic circumpolar habitats of Antarctic krill. *Marine Ecology Progress Series* 362, 1–23.
- de Baar, H.J.W., 1994. von Liebig's Law of the Minimum and plankton ecology (1899-1991). *Progress in Oceanography* 33, 347–386.
- de Baar, H.J.W., de Jong, J.T.M., Bakker, D.C.E., Löscher, B.M., Veth, C., Bathmann, U.V., Smetacek, V., 1995. Importance of iron for plankton blooms and carbon dioxide drawdown in the Southern Ocean. *Nature* 373, 412–415.
- Boyd, P.W., 2002. Environmental factors controlling phytoplankton processes in the Southern Ocean. *Journal of Phycology* 38, 844–861.
- Bracegirdle, T.J., Connolley, W.M., Turner, J., 2008. Antarctic climate change over the twenty first century. *Journal of Geophysical Research* 113, D03103.
- Brown, M., 2010. Environmental Effects on the Growth, Maturation and Physiology in Antarctic Krill (*Euphausia superba*) Over an Annual Cycle: An Experimental Approach. PhD thesis. University of Tasmania.
- Brown, M., Kawaguchi, S., King, R.A., Virtue, P., Nicol, S., 2011. Flexible adaptation of the seasonal krill maturity cycle in the laboratory. *Journal of Plankton Research* 33, 821–826.
- Buchholz, F., 1991. Molt Cycle and Growth of Antarctic Krill *Euphausia superba* in the Laboratory. *Marine Ecology Progress Series* 69, 217–229.
- Campolongo, F., Cariboni, J., Saltelli, A., 2007. An effective screening design for sensitivity analysis of large models. *Environmental Modelling and Software* 22, 1509–1518.
- Candy, S.G., Kawaguchi, S., 2006. Modelling growth of Antarctic krill. II. Novel approach to describing the growth trajectory. *Marine Ecology Progress Series* 306, 17–30.
- Capella, J.E., Quetin, L.B., Hofmann, E.E., Ross, R.M., 1992. Models of the early life history of *Euphausia superba*—Part II. Lagrangian calculations. *Deep-Sea Research Part A* 39, 1201–1220.
- Clarke, A., 1988. Seasonality in the Antarctic marine environment. *Comparative Biochemistry and Physiology* 90B, 461–473.

- Coale, K.H., Wang, X., Tanner, S.J., Johnson, K.S., 2003. Phytoplankton growth and biological response to iron and zinc addition in the Ross Sea and Antarctic Circumpolar Current along 170°W. *Deep-Sea Research Part II* 50, 635–653.
- Constable, A.J., Kawaguchi, S., 2012. Modelling growth and reproduction of Antarctic krill: implications of spatial and temporal trends in temperature and food for ecosystem-based management of krill fisheries. Report of the Working Group on Ecosystem Monitoring and Management , WG–EMM–12/38.
- Constable, A.J., Melbourne-Thomas, J., Corney, S.P., Arrigo, K.R., Barbraud, C., Barnes, D.K.A., Bindoff, N.L., Boyd, P.W., Brandt, A., Costa, D.P., Davidson, A.T., Ducklow, H.W., Emmerson, L., Fukuchi, M., Gutt, J., Hindell, M.A., Hofmann, E.E., Hosie, G.W., Iida, T., Jacob, S., Johnston, N.M., Kawaguchi, S., Kokubun, N., Koubbi, P., Lea, M.A., Makhado, A., Massom, R.A., Meiners, K., Meredith, M.P., Murphy, E.J., Nicol, S., Reid, K., Richerson, K., Riddle, M.J., Rintoul, S.R., Smith Jr, W.O., Southwell, C., Stark, J.S., Sumner, M., Swadling, K.M., Takahashi, K.T., Trathan, P.N., Welsford, D.C., Weimerskirch, H., Westwood, K.J., Wienecke, B.C., Wolf-Gladrow, D.A., Wright, S.W., Xavier, J.C., Ziegler, P., 2014. Climate change and Southern Ocean ecosystems I: How changes in physical habitats directly affect marine biota. *Global Change Biology* 20, 3004–3025.
- Cota, G.F., Legendre, L., Gosselin, M., Ingram, R.G., 1991. Ecology of bottom ice algae: I. Environmental controls and variability. *Journal of Marine Systems* 2, 257–277.
- Cota, G.F., Smith, R.E.H., 1991. Ecology of bottom ice algae: II. Dynamics, distributions and productivity. *Journal of Marine Systems* 2, 279–295.
- Daly, K.L., 1990. Overwintering development, growth, and feeding of larval *Euphausia superba* in the Antarctic marginal ice zone. *Limnology and Oceanography* 35, 1546–1576.
- Daly, K.L., Macaulay, M.C., 1991. Influence of physical and biological mesoscale dynamics on the seasonal distribution and behavior of *Euphausia superba* in the Antarctic marginal ice zone. *Marine Ecology Progress Series* 79, 37–66.
- Ebenhöh, W., Baretta-Bekker, J.G., Baretta, J.W., 1997. The primary production module in the marine ecosystem model ERSEM II, with emphasis on the light forcing. *Journal of Sea Research* 38, 173–193.
- El-Sayed, S.Z., 1988. Productivity of the southern ocean: a closer look. *Comparative Biochemistry and Physiology* 90B, 489–498.
- Everson, I., 2000. Krill: biology, ecology and fisheries. Blackwell Science, Oxford, UK.
- Fach, B.A., Hofmann, E.E., Murphy, E.J., 2002. Modeling studies of Antarctic krill *Euphausia superba* survival during transport across the Scotia Sea. *Marine Ecology Progress Series* 231, 187–203.

- Fach, B.A., Hofmann, E.E., Murphy, E.J., 2006. Transport of Antarctic krill (*Euphausia superba*) across the Scotia Sea. Part II: Krill growth and survival. *Deep-Sea Research Part I* 53, 1011–1043.
- Fach, B.A., Klinck, J.M., 2006. Transport of Antarctic krill (*Euphausia superba*) across the Scotia Sea. Part I: Circulation and particle tracking simulations. *Deep-Sea Research Part I* 53, 987–1010.
- Fach, B.A., Meyer, B., Wolf-Gladrow, D.A., Bathmann, U.V., 2008. Biochemically based modeling study of Antarctic krill *Euphausia superba* growth and development. *Marine Ecology Progress Series* 360, 147–161.
- Fenton, N., Priddle, J., Tett, P., 1994. Regional variations in bio-optical properties of the surface waters in the Southern Ocean. *Antarctic Science* 6, 443–448.
- Fielding, S., Watkins, J.L., Trathan, P.N., Enderlein, P., Waluda, C.M., Stowasser, G., Tarling, G.A., Murphy, E.J., 2014. Interannual variability in Antarctic krill (*Euphausia superba*) density at South Georgia, Southern Ocean: 1997–2013. *ICES Journal of Marine Science* 71, 2578–2588.
- Flores, H., Atkinson, A., Kawaguchi, S., Krafft, B.A., Milinevsky, G., Nicol, S., Reiss, C.S., Tarling, G.A., Werner, R., Bravo Rebolledo, E., Cirelli, V., Cuzin-Roudy, J., Fielding, S., Groeneveld, J.J., Haraldsson, M., Lombana, A., Marschoff, E., Meyer, B., Pakhomov, E.A., Rombolá, E., Schmidt, K., Siegel, V., Teschke, M., Tonkes, H., Toullec, J.Y., Trathan, P.N., Tremblay, N., Van De Putte, A.P., van Franeker, J.A., Werner, T., 2012a. Impact of climate change on Antarctic krill. *Marine Ecology Progress Series* 458, 1–19.
- Flores, H., van Franeker, J.A., Siegel, V., Haraldsson, M., Strass, V.H., Meesters, E.H., Bathmann, U.V., Wolff, W.J., 2012b. The association of Antarctic krill *Euphausia superba* with the under-ice habitat. *PLoS ONE* 7, e31775.
- Fraser, F.C., 1936. On the development and distribution of the young stages of krill (*Euphausia superba*). *Discovery Reports* 14, 1–192.
- Fraser, W.R., Hofmann, E.E., 2003. A predator's perspective on causal links between climate change, physical forcing and ecosystem response. *Marine Ecology Progress Series* 265, 1–15.
- Gilstad, M., Sakshaug, E., 1990. Growth rates of ten diatom species from the Barents Sea at different irradiances and day lengths. *Marine Ecology Progress Series* 64, 169–173.
- Gran, H.H., 1931. On the conditions for the production of plankton in the sea. *Rapports et Procès-verbaux des Reunions, Conseil International pour L'Exploration de la Mer* 75, 37–46.
- Groeneveld, J., Johst, K., Kawaguchi, S., Meyer, B., Teschke, M., Grimm, V., 2015. How biological clocks and changing environmental conditions determine local population

- growth and species distribution in Antarctic krill (*Euphausia superba*): a conceptual model. *Ecological Modelling* 303, 78–86.
- Gwinner, E., 1986. Circannual rhythms: endogenous annual clocks in the organization of seasonal processes. Springer-Verlag, Berlin.
- Hagen, W., Kattner, G., Terbrüggen, A., Van Vleet, E.S., 2001. Lipid metabolism of the Antarctic krill *Euphausia superba* and its ecological implications. *Marine Biology* 139, 95–104.
- Hamberg, F., 1996. CEMoS, eine Programmierumgebung zur Simulation komplexer Modelle. Diploma thesis. Carl von Ossietzky Universität Oldenburg.
- Hart, T., 1934. On the phytoplankton of the Southwest Atlantic and the Bellinghausen Sea, 1929-1931. *Discovery Reports* 8, 3–270.
- Hewitt, R.P., Demer, D.A., Emery, J.H., 2003. An 8-year cycle in krill biomass density inferred from acoustic surveys conducted in the vicinity of the South Shetland Islands during the austral summers of 1991-1992 through 2001-2002. *Aquatic Living Resources* 16, 205–213.
- Hill, S.L., Phillips, T., Atkinson, A., 2013. Potential Climate Change Effects on the Habitat of Antarctic Krill in the Weddell Quadrant of the Southern Ocean. *PLoS ONE* 8, e72246.
- Hofmann, E.E., Capella, J.E., Ross, R.M., Quetin, L.B., 1992. Models of the early life history of *Euphausia superba*-Part I. Time and temperature dependence during the descent-ascent cycle. *Deep-Sea Research Part A* 39, 1177–1200.
- Hofmann, E.E., Hüsrevoglu, Y.S., 2003. A circumpolar modeling study of habitat control of Antarctic krill (*Euphausia superba*) reproductive success. *Deep-Sea Research Part II* 50, 3121–3142.
- Hofmann, E.E., Lascara, C.M., 2000. Modeling the growth dynamics of Antarctic krill *Euphausia superba*. *Marine Ecology Progress Series* 194, 219–231.
- Holm-Hansen, O., Huntley, M., 1984. Feeding requirements of krill in relation to food sources. *Journal of Crustacean Biology* 4, 156–173.
- Holm-Hansen, O., Naganobu, M., Kawaguchi, S., Kameda, T., Krasovski, I., Tchernyshkov, P., Priddle, J., Korb, R.E., Brandon, M.A., Demer, D.A., Hewitt, R.P., Kahru, M., Hewes, C.D., 2004. Factors influencing the distribution, biomass, and productivity of phytoplankton in the Scotia Sea and adjoining waters. *Deep-Sea Research Part II* 51, 1333–1350.
- Ikeda, T., Dixon, P., 1982. Body shrinkage as a possible over-wintering mechanism of the Antarctic krill, *Euphausia superba* DANA. *Journal of Experimental Marine Biology and Ecology* 62, 143–151.
- Jager, T., Ravagnan, E., 2015. Parameterising a generic model for the dynamic energy budget of Antarctic krill *Euphausia superba*. *Marine Ecology Progress Series* 519, 115–128.

- Jia, Z., Virtue, P., Swadling, K.M., Kawaguchi, S., 2014. A photographic documentation of the development of Antarctic krill (*Euphausia superba*) from egg to early juvenile. *Polar Biology* 37, 165–179.
- Jolliff, J.K., Kindle, J.C., Shulman, I., Penta, B., Friedrichs, M.A.M., Helber, R., Arnone, R.A., 2009. Summary diagrams for coupled hydrodynamic-ecosystem model skill assessment. *Journal of Marine Systems* 76, 64–82.
- Kawaguchi, K., Ishikawa, S., Matsuda, O., 1986. The overwintering strategy of Antarctic krill (*Euphausia superba* DANA) under the coastal fast ice off the Ongul islands in Lützow-Holm Bay, Antarctica. *Memoirs of National Institute of Polar Research* 44, 67–85.
- Kawaguchi, S., Candy, S.G., King, R.A., Naganobu, M., Nicol, S., 2006. Modelling growth of Antarctic krill. I. Growth trends with sex, length, season, and region. *Marine Ecology Progress Series* 306, 1–15.
- Kawaguchi, S., Ishida, A., King, R.A., Raymond, B., Waller, N., Constable, A.J., Nicol, S., Wakita, M., Ishimatsu, A., 2013. Risk maps for Antarctic krill under projected Southern Ocean acidification. *Nature Climate Change* 3, 843–847.
- Kawaguchi, S., Kurihara, H., King, R.A., Hale, L., Berli, T., Robinson, J.P., Ishida, A., Wakita, M., Virtue, P., Nicol, S., Ishimatsu, A., 2011. Will krill fare well under Southern Ocean acidification? *Biology letters* 7, 288–291.
- Kawaguchi, S., Yoshida, T., Finley, L.A., Cramp, P., Nicol, S., 2007. The krill maturity cycle: A conceptual model of the seasonal cycle in Antarctic krill. *Polar Biology* 30, 689–698.
- Kennicutt II, M.C., Chown, S.L., Cassano, J.J., Liggett, D., Peck, L.S., Massom, R.A., Rintoul, S.R., Storey, J.W.V., Vaughan, D.G., Wilson, T.J., Allison, I., Ayton, J., Badhe, R., Baeseman, J., Barrett, P.J., Bell, R.E., Bertler, N., Bo, S., Brandt, A., Bromwich, D., Cary, S.C., Clark, M.S., Convey, P., Costa, E.S., Cowan, D., Deconto, R., Dunbar, R., Elfring, C., Escutia, C., Francis, J., Fricker, H.A., Fukuchi, M., Gilbert, N., Gutt, J., Havermans, C., Hik, D., Hosie, G.W., Jones, C., Kim, Y.D., Le Maho, Y., Lee, S.H., Leppe, M., Leitchenkov, G., Li, X., Lipenkov, V., Lochte, K., López-Martínez, J., Lüdecke, C., Lyons, W., Marensi, S., Miller, H., Morozova, P., Naish, T., Nayak, S., Ravindra, R., Retamales, J., Ricci, C.A., Rogan-Finnemore, M., Ropert-Coudert, Y., Samah, A.A., Sanson, L., Scambos, T., Schloss, I.R., Shiraishi, K., Siegert, M.J., Simões, J.C., Storey, B., Sparrow, M.D., Wall, D.H., Walsh, J.C., Wilson, G., Winther, J.G., Xavier, J.C., Yang, H., Sutherland, W.J., 2015. A roadmap for Antarctic and Southern Ocean science for the next two decades and beyond. *Antarctic Science* 27, 3–18.
- Klunder, M.B., Laan, P., Middag, R., de Baar, H.J.W., van Ooijen, J.C., 2011. Dissolved iron in the Southern Ocean (Atlantic sector). *Deep-Sea Research Part II* 58, 2678–2694.
- Knox, G.A., 2006. *The biology of the Southern Ocean*. 2nd ed., CRC Press, Boca Raton.
- Kopp, G., Lean, J.L., 2011. A new, lower value of total solar irradiance: Evidence and climate significance. *Geophysical Research Letters* 38, 1–7.

- Lancelot, C., Hannon, E., Becquevort, S., Veth, C., de Baar, H.J.W., 2000. Modeling phytoplankton blooms and carbon export production in the Southern Ocean: Dominant controls by light and iron in the Atlantic sector in Austral spring 1992. *Deep-Sea Research Part I* 47, 1621–1662.
- Loeb, V.J., Hofmann, E.E., Klinck, J.M., Holm-Hansen, O., White, W.B., 2009. ENSO and variability of the Antarctic Peninsula pelagic marine ecosystem. *Antarctic Science* 21, 135.
- Loeb, V.J., Siegel, V., Holm-Hansen, O., Hewitt, R.P., Fraser, W.R., Trivelpiece, W., Trivelpiece, S., 1997. Effects of sea-ice extent and krill or salp dominance on the Antarctic food web. *Nature* 387, 879–900.
- Löscher, B.M., de Baar, H.J.W., de Jong, J.T.M., Veth, C., Dehairs, F., 1997. The distribution of Fe in the Antarctic Circumpolar Current. *Deep-Sea Research Part II* 44, 143–187.
- Lowe, A.T., Ross, R.M., Quetin, L.B., Vernet, M., Fritsen, C.H., 2012. Simulating larval Antarctic krill growth and condition factor during fall and winter in response to environmental variability. *Marine Ecology Progress Series* 452, 27–43.
- Mackey, A.P., Atkinson, A., Hill, S.L., Ward, P., Cunningham, N.J., Johnston, N.M., Murphy, E.J., 2012. Antarctic macrozooplankton of the southwest Atlantic sector and Bellingshausen Sea: Baseline historical distributions (Discovery Investigations, 1928-1935) related to temperature and food, with projections for subsequent ocean warming. *Deep-Sea Research Part II: Topical Studies in Oceanography* 59-60, 130–146.
- Marr, J., 1962. The natural history and geography of the Antarctic krill (*Euphausia superba* DANA). *Discovery Reports* 32, 33–464.
- Marschall, H.P., 1988. The overwintering strategy of Antarctic krill under the pack-ice of the Weddell Sea. *Polar Biology* 9, 129–135.
- Martin, J.H., 1990. Glacial-Interglacial CO₂ change: The Iron Hypothesis. *Paleoceanography* 5, 1–13.
- Martin, J.H., 1991. Iron, Liebig's Law, and the Greenhouse. *Oceanography* 4, 52–55.
- McMinn, A., Skerratt, J., Trull, T., Ashworth, C., Lizotte, M.P., 1999. Nutrient stress gradient in the bottom 5 cm of fast ice, McMurdo Sound, Antarctica. *Polar Biology* 21, 220–227.
- Meyer, B., 2012. The overwintering of Antarctic krill, *Euphausia superba*, from an ecophysiological perspective. *Polar Biology* 35, 15–37.
- Meyer, B., Atkinson, A., Blume, B., Bathmann, U.V., 2003. Feeding and energy budgets of larval Antarctic krill *Euphausia superba* in summer. *Marine Ecology Progress Series* 257, 167–177.
- Meyer, B., Atkinson, A., Stübing, D., Oettl, B., Hagen, W., Bathmann, U.V., 2002. Feeding and energy budgets of Antarctic krill *Euphausia superba* at the onset of winter—I. Furcilia III larvae. *Limnology and Oceanography* 47, 943–952.

- Meyer, B., Auerswald, L., Siegel, V., Spahić, S., Pape, C., Fach, B.A., Teschke, M., Lopata, A.L., Fuentes, V., 2010. Seasonal variation in body composition, metabolic activity, feeding, and growth of adult krill *Euphausia superba* in the Lazarev Sea. *Marine Ecology Progress Series* 398, 1–18.
- Meyer, B., Fuentes, V., Guerra, C., Schmidt, K., Atkinson, A., Spahić, S., Cisewski, B., Freier, U., Olariaga, A., Bathmann, U.V., 2009. Physiology, growth, and development of larval krill *Euphausia superba* in autumn and winter in the Lazarev Sea, Antarctica. *Limnology and Oceanography* 54, 1595–1614.
- Miller, D.G.M., Hampton, I., Henry, J., Abrams, R.W., Cooper, J., 1985. The Relationship Between Krill Food Requirements and Phytoplankton Production in a Sector of the Southern Indian Ocean, in: Siegfried, W.R., Condy, P.R., Laws, R.M. (Eds.), *Antarctic Nutrient Cycles and Food Webs*. Springer-Verlag, pp. 362–371.
- Moline, M.A., Prézelin, B.B., 1997. High-resolution time-series data for 1991/1992 primary production and related parameters at a Palmer LTER coastal site: Implications for modeling carbon fixation in the Southern Ocean. *Polar Biology* 17, 39–53.
- Morel, F.M.M., Rueter, J.G., Price, N.M., 1991. Iron nutrition of phytoplankton and its possible importance in the ecology of ocean regions with high nutrient and low biomass. *Oceanography* 4, 56–61.
- Morris, M.D., 1991. Factorial Sampling Plans for Preliminary Computational Experiments. *Technometrics* 33, 161–174.
- Murphy, E.J., Reid, K., 2001. Modelling Southern Ocean krill population dynamics: Biological processes generating fluctuations in the South Georgia ecosystem. *Marine Ecology Progress Series* 217, 175–189.
- Murphy, E.J., Watkins, J.L., Reid, K., Trathan, P.N., Everson, I., Croxall, J.P., Priddle, J., Brandon, M.A., Brierley, A.S., Hofmann, E.E., 1998. Interannual variability of the South Georgia marine ecosystem: Biological and physical sources of variation in the abundance of krill. *Fisheries Oceanography* 7, 381–390.
- Nicol, S., 2006. Krill, Currents, and Sea Ice: *Euphausia superba* and Its Changing Environment. *BioScience* 56, 111–120.
- Nicol, S., Constable, A.J., Pauly, T., 2000. Estimates of circumpolar abundance of Antarctic krill based on recent acoustic density measurements. *CCAMLR Science* 7, 87–99.
- Nicol, S., Foster, J., 2003. Recent trends in the fishery for Antarctic krill. *Aquatic Living Resources* 16, 42–45.
- Nicol, S., Foster, J., Kawaguchi, S., 2012. The fishery for Antarctic krill - recent developments. *Fish and Fisheries* 13, 30–40.

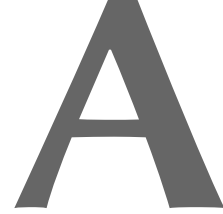
- Nicol, S., de la Mare, W.K., Stolp, M., 1995. The energetic cost of egg production in Antarctic krill (*Euphausia superba* DANA). *Antarctic Science* 7, 25–30.
- Pakhomov, E.A., 1995. Natural age-dependent mortality rates of Antarctic krill *Euphausia superba* DANA in the Indian sector of the Southern Ocean. *Polar Biology* 15, 69–71.
- Palmisano, A.C., Beeler SooHoo, J., Moe, R.L., Sullivan, C.W., 1987a. Sea ice microbial communities. VII. Changes in under-ice spectral irradiance during the development of Antarctic sea ice microalgal communities. *Marine Ecology Progress Series* 35, 165–173.
- Palmisano, A.C., Beeler SooHoo, J., Sullivan, C.W., 1987b. Effects of four environmental variables on photosynthesis-irradiance relationships in Antarctic sea-ice microalgae. *Marine Biology* 94, 299–306.
- Palmisano, A.C., Kottmeier, S.T., Moe, R.L., Sullivan, C.W., 1985. Sea ice microbial communities. IV. The effect of light perturbation on microalgae at the ice-seawater interface in McMurdo Sound, Antarctica. *Marine Ecology Progress Series* 21, 37–45.
- Pinkerton, M.H., Bradford-Grieve, J.M., Hanchet, S.M., 2010. A balanced model of the food web of the Ross Sea, Antarctica. *CCAMLR Science* 17, 1–31.
- Piñones, A., Hofmann, E.E., Daly, K.L., Dinniman, M.S., Klinck, J.M., 2013. Modeling environmental controls on the transport and fate of early life stages of Antarctic krill (*Euphausia superba*) on the western Antarctic Peninsula continental shelf. *Deep-Sea Research Part I* 82, 17–31.
- Piñones, A., Hofmann, E.E., Dinniman, M.S., Davis, L.B., 2016. Modeling the transport and fate of euphausiids in the Ross Sea. *Polar Biology* 39, 177–187.
- Price, H.J., Boyd, K.R., Boyd, C.M., 1988. Omnivorous feeding behavior of the Antarctic krill *Euphausia superba*. *Marine Biology* 97, 67–77.
- Quetin, L.B., Ross, R.M., 1991. Behavioral and Physiological Characteristics of the Antarctic Krill, *Euphausia superba*. *American Zoologist* 31, 49–63.
- Quetin, L.B., Ross, R.M., 2001. Environmental Variability and Its Impact on the Reproductive Cycle of Antarctic Krill. *American Zoologist* 41, 74–89.
- Quetin, L.B., Ross, R.M., 2003. Episodic recruitment in Antarctic krill *Euphausia superba* in the Palmer LTER study region. *Marine Ecology Progress Series* 259, 185–200.
- Quetin, L.B., Ross, R.M., 2009. Life under Antarctic pack ice: a krill perspective, in: Krupnik, I., Lang, M.A., Miller, S.E. (Eds.), *Smithsonian at the Poles*. Smithsonian Institution Scholarly Press, Washington DC, pp. 285–298.
- Quetin, L.B., Ross, R.M., Frazer, T.K., Haberman, K.L., 1996. Factors affecting distribution and abundance of zooplankton, with an emphasis on Antarctic Krill, *Euphausia superba*. *Antarctic Research Series* 70, 357–371.

- Redfield, A.C., 1934. On the proportions of organic derivatives in sea water and their relation to the composition of plankton. University Press of Liverpool, James Johnstone Memorial Volume , 177–192.
- Ross, R.M., Quetin, L.B., 1983. Spawning frequency and fecundity of the Antarctic krill *Euphausia superba*. *Marine Biology* 77, 201–205.
- Ross, R.M., Quetin, L.B., 1986. How productive are Antarctic Krill? *BioScience* 36, 264–269.
- Ross, R.M., Quetin, L.B., 1988. *Euphausia superba*: A critical review of estimates of annual production. *Comparative Biochemistry and Physiology* 90B, 499–505.
- Ross, R.M., Quetin, L.B., 1989. Energetic cost to develop to the first feeding stage of *Euphausia superba* DANA and the effect of delays in food availability. *Journal of Experimental Marine Biology and Ecology* 133, 103–127.
- Ross, R.M., Quetin, L.B., Baker, K.S., Vernet, M., Smith, R.C., 2000. Growth limitation in young *Euphausia superba* under field conditions. *Limnology and Oceanography* 45, 31–43.
- Ross, R.M., Quetin, L.B., Newberger, T., Shaw, C.T., Jones, J.L., Oakes, S.A., Moore, K.J., 2014. Trends, cycles, interannual variability for three pelagic species west of the Antarctic Peninsula 1993–2008. *Marine Ecology Progress Series* 515, 11–32.
- Saba, G.K., Fraser, W.R., Saba, V.S., Iannuzzi, R.a., Coleman, K.E., Doney, S.C., Ducklow, H.W., Martinson, D.G., Miles, T.N., Patterson-Fraser, D.L., Stammerjohn, S.E., Steinberg, D.K., Schofield, O.M., 2014. Winter and spring controls on the summer food web of the coastal West Antarctic Peninsula. *Nature Communications* 5, 4318.
- Saba, G.K., Schofield, O., Torres, J.J., Ombres, E.H., Steinberg, D.K., 2012. Increased Feeding and Nutrient Excretion of Adult Antarctic Krill, *Euphausia superba*, Exposed to Enhanced Carbon Dioxide (CO₂). *PLoS ONE* 7, 1–12.
- Saito, M.A., Goepfert, T.J., Ritt, J.T., 2008. Some thoughts on the concept of colimitation: Three definitions and the importance of bioavailability. *Limnology and Oceanography* 53, 276–290.
- Sakshaug, E., Slagstad, D., 1991. Light and productivity of phytoplankton in polar marine ecosystems: a physiological view. *Polar Research* 10, 69–85.
- Saltelli, A., Tarantola, S., Campolongo, F., Ratto, M., 2004. *Sensitivity Analysis in Practice: A Guide to Assessing Scientific Models*. John Wiley & Sons, New York.
- Schaafsma, F.L., David, C.L., Pakhomov, E.A., Hunt, B.P.V., Lange, B.A., Flores, H., van Franeker, J.A., 2016. Size and stage composition of age class 0 Antarctic krill (*Euphausia superba*) in the ice–water interface layer during winter/early spring. *Polar Biology* , 1–12.
- Schmidt, K., Atkinson, A., Pond, D.W., Ireland, L.C., 2014. Feeding and overwintering of Antarctic krill across its major habitats: The role of sea ice cover, water depth, and phytoplankton abundance. *Limnology and Oceanography* 59, 17–36.

- Siegel, V., 2000. Krill (Euphausiacea) demography and variability in abundance and distribution. *Canadian Journal of Fisheries and Aquatic Sciences* 57, 151–167.
- Siegel, V., 2005. Distribution and population dynamics of *Euphausia superba*: Summary of recent findings. *Polar Biology* 29, 1–22.
- Siegel, V. (Ed.), 2016. *Biology and Ecology of Antarctic krill*. 1 ed., Springer International Publishing.
- Siegel, V., Loeb, V.J., 1994. Length and age at maturity of Antarctic krill. *Antarctic Science* 6, 479–482.
- Siegel, V., Loeb, V.J., 1995. Recruitment of Antarctic krill *Euphausia superba* and possible causes for its variability. *Marine Ecology Progress Series* 123, 45–56.
- Siegel, V., Watkins, J.L., 2016. Distribution, Biomass and Demography of Antarctic Krill, *Euphausia superba*, in: Siegel, V. (Ed.), *Biology and Ecology of Antarctic Krill*. 1 ed.. Springer International Publishing. Chapter 2, pp. 21–100.
- Smith Jr, W.O., Sakshaug, E., 1990. Polar phytoplankton, in: Smith Jr, W.O. (Ed.), *Polar Oceanography. Part B: Chemistry, Biology and Geology*. Academic Press. Chapter 9, pp. 477–526.
- Sommer, U., 1989. Maximal growth rates of Antarctic phytoplankton: Only weak dependence on cell size. *Limnology and Oceanography* 34, 1109–1112.
- Stambler, N., 2003. Primary production, light absorption and quantum yields of phytoplankton from the Bellingshausen and Amundsen Seas (Antarctica). *Polar Biology* 26, 438–451.
- Stammerjohn, S., Massom, R., Rind, D., Martinson, D., 2012. Regions of rapid sea ice change: An inter-hemispheric seasonal comparison. *Geophysical Research Letters* 39, L06501.
- Stammerjohn, S.E., Martinson, D.G., Smith, R.C., Yuan, X., Rind, D., 2008. Trends in Antarctic annual sea ice retreat and advance and their relation to El Niño–Southern Oscillation and Southern Annular Mode variability. *Journal of Geophysical Research* 113, C03S90.
- Steinberg, D.K., Ruck, K.E., Gleiber, M.R., Garzio, L.M., Cope, J.S., Bernard, K.S., Stammerjohn, S.E., Schofield, O.M., Quetin, L.B., Ross, R.M., 2015. Long-term (1993–2013) changes in macrozooplankton off the western antarctic peninsula. *Deep-Sea Research Part I* 101, 54–70.
- Sunda, W.G., Huntsman, S.A., 1997. Interrelated influence of iron, light and cell size on marine phytoplankton growth. *Nature* 390, 389–392.
- Tagliabue, A., Sallée, J.B., Bowie, A.R., Lévy, M., Swart, S., Boyd, P.W., 2014. Surface-water iron supplies in the Southern Ocean sustained by deep winter mixing. *Nature Geoscience* 7, 314–320.

- Tarling, G.A., Cuzin-Roudy, J., Thorpe, S.E., Shreeve, R.S., Ward, P., Murphy, E.J., 2007. Recruitment of Antarctic krill *Euphausia superba* in the South Georgia region: Adult fecundity and the fate of larvae. *Marine Ecology Progress Series* 331, 161–179.
- Tarling, G.A., Shreeve, R.S., Hirst, A.G., Atkinson, A., Pond, D.W., Murphy, E.J., Watkins, J.L., 2006. Natural growth rates in Antarctic krill (*Euphausia superba*): I. Improving methodology and predicting intermolt period. *Limnology and Oceanography* 51, 959–972.
- Taylor, K.E., 2001. Summarizing multiple aspects of model performance in a single diagram. *Journal of Geophysical Research* 106, 7183.
- Taylor, M.H., Losch, M., Bracher, A., 2013. On the drivers of phytoplankton blooms in the Antarctic marginal ice zone: A modeling approach. *Journal of Geophysical Research: Oceans* 118, 63–75.
- Teschke, M., 2007. Influence of Seasonal Light Conditions on the Physiology of Antarctic Krill: Implications for Over-Winter Biology and Maturity Development. PhD thesis. Universität Bremen.
- Teschke, M., Kawaguchi, S., Meyer, B., 2007. Simulated light regimes affect feeding and metabolism of Antarctic krill, *Euphausia superba*. *Limnology and Oceanography* 52, 1046–1054.
- Teschke, M., Kawaguchi, S., Meyer, B., 2008. Effects of simulated light regimes on maturity and body composition of Antarctic krill, *Euphausia superba*. *Marine Biology* 154, 315–324.
- Thimijan, R.W., Heins, R.D., 1983. Photometric, radiometric, and quantum light units of measure: a review of procedures for interconversion. *HortScience* 18, 818–822.
- Thomas, P.G., Ikeda, T., 1987. Sexual regression, shrinkage, re-maturation and growth of spent female *Euphausia superba* in the laboratory. *Marine Biology* 95, 357–363.
- Thorpe, S.E., Murphy, E.J., Watkins, J.L., 2007. Circumpolar connections between Antarctic krill (*Euphausia superba* DANA) populations: Investigating the roles of ocean and sea ice transport. *Deep-Sea Research Part I: Oceanographic Research Papers* 54, 792–810.
- Timmermans, K.R., Gerringa, L.J.a., de Baar, H.J.W., van der Wagt, B., Veldhuis, M.J.W., de Jong, J.T.M., Croot, P.L., Boye, M., 2001. Growth rates of large and small Southern Ocean diatoms in relation to availability of iron in natural seawater. *Limnology and Oceanography* 46, 260–266.
- Torres, J.J., Donnelly, J., Hopkins, T.L., Lancraft, T.M., Aarset, A.V., Ainley, D.G., 1994. Proximate composition and overwintering strategies of Antarctic micronektonic Crustacea. *Marine Ecology Progress Series* 113, 221–232.
- Trivelpiece, W.Z., Hinke, J.T., Miller, A.K., Reiss, C.S., Trivelpiece, S.G., Watters, G.M., 2011. Variability in krill biomass links harvesting and climate warming to penguin population changes in Antarctica. *Proceedings of the National Academy of Sciences* 108, 7625–7628.

- Turner, J., Barrand, N.E., Bracegirdle, T.J., Convey, P., Hodgson, D.A., Jarvis, M., Jenkins, A., Marshall, G., Meredith, M.P., Roscoe, H., Shanklin, J., French, J., Goosse, H., Guglielmin, M., Gutt, J., Jacobs, S., Kennicutt, M.C., Masson-Delmotte, V., Mayewski, P.A., Navarro, F., Robinson, S.A., Scambos, T., Sparrow, M.D., Summerhayes, C.P., Speer, K., Klepikov, A., 2014. Antarctic climate change and the environment: an update. *Polar Record* 50, 237–259.
- Vaughan, D.G., Comiso, J.C., Allison, I., Carrasco, J., Kaser, G., Kwok, R., Mote, P., Murray, T., Paul, F., Ren, J., Rignot, E., Solomina, O., Steffen, K., Zhang, T., 2013. Observations: Cryosphere, in: Stocker, T., Qin, D., Plattner, G.K., Tignor, M., Allen, S.K., Boschung, J., Nauels, A., Xia, Y., Bex, V., Midgley, P.M. (Eds.), *Climate Change 2013: The Physical Science Basis. Contribution of Working Group I to the Fifth Assessment Report of the Intergovernmental Panel on Climate Change*. Cambridge University Press, Cambridge, United Kingdom and New York, NY, USA. Chapter 4, pp. 317–382.
- Weber, L., Völker, C., Schartau, M., Wolf-Gladrow, D.A., 2005. Modeling the speciation and biogeochemistry of iron at the Bermuda Atlantic Time-series Study site. *Global Biogeochemical Cycles* 19, GB1019.
- Whitehouse, M.J., Meredith, M.P., Rothery, P., Atkinson, A., Ward, P., Korb, R.E., 2008. Rapid warming of the ocean around South Georgia, Southern Ocean, during the 20th century: Forcings, characteristics and implications for lower trophic levels. *Deep-Sea Research Part I: Oceanographic Research Papers* 55, 1218–1228.
- Wiedenmann, J., Cresswell, K.A., Mangel, M., 2008. Temperature-dependent growth of Antarctic krill: Predictions for a changing climate from a cohort model. *Marine Ecology Progress Series* 358, 191–202.
- Yoshida, T., 2009. Environmental influences on reproduction in Antarctic krill, *Euphausia superba*. PhD thesis. University of Tasmania.



APPENDIX

A.1. CALCULATION OF THE SEA ICE FORCING

The function for the sea ice forcing is described by the following Fourier series:

$$f_{\text{ice}}(t) = a_0 + \sum_{k=1}^{10} \left(a_k \cdot \cos\left(\frac{2\pi kt}{365}\right) + b_k \cdot \sin\left(\frac{2\pi kt}{365}\right) \right),$$

where t is the day of the year, $a_0 = 0.2608$ the mean of the data. a_k and b_k are the Fourier coefficients, which are given by the following sums:

$$a_k = \frac{2}{N} \sum_{i=1}^N y_i \cdot \cos\left(2\pi k \frac{t_i}{365}\right),$$
$$b_k = \frac{2}{N} \sum_{i=1}^N y_i \cdot \sin\left(2\pi k \frac{t_i}{365}\right),$$

where y_i are the values of the data at time t_i . The values of the parameters can be found in Table A1.

A.2. CALCULATION OF THE ASTRONOMICAL IRRADIANCE AND DAYLENGTH

The astronomical irradiance at the top of the atmosphere is a function of the date t , the time of day α and the geographical latitude ϕ . Following Ebenh oh et al. (1997), the day of the year

TABLE A1.: Coefficients of the sea ice fourier transformation.

k	a	b	k	a	b
1	0.1093	-0.2435	6	-0.0038	-0.0047
2	-0.0088	-0.0072	7	0.0001	0.0006
3	-0.0054	-0.0102	8	-0.0007	-0.0014
4	0.0005	-0.016	9	0.0014	0.0002
5	-0.0031	-0.0079	10	0.0003	-0.0008

is expressed as an angle β between $-\pi$ and π with $\beta = 0$ at June 21:

$$\beta = \frac{2\pi(t - 172)}{365}.$$

In the same way, the time of day α is described as an angle $[-\pi, \pi]$ with $\alpha = 0$ at noon. With these notations, the angle between the sun and the pole axis γ can be calculated, which depends on the day of the year β and the inclination of the pole axis $\rho = 23.5^\circ$:

$$\cos(\gamma) = \sin(\rho) \cos(\beta).$$

Using this angle, the solar zenith angle σ (the angle between the normal vector at the current location and the direction to the sun) can be calculated:

$$\cos(\sigma) = \sin(\phi) \cos(\gamma) + \cos(\phi) \sin(\gamma) \cos(\alpha).$$

When the sun is aligned with the horizon, $\cos(\sigma)$ becomes zero. These are the times of sunrise and sunset $\pm\alpha_n$:

$$\alpha_n = \begin{cases} \arccos\left(-\frac{\sin(\phi) \cos(\gamma)}{\cos(\phi) \sin(\gamma)}\right) & \text{if } |(\cdot)| \leq 1, \\ 0 & \text{if } (\cdot) > 1, \\ \pi & \text{if } (\cdot) < -1, \end{cases}$$

where (\cdot) denotes the arguments of the arccosine.

The last two cases only apply for latitudes beyond the polar circle ($>66.5^\circ\text{S}$), when the sun does not set or rise above the horizon (polar day/night). When the sun is at its zenith ($\sigma = 0$), this function has its maximum and can thus be used as a measure for the relative irradiance I_{rel} . The daily averaged irradiance can be obtained by solving the following integral:

$$I_{\text{rel}}(\phi, \beta) = \frac{1}{2\pi} \int_{-\pi}^{\pi} \max(0, \cos(\sigma)) d\alpha.$$

The maximum function is needed to prevent from incorrect integration over times when the sun is below the horizon ($\cos(\sigma) < 0$). Instead of the maximum function, the domain of integration can be changed to only integrate from sunrise to sunset:

$$\begin{aligned} I_{\text{rel}}(\phi, \beta) &= \frac{1}{2\pi} \int_{-\alpha_n}^{\alpha_n} \cos(\sigma) d\alpha \\ &= \frac{1}{2\pi} \int_{-\alpha_n}^{\alpha_n} \left(\sin(\phi) \cos(\gamma) + \cos(\phi) \sin(\gamma) \cos(\alpha) \right) d\alpha \\ &= \frac{1}{\pi} \left(\sin(\phi) \cos(\gamma) \alpha_n + \cos(\phi) \sin(\gamma) \sin(\alpha_n) \right). \end{aligned}$$

To get the absolute astronomical irradiance, the relative irradiance is multiplied with the solar constant $I_{\text{solar}} = 1368 \text{ W/m}^{-2}$:

$$I_{\text{ast}}(\phi, \beta) = I_{\text{rel}}(\phi, \beta) \cdot I_{\text{solar}}.$$

The daylength – or more precisely the length of the photoperiod – can then be calculated from the times of sunrise and sunset $\pm\alpha_n$:

$$b = \frac{\alpha_n}{\pi}.$$

A.3. CALCULATION OF THE LIGHT-DEPENDENT GROWTH FACTOR

PELAGIC PHYTOPLANKTON

The light-dependent growth factor e_{PI} is a dimensionless parameter that is defined according to Ebenhöf et al. (1997) as:

$$e_{PI} = \frac{prod}{p_0},$$

where $prod$ is the daily average production in the mixed layer and p_0 the maximum production rate. It is calculated by averaging the productivity p over the depth of the mixed layer z and the time of the day α :

$$prod = \frac{1}{2\pi} \int_{\alpha=-\pi}^{\alpha=\pi} \frac{1}{D} \int_{z=0}^{z=D} p(I(\alpha, z)) dz d\alpha.$$

Through substitution with $I(\alpha, z) = I_{net}(\alpha, 0) \cdot e^{-\sigma z}$ the integral over the depth is changed to an integral over the light intensity in the water column:

$$\begin{aligned} prod &= \frac{1}{2\pi D} \int_{\alpha=-\pi}^{\alpha=\pi} \int_{z=0}^{z=D} p(I(\alpha, z)) dz d\alpha \\ &= \frac{1}{2\pi\sigma D} \int_{-\pi}^{\pi} \int_{I(\alpha, D)}^{I(\alpha, 0)} \frac{p(I)}{I} dI d\alpha. \end{aligned}$$

For the chosen Monod-type productivity-irradiance function this leads to:

$$\begin{aligned} prod &= \frac{1}{2\pi\sigma D} \int_{-\pi}^{\pi} \int_{I(\alpha, D)}^{I(\alpha, 0)} p_0 \frac{I}{H_{PI} + I} dI d\alpha \\ &= \frac{p_0}{2\pi\sigma D} \int_{-\pi}^{\pi} \left[\ln(H_{PI} + I) \right]_{I(\alpha, D)}^{I(\alpha, 0)} d\alpha \\ &= \frac{p_0}{2\pi\sigma D} \int_{-\pi}^{\pi} \ln \left(\frac{H_{PI} + I(\alpha, 0)}{H_{PI} + I(\alpha, 0)e^{-\sigma D}} \right) d\alpha. \end{aligned}$$

Because $I(\alpha, 0)$ is symmetric around $\alpha = 0$ the integral can be changed to:

$$prod = 2 \cdot \frac{p_0}{2\pi\sigma D} \int_0^{\pi} \ln \left(\frac{H_{PI} + I(\alpha, 0)}{H_{PI} + I(\alpha, 0)e^{-\sigma D}} \right) d\alpha.$$

Since there is no productivity after sunset, i.e. $p(I) = 0$ for $\alpha > \alpha_n$, the upper limit of the integral can be replaced by α_n and the integral can finally be approximated with Simpson's rule:

$$\begin{aligned} prod &= \frac{p_0}{\pi\sigma D} \int_0^{\alpha_n} \ln \left(\frac{H_{PI} + I(\alpha, 0)}{H_{PI} + I(\alpha, 0)e^{-\sigma D}} \right) d\alpha \\ &= \frac{p_0 b}{6\sigma D} \left[\ln \left(\frac{H_{PI} + I(0, n)}{H_{PI} + I(0, n)e^{-\sigma D}} \right) + 4 \cdot \ln \left(\frac{H_{PI} + I(0, a)}{H_{PI} + I(0, a)e^{-\sigma D}} \right) \right], \end{aligned}$$

where $I(0, n)$ is the irradiance at the sea surface at noon and $I(0, a)$ the irradiance at the sea surface in the afternoon, i.e. the midpoint between noon and sunset.

The light-dependent growth factor e_{PI} is then given by:

$$e_{PI} \approx \frac{b}{6\sigma D} \left[\ln \left(\frac{H_{PI} + I(0, n)}{H_{PI} + I(0, n)e^{-\sigma D}} \right) + 4 \cdot \ln \left(\frac{H_{PI} + I(0, a)}{H_{PI} + I(0, a)e^{-\sigma D}} \right) \right].$$

SEA ICE PHYTOPLANKTON

The light-dependent growth factor for sea ice phytoplankton e_{SI} is calculated similar to the one for pelagic phytoplankton. It is defined according to Ebenhöf et al. (1997) as:

$$e_{SI} = \frac{prod_S}{p_{0S}},$$

where $prod_S$ is the daily average production and p_{0S} the maximum production rate. In contrast to the pelagic phytoplankton production, the production of sea ice phytoplankton only needs to be averaged over the length of the photoperiod and not the depth. All assumptions and substitutions are the same as described above for pelagic phytoplankton:

$$\begin{aligned} prod_S &= \frac{1}{2\pi} \int_{\alpha=-\pi}^{\alpha=\pi} p(I(\alpha,0)) d\alpha \\ &= \frac{1}{2\pi} \int_{\alpha=-\pi}^{\alpha=\pi} p_{0S} \frac{I(\alpha,0)}{H_{SI} + I(\alpha,0)} d\alpha \\ &= \frac{p_{0S}}{\pi} \int_{\alpha=0}^{\alpha=\alpha_n} \frac{I(\alpha,0)}{H_{SI} + I(\alpha,0)} d\alpha \\ &\approx \frac{p_{0S} \cdot b}{6} \left[\frac{I(n,0)}{H_{SI} + I(n,0)} + 4 \frac{I(a,0)}{H_{SI} + I(a,0)} \right]. \end{aligned}$$

The light-dependent growth factor e_{SI} is then given by:

$$e_{SI} \approx \frac{b}{6} \left[\frac{I(n,0)}{H_{SI} + I(n,0)} + 4 \frac{I(a,0)}{H_{SI} + I(a,0)} \right].$$

A.4. CALCULATION OF THE CONCEPTUAL ICE

The conceptual sea ice f_{ice}^* as a function of the day of the year t can be calculated using the following equation (Figure A1):

$$f_{ice}^*(t) = \begin{cases} \frac{ice_{max}}{\Delta_{freezing}} \cdot (t - t_{start}) & \text{for } t_{start} \leq t \leq (t_{start} + \Delta_{freezing}), \\ ice_{max} & \text{for } (t_{start} + \Delta_{freezing}) < t < (t_{start} + \Delta_{freezing} + \Delta_{const}), \\ -\frac{ice_{max}}{\Delta_{melting}} \cdot (t - t_{end}) & \text{for } (t_{start} + \Delta_{freezing} + \Delta_{const}) \leq t \leq t_{end} \\ & \text{and } t_{ice_max} < t_{end}, \\ -\frac{ice_{max}}{\Delta_{melting}} \cdot (t - t_{end}) & \text{for } t < t_{end} \text{ and } t_{end} < t_{max}, \\ -\frac{ice_{max}}{\Delta_{melting}} \cdot (t - (t_{end} + 365)) & \text{for } t > (t_{start} + \Delta_{freezing} + \Delta_{const}) \text{ and } t_{end} < t_{max}, \\ 0 & \text{otherwise.} \end{cases}$$

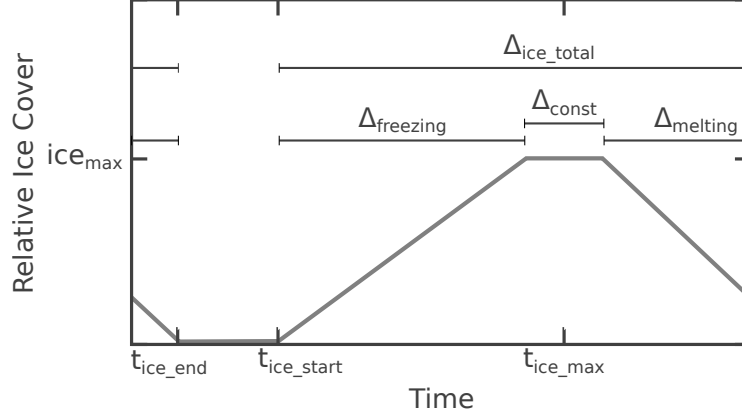


FIGURE A1.: Sketch of the conceptual sea ice function.

The fourth and the fifth case account for conditions, where the melting of the sea ice continues into the next year.

By fitting this function to the ice forcing function f_{ice} (Equation A.1), the parameters have been determined as follows:

$$\begin{aligned}
 ice_{max_REF} &= 0.53268, \\
 \Delta_{ice_total_REF} &= 300, \\
 t_{ice_max} &= 256, \\
 \Delta_{freezing} &= 0.49 \cdot \Delta_{ice_total_REF}, \\
 \Delta_{const} &= 0.13 \cdot \Delta_{ice_total_REF}, \\
 \Delta_{melting} &= 0.38 \cdot \Delta_{ice_total_REF}.
 \end{aligned}$$

For the simulations with shorter ice season durations Δ_{ice_total} , t_{ice_max} and the ratios of $\Delta_{freezing}$, Δ_{const} and $\Delta_{melting}$ are kept constant, while ice_{max} is scaled down proportionally to the shortening of the ice season:

$$ice_{max} = ice_{max_REF} \frac{\Delta_{ice_total}}{\Delta_{ice_total_REF}}.$$

By doing so, the start of the ice season t_{ice_start} is given by:

$$t_{ice_start} = t_{ice_max} - \left(\Delta_{freezing} + \frac{\Delta_{const}}{2} \right)$$

and the end of the ice season t_{ice_end} by:

$$t_{ice_end} = \left[t_{ice_max} + \left(\Delta_{melting} + \frac{\Delta_{const}}{2} \right) \right] \text{ mod } 365,$$

where the modulo is due to the fact that the ice season can reach into the next year.

A.5. THE EFFECT OF CLIMATE CHANGE ON THE ABSOLUTE KRILL DENSITIES

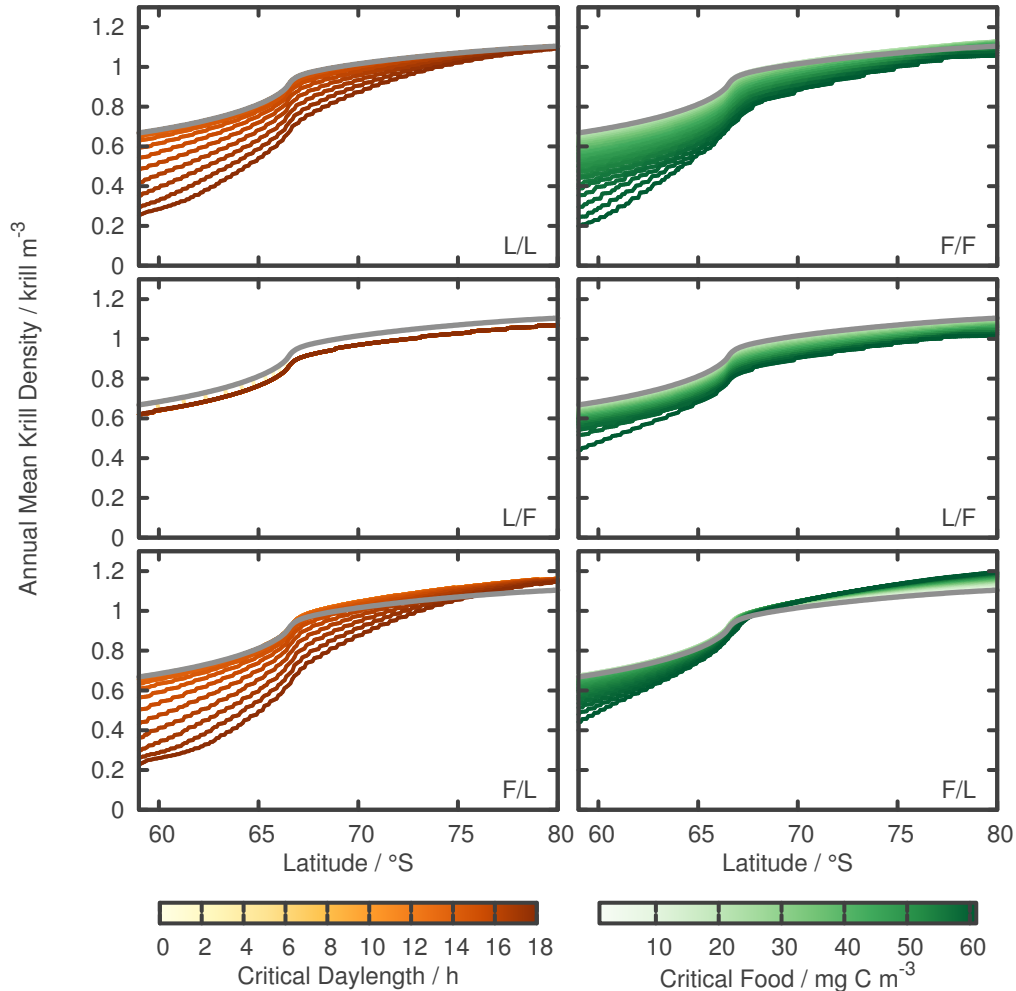


FIGURE A2.: Absolute change in annual mean krill density in dependence on the latitude. Shown are the results for the light/light clock (top left), the food/food clock (top right), the light/food clock (middle) and the food/light clock (bottom) for different values of the critical daylength and critical food concentration. The grey line shows the results of the reference run (i.e. without a clock). For the variation in critical daylength of the light/food and food/light clock, the critical food concentration was kept constant at 35 mg C m^{-3} . For the variation in critical food of these two clocks, the critical daylength was kept constant at 12 hours.

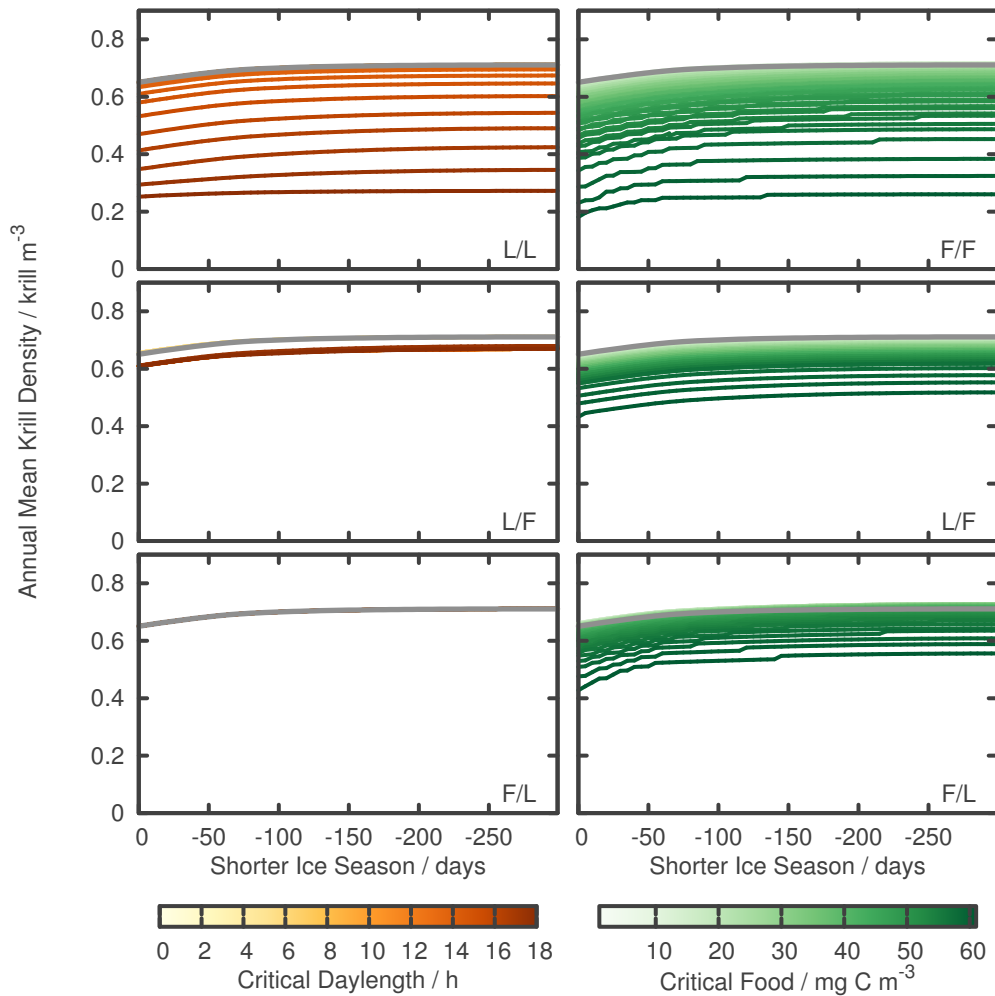


FIGURE A3: Absolute change in annual mean krill density in dependence on the length of the sea ice season. Shown are the results for the light/light clock (top left), the food/food clock (top right), the light/food clock (middle) and the food/light clock (bottom) for different values of the critical daylength and critical food concentration. The grey line shows the results of the reference run (i.e. without a clock). For the variation in critical daylength of the light/food and food/light clock, the critical food concentration was kept constant at 35 mg C m^{-3} . For the variation in critical food of these two clocks, the critical daylength was kept constant at 12 hours.

LIST OF FIGURES

1.1. Graphical summary of the model.	10
1.2. Temporal dynamics of the relative ice cover over the course of one year. . .	12
1.3. Temporal dynamics of the daily averaged light intensity at the sea surface and the daylength over the course of one year for 59°S.	13
1.4. Temporal dynamics of the mixed layer depth over the course of one year. . .	14
1.5. Dependence of the maturation function q_{mat} on the food per juvenile krill for different values of the steepness of the maturation function n	21
1.6. Example of a Taylor diagram and a Target diagram.	30
1.7. Annual dynamics of the reference run.	34
1.8. Mean values of the fluxes describing pelagic phytoplankton.	35
1.9. Factors limiting pelagic phytoplankton growth.	36
1.10. Annual dynamics of the reproduction of adult krill and the maturation of juvenile krill.	37
1.11. Results of the Morris Screening.	38
1.12. Taylor, Target and Time diagram showing the effect of the maximum growth rate of pelagic phytoplankton μ_P on juvenile krill and adult krill.	40
1.13. Taylor, Target and Time diagram showing the effect of the typical amount of food per krill needed for maturation F_{crit} on adult krill.	40
1.14. Taylor, Target and Time diagram showing the effect of the mortality rate of pelagic phytoplankton m_P on juvenile krill.	41
1.15. Taylor, Target and Time diagram showing the effect of the maximum repro- duction rate $q_{\text{rep}0}$ on adult krill.	42
1.16. Taylor, Target and Time diagram showing the effect of the mortality rate of juvenile krill m_J on juvenile krill.	42
1.17. Taylor, Target and Time diagram showing the effect of the half-saturation constant of pelagic phytoplankton for light H_{PI} on adult krill.	43
1.18. Taylor, Target and Time diagram showing the effect of the half-saturation constant of adult krill for food uptake H_A on adult krill.	44
1.19. Taylor, Target and Time diagram showing the effect of the mortality rate of adult krill m_A on adult krill.	45
1.20. Qualitative comparison of an annual and a multi-annual cycle in krill dynamics.	46

1.21.	Dependence of the number of different maxima in juvenile krill density on the maximum maturation rate q_{mat0} and the steepness of the maturation function n	48
1.22.	Bifurcation diagram of the annual maxima of juvenile krill as a function of the steepness of the maturation function n for $q_{mat0} = 0.6$ and two corresponding time series.	49
1.23.	Bifurcation diagrams of the annual maxima of juvenile krill as a function of the steepness of the maturation function n for four different values of q_{mat0}	50
1.24.	Bifurcation diagrams of the annual maxima of juvenile krill as a function of the maximum maturation rate q_{mat0} for two different values of n	50
2.1.	Overview of the krill maturity cycle proposed by Kawaguchi et al. (2007).	55
2.2.	Illustration of the biological clock, which regulates the reproduction.	56
2.3.	Relative change in annual mean krill density in dependence on the critical values of the light/light clock setup and the food/food clock setup.	58
2.4.	Temporal dynamics of the reproduction over the course of one year for the light/light clock setup.	60
2.5.	Temporal dynamics of the reproduction over the course of one year for the food/food clock setup.	61
2.6.	Relative change in annual mean krill density in dependence on the critical values of the light/food clock setup and the food/light clock setup.	62
2.7.	Relative frequencies of the relative changes in mean krill density and the shortening of the reproductive season for the four different clock setups.	63
3.1.	Temporal dynamics of the daily averaged light intensity at the sea surface and length of the photoperiod over the course of one year for 59°S and 80°S.	68
3.2.	Temporal dynamics of the simple ice cover over the course of one year.	69
3.3.	Relative change in annual mean krill density in dependence on the latitude for the different clock setups.	71
3.4.	Dependence of the light-dependent growth factor for pelagic phytoplankton on the time of the year for the two climate change scenarios.	72
3.5.	Temporal dynamics of the state variables over the course of one year for the two climate change scenarios.	73
3.6.	Relative change in annual mean krill density in dependence on the length of the sea ice season for the different clock setups.	75
4.1.	Dependence of a light-mediated biological clock on the daylength and the latitude.	81
4.2.	Daylength in dependence on the day of the year and the latitude.	83
A1.	Sketch of the conceptual sea ice function.	108
A2.	Absolute change in annual mean krill density in dependence on the latitude for the different clock setups.	109

A3. Absolute change in annual mean krill density in dependence on the length of the sea ice season for the different clock setups. 110

LIST OF TABLES

1.1. Overview of the parameter values used in the reference run and the corresponding values found in the literature. 26

2.1. Overview of the four different clock setups. 57

A1. Coefficients of the sea ice fourier transformation. 104



SIRI RACKEBRANDT

✉ siri.rackebrandt@uni-oldenburg.de

born on 2 September 1988 in Göttingen (Germany)

Education	PhD Student in Marine Environmental Sciences University of Oldenburg (Germany)	since 2012
	Master of Science in Marine Environmental Sciences University of Oldenburg (Germany) Thesis: „Modelling the effects of nutrient fluxes across the sediment-water interface of an intertidal flat – Sensitivity studies and budget estimates with the complex ecosystem model EcoTiM for the backbarrier area of Spiekeroog“	2009–2012
	Bachelor of Science in Environmental Sciences University of Oldenburg (Germany) Thesis: „Manganese depletion by phytoplankton: a model study“	2006–2009
	Ontario Secondary School Diploma Fieldstone Day School Toronto (Canada)	2004–2006
Work Experience	Scientist Research Group Mathematical Modelling Institute for Chemistry and Biology of the Marine Environment, Oldenburg (Germany)	2012–2015
	Scientific Assistant different research groups Institute for Chemistry and Biology of the Marine Environment & Institute for Mathematics, Oldenburg (Germany)	2007–2012
Publications	Gansel, L. C., Rackebrandt, S. , Oppedal, F., McClimans, T. A. (2014). <i>Flow Fields Inside Stocked Fish Cages and the Near Environment</i> . Journal of Offshore Mechanics and Arctic Engineering 136(3): 031201	
	Osterholz H., Simon H., Beck M., März J., Rackebrandt S. , Brumsack H.-J., Feudel U., Simon M. (2014). <i>Impact of diatom growth on trace metal dynamics (Mn, Mo, V, U)</i> . Journal of Sea Research, 87: 35-45	
	Gansel, L. C., Rackebrandt, S. , Oppedal, F., McClimans, T. A. (2011). <i>Flow Fields Inside Stocked Fish Cages and the Near Environment</i> . ASME Conference Proceedings: 201 - 209	

ERKLÄRUNG

Hiermit versichere ich, dass ich die vorliegende Arbeit unter Berücksichtigung der Leitlinien guter wissenschaftlicher Praxis an der Carl von Ossietzky Universität Oldenburg selbstständig angefertigt und keine anderen als die angegebenen Quellen und Hilfsmittel verwendet habe. Zusätzlich erkläre ich, dass diese Dissertation weder in ihrer Gesamtheit noch in Teilen einer anderen wissenschaftlichen Hochschule zur Begutachtung in einem Promotionsvorhaben vorliegt oder vorgelegen hat und dass im Zusammenhang mit dem Promotionsvorhaben keine kommerziellen Vermittlungs- oder Beratungsdienste in Anspruch genommen worden sind.

Oldenburg, den 8. Dezember 2016

Siri Rackebrandt